R88-917779-2

AD-A202 225

INTERFACIAL STUDIES OF CHEMICAL VAPOR INFILTRATED (CVI) CERAMIC MATRIX COMPOSITES

Prepared by
J.J. Brennan

Annual Report

Contract N00014-87-C-0699

for

Department of the Navy
Office of Naval Research
Arlington, VA 22217

October 1, 1988

DTIC
ELECTE
NOV 0 8 1988
S E

UNITED TECHNOLOGIES RESEARCH CENTER

DISTRIBUTION: UNLIMITED

88 11 08 046

UNCLASSIFIED
SECURITY CLASSIFICATION OF THIS PAGE

REPORT DOCUMENTATION PAGE

1a REPORT SECURITY CLASSIFICATION Unclassified	1b. RESTRICTIVE MARKINGS
2a SECURITY CLASSIFICATION AUTHORITY	3 DISTRIBUTION / AVAILABILITY OF REPORT Unlimited Distribution
2b DECLASSIFICATION / DOWNGRADING SCHEDULE	
4 PERFORMING ORGANIZATION REPORT NUMBER(S) R88-917779-2	5. MONITORING ORGANIZATION REPORT NUMBER(S)
6a NAME OF PERFORMING ORGANIZATION United Technologies Research Center; 6b OFFICE SYMBOL (If applicable)	7a NAME OF MONITORING ORGANIZATION See 8a
6c ADDRESS (City, State, and ZIP Code) Silver Lane East Hartford, CT 06108	7b ADDRESS (City, State, and ZIP Code) See 8c
8a. NAME OF FUNDING / SPONSORING ORGANIZATION Office of Naval Research; 8b OFFICE SYMBOL (If applicable)	9 PROCUREMENT INSTRUMENT IDENTIFICATION NUMBER N00014-87-C-0699
8c. ADDRESS (City, State, and ZIP Code) Arlington, VA 22217	10 SOURCE OF FUNDING NUMBERS

PROGRAM ELEMENT NO	PROJECT NO.	TASK NO	WORK UNIT ACCESSION NO
61153N22	4312	N.A.	4312616

11 TITLE (Include Security Classification)
INTERFACIAL STUDIES OF CHEMICAL VAPOR INFILTRATED (CVI) CERAMIC MATRIX COMPOSITES

12. PERSONAL AUTHOR(S)
J. J. Brennan

13a. TYPE OF REPORT	13b. TIME COVERED	14. DATE OF REPORT (Year, Month, Day)	15. PAGE COUNT
Annual	FROM 8/1/87 TO 7/31/88	Oct. 1, 1988	78

16. SUPPLEMENTARY NOTATION

17. COSATI CODES		
FIELD	GROUP	SUB-GROUP

18. SUBJECT TERMS (Continue on reverse if necessary and identify by block number)
CVI SiC matrix composites
Ceramic composite interfaces
Nicalon and Nextel 440 fiber/ceramic matrix composites

19. ABSTRACT (Continue on reverse if necessary and identify by block number) Chemical Vapor Infiltration Silicon Carbide
The objective of this program is to investigate the fiber/matrix interfacial chemistry in ~~CVI SiC~~ matrix composites utilizing Nicalon SiC and Nextel 440 mullite fibers and how this interface influences composite properties such as strength, toughness, and environmental stability. The SiC matrix was deposited using three different reactants; methyldichlorosilane (MDS), methyltrichlorosilane (MTS), and dimethyldichlorosilane (DMDS).

It was found that by varying the reactant gas flow rates, the ratio of carrier gas to reactant gas, the type of carrier gas (hydrogen or argon), the flushing gas used in the reactor prior to deposition (hydrogen or argon), or the type of silane reactant gas used, the composition of the deposited SiC could be varied from very silicon rich (75 at%) to carbon rich (60%) to almost pure carbon. Stoichiometric SiC was found to bond very strongly to both Nicalon and Nextel fibers, resulting in a weak and brittle composite. A thin carbon interfacial layer deposited either deliberately by the decomposition of methane or inadvertently by the introduction of argon into the reactor prior to silane flow, resulted in a weakly bonded fiber/matrix interface and strong and tough composites. However, composites with this type of interface were not oxidatively stable. Preliminary results point to the use of a carbon rich SiC interfacial zone to achieve a relatively weak, crack deflecting fiber/matrix bond but also exhibiting oxidative stability.

20. DISTRIBUTION / AVAILABILITY OF ABSTRACT ☐ UNCLASSIFIED/UNLIMITED ☒ SAME AS RPT ☐ DTIC USERS	21 ABSTRACT SECURITY CLASSIFICATION Unclassified
22a. NAME OF RESPONSIBLE INDIVIDUAL Dr. S. G. Fishman	22b TELEPHONE (Include Area Code) (202) 696-4401; 22c. OFFICE SYMBOL ONR/1131

DD FORM 1473, 84 MAR — 83 APR edition may be used until exhausted. All other editions are obsolete.

SECURITY CLASSIFICATION OF THIS PAGE
UNCLASSIFIED

UNITED TECHNOLOGIES RESEARCH CENTER
East Hartford, Connecticut 06108

R88-917779-2

Interfacial Studies of Chemical Vapor Infiltrated (CVI) Ceramic Matrix Composites

ANNUAL REPORT

Contract N00014-87-C-0699

REPORTED BY J. J. Brennan

APPROVED BY K. M. Prewo, Manager of Materials Sciences

DATE 10/1/88

NO. OF PAGES ________ COPY NO. ________

TABLE OF CONTENTS

Accession For
NTIS GRA&I ☒
DTIC TAB ☐
Unannounced ☐
Justification
By
Distribution/
Availability Codes
Avail and/or
Dist Special
A-1

DTIC
COPY
INSPECTED
6

Interfacial Studies of Chemical Vapor Infiltrated (CVI) Ceramic Matrix Composites

SUMMARY

The main objective of this program is the investigation of the fiber/matrix interface in CVI composites and how the microstructure and chemistry of this interface influence composite properties such as strength, toughness, and environmental stability. The long range goal of this investigation is to develop a CVI ceramic matrix composite that combines toughness and strength and can operate under stress in oxidizing conditions to temperatures approaching 1300°C. The CVI matrix system studied during the first year of this contract consisted of SiC deposited from three different reactant gases; methyldichlorosilane (MDS), methyltrichlorosilane (MTS), and dimethyldichlorosilane (DMDS). The fibers utilized were Nicalon SiC and Nextel 440 mullite. The chemistry and microstructure of the fiber/matrix interfacial area were studied through the use of scanning electron microscopy (SEM) of fracture surfaces, scanning Auger multiprobe (SAM) analysis of the elemental composition of the interface from depth profiles of fiber surfaces and matrix troughs that lie on composite fracture surfaces, and transmission electron microscopy (TEM) of polished surface replicas and ion beam thinned foils.

A number of CVI SiC matrix composites were fabricated and analyzed. It was found that composites utilizing Nicalon or Nextel 440 fibers that contained a thin carbon interfacial layer, whether deliberately or inadvertantly deposited, exhibited high toughness and strength due to the weakly bonded carbon interface's ability to deflect matrix cracks. However, this type of interface is not oxidatively stable and, when oxidized, leads to severe degradation of composite properties.

From studies of deposited SiC layers on Nicalon and Nextel 440 fibers utilizing MDS and MTS precursors, it was found that the use of an argon flushing gas in the reactor pricr to the introduction of the reactant gases initially disrupts the deposition of SiC such that a thin carbon layer is formed on the surface of the fibers prior to SiC deposition. While this situation results in a tough composite structure, the lack of oxidative stability, as mentioned previously, is undesirable. Overcoating this type of composite structure with CVD SiC to seal the fiber/matrix interface is practiced, but the likelihood of cracking in the coating is high, especially under stress, so that this approach is not considered to be a long term solution.

When hydrogen was used as the reactor flushing gas, no carbon interfacial layer was formed and the deposited SiC bonded very strongly to both Nicalon and Nextel 440 fibers, resulting in weak and brittle composites. However, the deposited SiC appeared to be more consistant in composition and contain less oxygen.

From studies of the bulk composition of SiC deposited on carbon plates utilizing MDS, MTS, and DMDS precursors, it was found that both MTS and DMDS could controllably yield compositions that ranged from very silicon rich to essentially stoichiometric SiC, depending on the hydrogen carrier gas to silane flow rate ratios. The utilization of MDS as a precursor to SiC appeared to yield more consistant depositions with compositions ranging from stoichiometric to slightly carbon rich SiC. The addition of large amounts of methane (CH_4) during the MDS deposition appeared to yield a product that was even more carbon rich (56-60 at %). Previous results on a different program indicated that a carbon rich SiC coating on Nicalon fibers (most likely a mixture of SiC + C) did not appear to bond very well to the fibers. It is likely that a coating of this composition would exhibit relatively good oxidative stability, especially when compared to the carbon interfacial layers.

Thus, the emphasis for the continuation of this investigation will be focused on the feasibility of utilizing a carbon rich SiC interfacial layer for both Nicalon and Nextel 440 fiber composites fabricated by CVI. In addition to carbon rich SiC as a weakly bonded, crack deflecting, oxidatively stable interface, the application of a CVD BN coating on the fiber surfaces prior to deposition of the SiC matrix will be studied. BN coatings on Nicalon fibers have been found recently to yield tough, strong, and relatively oxidatively stable glass-ceramic matrix composites at UTRC.

I. Introduction

During the past decade, the interest in ceramic matrix composites for high temperature structural applications, especially for use in heat engines, has increased to the point that a large number of industrial organizations as well as universities and government laboratories throughout the world are actively performing research into a myriad of different systems and different processing procedures for these materials. Among the types of ceramic matrix composites under investigation are whisker reinforced glasses and glass-ceramics[1] as well as whisker reinforced crystalline ceramics[2-18], and continuous fiber reinforced ceramics produced by methods that include hot-pressing of glasses and glass-ceramics[19-33], sol-gel infiltration and pyrolysis of ceramics[34], polymer precursor infiltration and pyrolysis[35], reactive oxidation of metals[36], reactive sintering[37], and chemical vapor infiltration (CVI) of silicon based ceramics[38-48].

It has been found in all of the above-mentioned ceramic composites that in order to achieve high strength and, in particular, high toughness, the bonding at the fiber/matrix interface must be controlled such that bonding is strong enough to allow load transfer from the matrix to the fibers under stress but weak enough so that an advancing matrix crack can be deflected by the fibers. In addition, the nature of the fiber/matrix interface must include resistance to oxidation at elevated temperature as well as resistance to other environmental effects.

For the past decade, research at United Technologies Research Center (UTRC) in the area of ceramic matrix composites has centered on systems based on the reinforcement of glass and glass-ceramic matrices with Nicalon polymer derived SiC fibers. In the past few years, this research has concentrated on the study of the fiber/matrix interface and the relationship of the interfacial chemistry and morphology to the composite mechanical and thermal properties[28,31]. The characterization of the interfaces in these composites has been accomplished primarily by a combination of scanning electron microscope (SEM) observations of composite fracture surfaces, transmission electron microscope (TEM) replica and thin foil analysis, and scanning Auger microprobe (SAM) analysis of composite fracture surfaces. This work has enabled a greater understanding to be reached of the reactions that occur and the phases formed in these systems and has led to the sucessful development of strong, tough, and oxidatively stable glass-ceramic matrix/Nicalon fiber composite systems for use to temperatures approaching 1000°C. While the attainment of much higher use temperature glass-ceramic matrices has been demonstrated, the inherent formation of a carbon rich interfacial layer between the Nicalon fibers and the glass-ceramic matrices during fabrication make the oxidative stability of these composites difficult to achieve in the temperature range of 1000-1300°C. Work in this area is being carried out at UTRC, primarily through the application of fiber coatings prior to composite fabrication. However, with the recent successful development of CVD coatings for carbon/carbon composites at UTRC[49], it was decided to use the knowledge gained in this area with the previous experience in fiber/matrix interfacial analysis of glass-ceramic matrix composites and apply them to a somewhat different class of ceramic matrix composites.

One of the most promising routes to the development of ceramic matrix composites that could potentially exhibit use temperatures to 1300°C or higher is that of chemical vapor infiltration (CVI) of silicon carbide or silicon nitride into fibrous preforms. Work in this type of ceramic matrix composite, pioneered by researchers at SEP in France[43], is now being carried out at a number of institutions[38-48]. Most of this work has concentrated on SiC matrices, since the deposition of crystalline silicon nitride can only be obtained at temperatures that are higher than the maximum stability temperature of fibers such as Nicalon. While CVI SiC reinforced with carbon or Nicalon fibers is now a commercially available ceramic composite from SEP, very little work has been reported on the fiber/matrix interfacial chemistry in these systems, with the exception of some recent research from Oak Ridge National Lab (ORNL)[50]. Since the nature of the fiber/matrix interface plays such an important role in the strength, toughness, and oxidative stability of these composites, it was decided to investigate the interfacial chemistry in the CVI SiC matrix composite systems reinforced with both Nicalon SiC and Nextel 440 mullite ($3AL_2O_3 \cdot 2SiO_2$) fibers. TEM and SAM analyses of the fiber/matrix interfacial regions in these systems constituted a major portion of this work.

II. Technical Discussion

A. Materials

The SiC fiber utilized for this program is that produced by Nippon Carbon Co. in Japan and distributed in the U. S. by Dow Corning Corp., Midland, Mich. under the trade name "Nicalon". The fiber used for this program is the lower oxygen level "Ceramic Grade". The fibers were obtained on spools of continuous length (500 m) tows of 500 fibers/tow with an average fiber diameter of 14 μm. The average tensile strength and elastic modulus of this fiber, as measured at UTRC, is 2400 MPa (350 ksi) and 193 GPa (28 x 10^6 psi), respectively. The mullite fiber (Nextel 440) was obtained from 3M Corp., Minneapolis, Minn. on spools of continuous length tows. According to 3M data, this fiber has a diameter of 7-11μm (somewhat oval shaped), a tensile strength of 1400-2000 MPa (200-300 ksi), and an elastic modulus of 205-240 GPa (30-35 x 10^6 psi). Some of the deposition runs utilized ATJ carbon plates as the substrate material.

Three different silane precursors were utilized to deposit SiC. Methlydichlorosilane (MDS), CH_3SiHCl_2, has long been used at UTRC to deposit SiC since its high vapor pressure (B. P. = 41.5°C) has allowed the transference of the saturated carrier to the reactor over long distances without heated lines. Methyltrichlorosilane (MTS), CH_3SiCl_3 (B.P.= 66.4°C), is used extensively by other researchers to deposit SiC and was also used in this program along with dimethyldichlorosilane (DMDS), $(CH_3)_2SiCl_2$ (B.P.= 70.5°C). All three of the silane precursors were obtained from Alfa Products, Danvers, Mass.

B. Sample Fabrication

The reactor utilized to deposit the CVD SiC coatings and to form the CVI SiC matrix composites is shown in Fig. 1. The reactant gases are introduced into the hollow quartz reaction cylinder at one end and the exhaust gases are removed at the other end. If the reaction is being run at reduced pressure, a vacuum pump is attached to the exhaust line.

A schematic of the quartz reaction chamber is shown in Fig. 2. The reactor has removable water cooled copper plates at each end. Pieces of carbon placed on the bottom of the reactor hold a hollow carbon cylindrical susceptor which is heated by an RF coil. When CVD coating either flat carbon plates or tows of fibers, carbon rods are inserted into the center of the susceptor to hold the samples being coated. When CVI matrix composites are fabricated, the fiber tows are wound around a solid carbon cylinder that is placed in the center of the reactor without utilizing the normal hollow carbon susceptor. Thus, the wound carbon rod is heated directly producing a temperature gradient from the inside of the fiber winding to the outside. This should allow deposition of the SiC to occur on the inside of the windings first so that the wound tows are not sealed off on the outside. The water cooled RF coil around the reactor also adds to the temperature gradient.

Reactant gases are introduced into the reactor through the copper end plates. The carrier gases; either hydrogen, argon, or methane, are passed through an evaporator containing the liquid silane and then through a water cooled condenser which insures that the carrier gas is saturated with the silane. The pressure in the evaporator is maintained at slightly more than one atmosphere. The ratio of carrier gas to silane can be controlled by varying the temperature in the condenser. The temperature in the condenser was usually held at RT for MTS and DMDS and 11°C for MDS, due to the lower vapor pressures of the former compared to the latter. In addition, for MTS and DMDS, the evaporator was moved closer to the reactor and the gas lines heated to prevent condensation.

Another inlet is also available into the reactor to add hydrogen or methane. This additional gas can be used to help control the ratio of carrier gas to silane. For high hydrogen to silane ratios, for example, the addition of hydrogen by this method was required.

At the beginning of each coating run, either argon or hydrogen gas is introduced into the reactor as a flushing gas while the temperature is being raised. When the desired reactor temperature is reached, a 15 to 20 minute stabilization period precedes introduction of the reactant gases. If the run is to take place at reduced pressure, the reactor chamber is evacuated and held at a pressure of approximately 30 microns.

C. CVI SiC Matrix Composites

Initial experiments under this program consisted of the fabrication of CVI SiC matrix composite rings utilizing MDS as the precursor and either Nicalon or Nextel 440 fibers as reinforcement. Figure 3 shows the fracture surface of composite #4-3-12 that consisted of wound Nicalon fiber tows that were first coated with a thin layer of pyrolytic graphite by the decomposition of methane (CH_4) (100 cc/min) plus hydrogen (500 cc/min) at 1100°C and then infiltrated with SiC. The SiC was deposited from MDS at 1080°C at a H_2/MDS flow rate ratio of 3.25/1 (50/15.4 cc/min, respectively). Total deposition time was 70 hrs. No attempt was made to optimize the fiber winding in order to obtain tight packing nor were any flexural tests performed on this composite.

From the fracture surface shown in Fig. 3, it can be seen that some of the regions fractured in a tough and fibrous manner while other areas exhibited a rather brittle mode of fracture with very little fiber pullout. The more fibrous regions tended to be located towards the inner diameter of the wound ring (next to the carbon mandrel) while the more brittle areas were located near the outer surface of the ring. Figure 4 shows the scanning Auger (SAM) depth profile taken from a fracture surface in the fibrous region of this composite. It can be seen that a very thin (50-100Å) carbon layer exists on the surface of the matrix trough from which a fiber has been fractured. Inside this carbon layer is an oxygen rich region of ~500Å in thickness which then grades to essentially stoichiometric SiC by a depth into the matrix of 2000Å.

Figures 5 and 6 show TEM thin foil micrographs and associated diffraction patterns and EDS analyses of the interfacial region for this composite taken from an area that was near the inner diameter of the ring. From these figures, it can be seen that a thin carbon layer exists at the fiber/matrix interface. From Fig. 6, it can also be seen that a small amount of Cl exists at the interface and in the CVD SiC matrix near the interface. HCl is a byproduct of the CVD reaction and if deposition conditions are not controlled correctly, it can be trapped during the SiC deposition. Figure 7 shows a TEM thin foil micrograph of the interfacial region from a brittle fracture area of this composite. No carbon layer exists at the fiber/matrix interface and the matrix next to the fiber is quite porous with a significant amount of oxygen and chlorine present.

It is apparent from the previous figures that the microstructure in composite #4-3-12 is very non-uniform with some regions exibiting fibrous fracture due to the presence of the deposited carbon interfacial layer and other regions exhibiting brittle fracture behavior due to the lack of a carbon interfacial layer and the added complication of a porous SiC deposition containing Cl and O. Apparently, the deposition of C from methane plus hydrogen was non-uniform throughout the wound fiber tows with adequate deposition occuring near the carbon mandrel and inadequate deposition occuring in the cooler regions away from the inductively heated carbon mandrel. The deposition of SiC was also non-uniform due to the initial temperature differences through the thickness of the wound ring. In the cooler regions, the SiC deposited in a very porous manner, apparently due to interference by residual HCl in the system. Oxygen contamination was also noted in the porous SiC regions and in the initial SiC that was deposited over the carbon layer in the fibrous regions of the composite.

It is apparent from the above results that a thin carbon layer deposited on Nicalon fibers before SiC deposition results in a tough composite with fibrous fracture behavoir. The lack of this carbon layer appears to result in a brittle composite, however, the added complication of Cl and O contamination resulting in the deposition of porous SiC clouds the issue somewhat. It was thus decided to evaluate the effectiveness of carbon layer interfaces in CVD SiC/ Nicalon fiber composites by investigating composites produced by Oak Ridge National Labs (ORNL). The ORNL process for depositing CVD SiC from MTS has been developed over a number of years and is considered to be a state-of-the-art CVD process[39,40,44-46,48,50].

Accordingly, two types of composites were obtained from ORNL[51], one with a rather thick carbon interfacial layer and one with no carbon interfacial layer. Both composites utilized a woven Nicalon fiber preform. Figure 8 shows the fracture surface of the composite with no carbon interfacial layer. From this figure, it can be seen that the fracture mode was quite brittle, with little or no fiber pullout and a rather well bonded fiber/matrix interface. The RT flexural strength of this composite was approximately 13 ksi (90 MPa). In contrast, Fig. 9 shows the fracture surface of a composite with a carbon interfacial layer of approximately 1 μm in thickness. This composite exhibits a very tough fracture surface with a large amount of fiber pullout and a RT flexural strength of 55 ksi (380 MPa). It is apparent that the presence of a weakly bonded carbon interface drastically alters the fracture behavior and increases the strength and toughness in CVI SiC matrix/Nicalon fiber composites.

While carbon interfaces have been found to also result in strong and tough composites in glass-ceramic matrix composites reinforced with Nicalon and other fibers (HPZ, MPDZ)[52], the presence of this type of interface results in severe degradation of composite properties when the composite is exposed to oxidizing environments at elevated temperatures. This is also the case for carbon interfaces in CVI SiC matrix composites. Figure 10 shows the fracture surface of an ORNL composite with a carbon interfacial layer that has been exposed to flowing oxygen at 1000°C for 70 hrs. It can be seen that while the fracture surface of this composite is still quite tough in appearance with a large amount of fiber pullout, the strength has dropped drastically to 11.2 ksi (77 MPa). At high magnification, it is apparent that the carbon layer has oxidized away leaving a gap between the fibers and matrix. While this gap results in a "tough" fracture appearance, load transfer from martix to fiber cannot take place, resulting in a very weak composite.

While the CVI SiC matrix/Nicalon fiber composite from ORNL without the intentionally deposited carbon interfacial layer was very weak and brittle, past work at UTRC with CVI SiC matrix/Nicalon fiber composites deposited from MDS precursor had resulted in composites that were quite strong with a tough and fibrous fracture behavior. These composites, however, were never characterized as to interfacial chemistry. It was thus decided to fabricate two wound composites, similar to #4-3-12 except with no deliberate carbon interfacial layer, utilizing both Nicalon and Nextel 440 fibers. Both composite rings were fabricated in the same run of 100 hrs at 1080° C using argon as the flushing gas and a hydrogen/MDS ratio of 3.25/1. No special attempt was made to wind the fiber tows around the carbon mandrel to achieve optimum fiber packing.

The fracture surface of a segment of the fiber wound ring utilizing Nicalon fibers in the CVI SiC matrix is shown in Fig. 11. Part of the fracture surface is quite fibrous in appearance while part is rather brittle. As was the case for composite #4-3-12, the fibrous fracture region is near the inner diameter of the ring segment while the brittle region is near the outer diameter. Figure 12 shows a polished cross-section through the composite ring. The areas containing a large amount of porosity are quite evident, reflecting the non-uniform winding of the fiber tows. Also evident is a reaction or change in morphology at the fiber/matrix interface near the outer diameter of the ring. Figure 13 shows this area in greater detail. From EDS analysis in the SEM (no light element detector), it is apparent that Cl contamination is again causing a porous SiC to deposit around the fibers in the initially cooler outer region of the wound composite ring. Also, a lighter colored region was seen to exist in the near surface area between the porous and dense SiC regions. This could be caused by oxygen contamination but confirmation of this was not obtained due to the lack of a light element detector on the SEM.

Scanning Auger analysis of a fiber surface and a matrix trough from a fibrous fracture area of the composite was conducted (Fig. 14) and showed that a very thick (6000Å) carbon layer was present at the fiber/matrix interface, most of which stayed on the fiber surface upon fracture. A small amount of oxygen (3-5 at%) was found to be present in the CVI SiC. The carbon layer was obviously responsible for the fibrous fracture mode of the inner diameter region of this composite, but was not uniform throughout the composite and not present at all near the outer surface. Since this carbon layer was not deposited deliberately, it must have resulted from the deposition conditions for the SiC present in the reactor at the beginning of the run.

Figures 15, 16, and 17 show the fracture surface and polished cross-sectional area of the Nextel 440 fiber composite (#7-8-18) that was fabricated during the same run as the Nicalon fiber composite discussed above. It can be seen that the fracture surface and reactivity near the outer composite surface appear very similar to the Nicalon fiber composite. Figure 18 shows again that during this run, Cl contamination has led to an area of porous SiC being formed around the fibers near the outer surface of the composite. The SAM depth profile analysis shown in Fig. 19 of an area in the fibrous region of the composite clearly shows that, as was the case in the Nicalon fiber composite, a rather thick carbon layer has been deposited on the fiber surface prior to deposition of SiC.

One-quarter segments of slices from the wound rings of composite #7-8-18 were tested in 3-pt flex at RT in the as-fabricated condition and after oxidation at 1000°C for 120 hrs. The inner diameter of the ring segments was the side in tension. The results of these tests are presented in Table I. It can be seen that the oxidation lowered the flexural strength of both the Nicalon and Nextel 440 composite rings substantially. It is obvious that carbon interfacial layers, whether deposited deliberately or inadvertantly, cannot withstand oxidizing environments at elevated temperatures. The solution to oxidation of these types of composites by applying a final overcoat of CVD SiC to cover any exposed carbon, as practiced by commercial vendors of SiC/SiC, will not work if the coating becomes cracked either from thermal or mechanical stresses.

During run #7-8-18, a few Nextel 440 fiber tows were wound around the end of the carbon mandrel at a point where the temperature was approximately 100°C less than the nominal 1080°C run temperature. These fibers were removed from the reactor after 10 hours. Figures 20 and 21 show the SAM depth profiles obtained for two different appearing fibers; one with a rough surface and one with a basically smooth surface with a few particles attached. Both fibers exhibited a carbon rich surface layer varying from 1000Å in thickness and approximately 80% C for the smooth fiber surface (Pt. #1 in Fig. 20) to 1500-2000Å of 60-80% C for the rough appearing fiber. From these results and the interfacial analyses conducted on the composites from run #7-8-18, it is apparent that during the initial stages of SiC deposition mostly carbon is deposited. It was thus decided that further experiments would consist of shorter time (2 hrs) deposition runs on fiber tows placed on carbon plates in the reactor, rather than long time deposition runs to produce composites, since it is the composition of the interface, ie, the first few hundred angstroms deposited, that controls many of the composite properties such as toughness and oxidative stability.

D. CVD SiC Coated Fiber Studies

It was decided that a series of deposition runs on both Nicalon and Nextel 440 fibers would be performed utilizing both MDS and MTS as precursors. Table II shows the coated fiber runs, as well as the previous composite runs, and brief comments on the results of each run.

The first runs consisted of 2 hr depositions on both Nextel 440 fibers (#7-9-14) and Nicalon fibers (#7-9-15) utilizing MDS with an Ar flush of the reactor prior to coating. Figure 22 shows the general appearance of the coated Nextel fibers. The coating appears to be rather thick (> 1 μm) and somewhat nonuniform and rather weakly bonded to the fibers. One of the coated fibers that had part of the coating fractured away was depth profiled in the SAM. Figure 23 shows the fiber that was analyzed and the SAM depth profile of the fiber surface (Pt. 2) under the coating. It can be seen that the surface of the Nextel fiber under the SiC coating is very high in carbon, accounting for the weak coating/fiber bonding. Figure 24 shows the SAM depth profile of the coating surface (Pt. 1) that indicates the coating itself is very close to stoichiometric SiC.

Examples of the coated Nicalon fibers from run #7-9-15 are shown in Fig. 25. The surfaces of the coated fibers ranged from quite smooth to very granular in appearance. Some evidence of fiber/coating debonding can be seen. A SAM depth profile of one of the coated Nicalon fibers, as shown in Fig. 26, indicates that the entire coating is high in carbon (70%) with 20% Si and 5-10% O. However, other coated fibers from this run, as shown in the TEM thin foil micrograph in Fig. 27, exhibited a distinct SiC coating over a carbon interfacial layer of about 2000Å in thickness. It is apparent that the composition and thickness of the coatings deposited during this run varied considerably and were not well controlled.

From the results obtained during the above experiments, one of the most puzzling findings is the presence of carbon at the interface between the CVD or CVI SiC and the Nicalon or Nextel fibers. It is obvious that during the initial stages of deposition, reactions are taking place that result in carbon formation rather than the deposition of SiC. In order to make sure this carbon deposition does not occur before the MDS and hydrogen are introduced into the reactor, Nicalon and Nextel fibers were placed in the reactor and heated to the deposition temperature (1080°C) only in the presence of the Ar flushing gas and held for 2 hrs. The results of this experiment (runs #7-10-2 and 7-10-6) showed that only minor surface carbon contamination was present on the fibers after the heat treatment. The SAM depth profile for a Nextel 440 fiber after heat treatment, as shown in Fig. 28, indicates that in addition to the minor surface carbon present, boron has diffused to the fiber surface region, being present at levels up to 9 at %, compared to an overall reported boron concentration of 3%. A minor amount of Fe contamination was also found in the near surface region.

Since the large amount of carbon deposition found on the fibers after the CVD or CVI SiC runs did not result from simply heating the fibers in the Ar flush atmosphere, it was theorized that the presence of Ar during the initial stages of decomposition of the MDS resulted in disruption of SiC formation and deposition of carbon instead. It was therefore decided to flush the reaction chamber with hydrogen prior to indroduction of the MDS in order to determine if this indeed was the case.

Figure 29 shows the fracture surface of Nextel 440 fibers with CVD SiC coatings deposited under the normal conditions except for the hydrogen rather than Ar flush (Run #7-10-22). It can be seen from the SEM photos of the fractured fiber ends that the fiber/matrix bonding is very strong, unlike previous runs where carbon was found at the interface. Figure 30 shows a TEM thin foil micrograph of a SiC coated Nextel fiber interface and the associated EDS analyses from the SiC coating, interface, and fiber. It is apparent that no carbon layer exists at the fiber/coating interface but instead an amorphous aluminosilicate interfacial layer has formed that is on the order of 1200Å in thickness and apparently quite well bonded to both fiber and SiC coating. The qualitative composition of this interfacial layer from the EDS analysis shows that it contains more Si than Al whereas the Nextel 440 mullite fiber contains more Al than Si. No SAM analysis of the interfacial composition for this composite could be done since the strong bonding across the interface precluded interfacial fracture.

The CVD SiC coated Nicalon fibers using hydrogen as the flushing gas (#7-10-23) also exhibited very strong bonding across the fiber/coating interface, as shown in Fig. 31. From the fractured ends of the coated fibers shown in Fig. 31 it is often difficult to discern the coating/matrix interface. Figure 32 shows a TEM thin foil micrograph and associated electron diffraction analyses of the Nicalon/SiC coating interfacial area. No distinct interfacial layer is seen in this system with the only discernable feature marking the interface being preferential thinning. Interestingly, the CVD SiC deposited on the Nicalon fibers is basically amorphous, in contrast to the very crystalline SiC that was deposited on the Nextel fibers over the thin aluminosilicate interfacial layer, as was shown in Fig. 30. As in the previous case, no SAM depth profiles of the fiber/coating interface could be done since the coating was so adherent that coating/fiber fracture was impossible.

CVD SiC coated Nicalon and Nextel 440 fibers utilizing both argon and hydrogen as the flushing gas were also evaluated with MTS rather than MDS as the silane precursor. The hydrogen carrier gas flow rate was 100 cc/min with the hydrogen/MTS ratio being fixed at 4.8/1. The higher hydrogen/MTS flow ratio compared to MDS was due to the lower vapor pressure of MTS necessitating that the condenser be run at RT in order to avoid having to heat the stainless steel flow lines to avoid MTS condensation.

Figure 33 shows the fractured fiber surfaces of run #8-1-14 utilizing MTS as the precursor for SiC deposition on Nextel 440 fibers with hydrogen as the flushing gas. Unlike the previous run using MDS with a hydrogen flush (#7-10-22), the bonding between the coating and fiber appears to be quite weak. Figure 34 shows the SAM depth profile taken from a coated fiber surface, a fiber under a fractured coating that had pulled away from the fiber, and the inside of a coating fragment. From this analysis, it appears that an extremely thin (25-50Å) carbon layer exists at the fiber/coating interface, accounting for the weak bond. Into the coating from this carbon layer was found a 1500-2000Å thick layer of silica with some carbon in it. The CVD coating surface appears to consist of stoichiometric or slightly carbon rich SiC. Trace amounts of chlorine were found throughout the coating as well as trace sulfur near the coating surface.

It appears that the formation of the very thin carbon layer and the high silica zone in the above run may have resulted from a leak in the CVD system rather than an inherent result of the MTS coating process. Figure 35 shows the fractured fiber ends of SiC coated Nicalon fibers utilizing MTS plus a hydrogen flush (Run #8-1-15). It is apparent from this figure that the fiber/matrix interfacial bonding is very strong for this system. Although the CVD coating was not able to be separated completely from the fiber, a SAM analysis of a fractured fiber end, as shown in Fig. 36, was attempted. The analysis of the four different areas shown in Fig. 36 indicated that no carbon layer existed at the fiber/coating interface and no evidence of a high silica containing layer was found. It thus appears that the MTS CVD process with a hydrogen flush yields a slightly carbon rich SiC containing a very small amount of oxygen (1-2%).

The results of MTS precursor coatings applied to Nextel 440 and Nicalon fibers preceded by an argon flush of the reactor are shown in Figs. 37-40. It can be seen from the SEM photos in Figs. 37 and 38 that a rather thick CVD coating with a somewhat dual nature is present on both types of fibers and is not bonded very strongly to them. A typical SAM depth profile of a fractured interface in the SiC/Nicalon system is shown in Fig. 39 and shows that a pure carbon layer of 2000-3000Å in thickness exists at the interface transitioning to a very carbon rich (69%) SiC overcoat. The SiC may become more stoichiometric towards its surface, but no SAM analysis of the coating surface region was attempted.

From the studies conducted on the deposition of CVD SiC onto Nicalon and Nextel 440 fibers from both MDS and MTS precursors, it has become apparent that utilizing an argon flushing gas prior to the introduction of the silane plus hydrogen mixture into the reactor results in initial deposition of a rather thick carbon layer. The presence of argon must disrupt the normal decomposition of the silanes from SiC + HCl to carbon plus a silicon containing gas such as $SiCl_4$. When the argon has been swept from the reaction chamber, the normal deposition of SiC takes place. While the presence of this carbon interfacial layer results in a weak fiber/matrix bond and thus imparts toughness to the composite structure, the poor oxidative stability of this type of system would be extremely detrimental to its use. Overcoating this type of composite structure with CVD SiC to seal the fiber/matrix interface is practiced, but the likelihood of cracking in the coating is high, especially under stress, so that this approach is not considered to be a long term solution.

Utilizing a hydrogen flushing gas prior to the introduction of the silane/hydrogen mix into the reaction chamber results in most cases in the deposition of stoichiometric or slightly carbon rich SiC directly on the surface of the fiber in the case of Nicalon and a glassy silicate formation under SiC in the case of Nextel. In both fiber systems, the fiber/matrix bonding is very strong such that the interface exhibits no crack stopping ability with the resultant composite being quite brittle with low toughness.

One other observation concerning the deposition of SiC from either MDS or MTS is that utilizing argon as a flushing gas, in addition to creating a carbon layer during initial deposition, results in wildly fluctuating compositions of SiC after the carbon deposition, including at times a large amount of oxygen in the deposited product. The majority of the deposited SiC, or bulk composition, appears to be uniform, however. Utilizing hydrogen as the flushing gas appears to result in somewhat more uniform SiC compositions during deposition with less oxygen impurity.

It was thus decided to investigate the bulk composition of deposited SiC utilizing MDS, MTS, and DMDS as the silane precursors under varying deposition conditions including type of flush gas, carrier gas to silane ratio, and the type of carrier gas. One of the purposes of this investigation was to determine if the carbon to silicon ratio of the deposited SiC could be controlled by varying the above parameters. Past work dealing with the deposition of CVD SiC on Nicalon fibers under another program[53] appeared to indicate that a carbon rich SiC (58 at% C, 40% Si, 2% O) did not bond particularly well to the fibers. It is also likely that a coating of this composition would exhibit relatively good oxidative stability. Thus, one of the objectives of this study was to determine if a CVD carbon rich SiC (actually, a mixture of carbon plus SiC) could be reproducibly obtained.

E. CVD SiC on Carbon Substrate Studies

CVD SiC layers were applied to small flat carbon substrates utilizing MDS, MTS, and DMDS precursors. After deposition, all samples were depth profiled in the SAM from the coating surface inward to a depth of 6000Å. Values for the bulk composition of each coating, as listed in the following tables, were taken at a depth where surface effects such as oxide formation would be negligible, normally 5000Å.

1. CVD SiC From MDS

MDS was utilized with a hydrogen carrier gas and an argon flush gas to produce CVD layers of SiC on carbon plates with the hydrogen to MDS flow rate ratio varying from 328/1 to 1/1. The results of the four runs performed and the conditions employed are shown in Table III. It can be seen from this data that varying the hydrogen/MDS ratio from 328/1 by an order of magnitude to 32.8/1 changes the bulk SiC deposition composition from essentially stoichiometric (+2% O) to somewhat carbon rich (53%C, 45%Si, 2% O). Reducing the hydrogen/MDS ratio further was found not to have an effect on the measured composition. Figures 40 and 41 show the SAM depth profiles and surface morphology for the 328/1 (#9-1-28) and the 3.28/1 (#9-1-25) SiC coatings, respectively. The coatings appear to be quite uniform in composition through the thickness that was analyzed except for slight surface contamination. The surface morphology appears slightly different, with the 328/1 sample exhibiting slightly smaller SiC grain size. If carbon layer formation or contamination was a problem with the argon flush gas used, it appears to have been limited to the coating/substrate interfacial area.

For the MDS system, it appears that the range of stoichiometry obtainable in a reproducible manner for SiC is quite limited for the conditions employed, at least in reasonable deposition times. Slightly carbon rich SiC can be obtained, but not at the level desired for interfacial deposition (~60% C) aimed at obtaining a weakly bonded but oxidatively stable composite.

2. CVD SiC From MTS

Five deposition runs were done utilizing MTS as the precursor at calculated hydrogen/MTS ratios varying from 48/1 to 1/1. Table IV shows the results of these experiments and the conditions employed. The 4.8/1 and 48/1 runs were done utilizing both argon and hydrogen as the flushing gas.

From Table IV, it can be seen that the 4.8/1 hydrogen/MTS ratio conditions produced a very silicon rich CVD product. The SAM depth profiles and coating morphologies for these runs are shown in Figs. 42 and 43. The only difference between the two runs is that the run utilizing an argon flushing gas resulted in a substantial amount of oxygen (7-10%) being present in the CVD SiC while the hydrogen flushed run resulted in a very Si rich SiC with essentially no oxygen present. By increasing the hydrogen/MTS ratio to 48/1 through the use of added hydrogen to the reactor, the deposited SiC composition became much closer to stoichiometry. However, even with hydrogen as the flushing gas, the oxygen content of both deposited coatings was in the range of 6-7%. While the composition of both coatings was similar, the morphology was quite different, as shown in Figs. 44 and 45. The argon flushed run, Fig. 44, resulted in a nodular coating of very fine grain size, especially when compared to the 4.8/1 coatings shown in Figs. 42 and 43. The hydrogen flushed coating, as shown in Fig. 45, was quite fibrous in nature. The depth profile shown was taken from one of the larger fibers. The 1/1 ratio of hydrogen to MTS run (#9-5-18) did not result in deposition of SiC but rather a very powdery layer of essentially carbon with small amounts of Si and O.

Within the deposition parameters investigated, which were chosen to be representative of feasible ranges for the deposition of SiC onto Nicalon or Nextel fibers utilizing MTS as the precursor, a range of composition could be obtained from silicon rich to almost pure carbon. However, it did not appear that the attainment of carbon rich SiC with this system was practical. It was thus decided to investigate deposition parameters within the dimethyldichlorosilane (DMDS) system.

3. CVD SiC From DMDS

It was thought at the beginning of this program that MDS and MTS, if properly deposited, should yield relatively stoichiometric SiC according to the following equations:

$$\text{(MTS)} - CH_3SiCl_3 \rightarrow SiC + 3HCl \qquad (1)$$

$$\text{(MDS)} - CH_3SiHCl_2 \rightarrow SiC + 2HCl + H2 \qquad (2)$$

However, DMDS should result in excess carbon in the SiC deposition according to the following equation:

$$\text{(DMDS)} - (CH_3)_2SiCl_2 \rightarrow SiC + C + 2HCl + 2H_2 \qquad (3)$$

Accordingly, deposition runs on carbon plates were done at hydrogen/DMDS ratios of from 38.5/1 to 1/1, utilizing both argon and hydrogen as flushing gases. The results of these experiments are shown in Table V. As can be seen from Table V, as the hydrogen/DMDS ratio is lowered, the CVD SiC coating goes from being very silicon rich to being essentially stoichiometric SiC. As in the case of MTS, at a 1/1 ratio the deposited coating was essentially pure carbon. Figures 46 and 47 show the surface morphologies and depth profiles for the 7.69/1 runs utilizing argon and hydrogen flushes, respectively. While the surface morphologies appear relatively similar, the compositions are quite different with the argon flushed coating being quite silicon rich with a large amount of oxygen (10%), while the hydrogen flushed system is essentially stoichiometric SiC by a depth of 1000Å from the surface with a very low oxygen content (2%). Even though from the chemistry of DMDS it was thought that a carbon rich SiC could be deposited, it was found that this was not the case. Although a high carbon containing deposit could be obtained at a hydrogen/DMDS ratio of 1/1, as in the case of MTS the control over excess carbon deposition could not be achieved such that a carbon/SiC mixture of ~60%C, 40%Si, would result.

4. CVD SIC From MDS Plus Methane

From the results of the experiments utilizing MDS, MTS, and DMDS as the precursors for the deposition of SiC, it appears that MDS is more controllable than the others as far as obtaining a carbon rich SiC deposit. It was thus decided that the final series of deposition experiments to be run during this reporting period would consist of MDS at a fixed carrier gas/MDS flow ratio of 3.28/1 with the variables being type of carrier gas (H_2, Ar, CH_4), type of flushing gas (H_2, Ar), and the effect of additions of methane at various flow rates to the reaction chamber during deposition. The results of these experiments are shown in Table VI.

From the results shown in Table VI, it is apparent that varying the carrier gas, flushing gas, deposition temperature, and the addition of methane at low flow rates (100 cc/min) does not affect the composition of the SiC deposited by a significant amount. All of these conditions result in a bulk SiC composition of from 53-57% C. Increasing the flow rate of the added methane gas from 100 cc/min to 600 cc/min does appear to slightly increase the carbon content but also leads to some inconsistant deposition, as shown in Fig. 48 for run #13-8-3A for a methane flow rate of 200 cc/min. Figure 49 shows the SAM depth profile and surface morphology for the 600 cc/min methane addition run. In general, while some variations in composition were noted, the coating was extremely low in oxygen and approached the 60% C content that has been set as an initial goal for composite fabrication. Work is continuing to evaluate methane additions to MDS in order to achieve this goal.

F. Conclusions and Recommendations

From the results of the first year's efforts under this program, certain conclusions can be made. It is obvious that applying a carbon interfacial layer to either Nicalon or Nextel 440 fibers prior to deposition of SiC results in a weakly bonded interface that imparts toughness to a CVI matrix composite through its ability to deflect matrix cracks. It is also obvious that this type of interface is not oxidatively stable and, when oxidized, leads to severe degradation of composite properties.

It has also been found that a carbon interfacial layer can form in these types of composites due to the argon flushing gas used during heat up of the reactor prior to introduction of the silane plus carrier gas interrupting the normal deposition of SiC. Since deposition of carbon was also found to occur in the MTS and DMDS systems at very low hydrogen/silane flow rate ratios of 1/1, the carbon interfacial layers found when utilizing argon flushing gas may simply be a result of dilution of the carrier gas as it enters the reactor. When hydrogen is used as the reactor flushing gas, no carbon interfacial layer is formed. Instead, the deposited SiC is found to bond very strongly to both Nicalon and Nextel fibers, resulting in weak and brittle composites. This has been found for MDS and MTS precursor depositions at UTRC and also found for MTS deposited SiC at ONRL.

From studies of the bulk composition of SiC deposited on carbon plates utilizing MDS, MTS, and DMDS precursors, it was found that both MTS and DMDS could controllably yield compositions that ranged from very silicon rich to essentially stoichiometric SiC. It was initially expected that DMDS, due to its chemistry, would yield carbon rich SiC but this was not the case. With very low flow rates of hydrogen carrier gas, both of these silanes also yielded depositions of almost pure carbon in a very powdery form. This carbon deposition did not appear to be controllable enough to combine carbon plus SiC deposition to yield a carbon rich SiC product, however. The utilization of MDS as a precursor to SiC appeared to yield more consistant depositions with compositions ranging from stoichiometric SiC to slightly carbon rich SiC. The addition of large amounts of methane (CH_4) during the deposition from MDS appeared to yield a product that was slightly more carbon rich (56-60 at%).

The interest in the controlled deposition of carbon rich SiC (actually, most likely a mixture of carbon plus SiC) stems from a previous observation that a CVD SiC coating on Nicalon fibers that was 58% C, 40% Si, and 2% O did not appear to bond very well to the fibers either as-deposited or after being incorporated into a glass-ceramic matrix composite. It also did not appear to bond particularly well to the glass-ceramic matrix either, unlike stoichiometric SiC coatings. It is likely that a coating of this composition would exhibit relatively good oxidative stability, especially when compared to the carbon interfacial layers. Thus, one of the objectives of this program was to determine if a carbon rich SiC could be reproducibly obtained by controlled deposition from a silane.

Certain recommendations for continued work in the area of interfacial studies of CVI matrix composites can be made as a result of the investigations performed during this past year. Further exploration into the feasibility of utilizing carbon rich SiC as an interfacial layer for both Nicalon and Nextel 440 fiber composites should be conducted. This will be accomplished using MDS as the precursor for SiC with and without additions of methane to the reactor. Only hydrogen will be utilized as the reactor flushing gas due to the carbon formation caused by argon and the generally increased oxygen contamination also associated with argon. Actual CVI matrix composites shall be fabricated utilizing woven fiber preforms that will be graded in composition from carbon rich SiC at the fiber/matrix interface to more stoichiometric SiC for the bulk of the matrix.

Another fiber/matrix interfacial layer will also be investigated for use as a weakly bonded crack deflector with increased oxidative stability. From experiments conducted at UTRC during the past year, CVD BN layers deposited on Nicalon fibers and incorporated into glass-ceramic matrices appeared to offer enhanced oxidative stability and tough and strong composites. Reaction of the BN coating with the glass-ceramic matrix during composite fabrication is a concern, however. This may not be as much of a problem in the CVI matrix composites, however, since deposition of both the BN interfacial layer and the SiC matrix can be done at the same temperature and possibly during the same run. Reactors to accomplish this are currently under construction at UTRC.

III. Acknowledgements

The author would like to thank Drs. F. Galasso and R. Veltri of UTRC for their guidance in the CVI and CVD SiC experiments and to Mr. J. Whittier for his part in the processing of the samples studied under this program. Thanks also go to Ms. J. Whitehead, Mr. G. McCarthy, and Mr. D. Delong and Dr. B. Laube for their contributions to the SEM, TEM, and SAM analyses, respectively, and to Dr. S. G. Fishman of ONR for his sponsorship of the program

REFERENCES

1. Gadkaree, K.P. and Chyung, Y.: Silicon-Carbide-Whisker-Reinforced Glass and Glass-Ceramic Composites, Am. Cer. Soc., Bull. 65 [2] (1986) 370-376.

2. Becher, P.F. and Wei, G.C.: Toughening Behavior in SiC Whisker Reinforced Alumina, Comm. Am. Cer. Soc. (Dec. 1984) C-267-269.

3. Wei, G.C. and Becher, P.F.: Development of SiC Whisker Reinforced Ceramics, Am. Cer. Soc. Bull., 64, (1985) 289-304.

4. Tiegs, T.N. and Echer, P.F.: Whisker Reinforced Ceramic Composites, Proceedings of "Tailoring Multiphase and Composite Ceramics", 21st Univ. Conf. on Ceramic Science Penn St. Univ. July 1985 Plenum Press NY (1986) 639-647.

5. Samanta, S.C. and Musikant, S.: SiC Whiskers-Reinforced Ceramic Matrix Composites, Cer. Engr. and Sci. Proc. (July-Aug 1985) 663-672.

6. Claussen, N. and Petzow, G.: Whisker Reinforced Zirconia Toughened Ceramics, Proceedings of "Tailoring Multiphase and Composite Ceramics", 21st Univ. Conf. on Ceramic Science Penn. St. Univ. (July 1985) Plenum Press NY (1986) 649-662.

7. Hermes, E.E. and Mazdiyasni, K.S.: SiC Whisker Reinforced $MgAl_2O_4$ Spinel, Proc. of NASA/DOD Conf. on Metal, Carbon, and Ceramic Matrix Composites Cocoa Beach FL (Jan. 1986) NASA Conf. Publication 2445, 143-155.

8. Shalek, P.D., Petrovic, J.J., Hurley, G.F. and Gac, F.D.: Hot-Pressed SiC Whisker/Si_3N_4 Matrix Composites, Am. Cer. Soc. Bull. Vol. 65 No. 2 (Feb 1986) 351-356.

9. Lundberg, R., Kahlman, L., Pompe, R., Carlsson, R. and Warren, R.: SiC Whisker-Reinforced Si_3N_4 Composites, Am. Cer. Soc. Bull. [66] 2 (1987) 330-333.

10. Tiegs, T.N and Becher, P.F.: Sintered Al_2O_3-SiC Whisker Composites, ibid, 339-343.

11. Porter, J.R., Lange, F.F. and Chokshi, A. H.: Processing and Creep Performance of SiC Whisker Reinforced Al_2O_3, ibid, 343-347.

12. Homeny, J., Vaughn, W.L. and Ferber, M.K.: Processing and Mechanical Properties of SiC-Whisker-Al_2O_3-Matrix Composites, ibid, 333-339.

13. Buljan, S.T., Baldoni, J.G. and Huckabee,M.L.: Si_3N_4-SiC Composites, ibid, 347-353.

14. Homeny, J. and Vaughn, W.L.: Whisker-Reinforced Ceramic Matrix Composites, MRS Bull. (Oct-Nov 1987) 66-71.

15. Buljan, S.T. and Sarin, V.K.: Silicon Nitride-Based Composites, Composites Vol. 18 No. 2 (Apr 1987) 99-106.

16. Kandori, T., Kobayashi, S., Wada, S and Kamigaito, O.: SiC Whisker Reinforced Si_3N_4 Composites, J. Mat. Sci. Let. 6 (1987) 1356-1358.

17. Becher, P.F. and Tiegs, T.N.: Toughening Behavior Involving Multiple Mechanisms: Whisker Reinforcement and Zirconia Toughening, J. Am. Cer. Soc. 70 [9] (1987) 651-654.

18. Akimune, Y., Katano, Y. and Shiehi, Y.: Mechanical Properties and Microstructure of an Air-Annealed SiC-Whisker/Y-TZP Composite, Ad. Cer. Mat. Vol 3 No. 2 (1988) 138-142.

19. Prewo, K.M. and Bacon, J.F.: Proc. of Second Intl. Conf. on Composite Materials, Toronto Canada (AIME New York 1978) 64.

20. Prewo, K.M., Bacon, J.F. and Dicus, D.L.: SAMPE Q. (1979) 42.

21. Prewo, K.M.: *Development of a New Dimensionally and Thermally Stable Composite*, Proceedings of "The Conference on Advanced Composites-Special Topics", (Dec 4-6, 1979) El Segundo CA.

22. Prewo, K.M. and Minford, E.J.: Graphite Fiber Reinforced Thermoplastic Matrix Composites for Use at 1000°F, SAMPE J. Vol 21-1 (March 1985).

23. Prewo, K.M.: A Compliant, High Failure Strain Fibre Reinforced Glass Matrix Composite, J. Mat. Sci. 17 (1982) 3549-3563.

24. Bacon, J.F. and Prewo, K.M.: Proc. Second Intl. Conf. on Composite Materials Toronto Canada (AIME New York 1978) 753.

25. Prewo, K.M. and Brennan, J.J.: High Strength Silicon Carbide Fiber-Reinforced Glass Matrix Composites, J. Mat. Sci. 15 (1980) 463-468.

26. Prewo, K.M. and Brennan, J.J.: Silicon Carbide Yarn Reinforced Glass Matrix Composites, J. Mat. Sci. 17 (1982) 1201-1206.

27. Brennan, J.J. and Prewo, K.M.: Silicon Carbide Fibre Reinforced Glass-Ceramic Matrix Composites Exhibiting High Strength and Toughness, J. Mat. Sci. 17 (1982) 2371-2383.

28. Brennan, J.J.: Interfacial Characterization of Glass and Glass-Ceramic Matrix/Nicalon SiC Fiber Composites, Proc. of the Conf. on Tailoring Multiphase and Composite Ceramics Penn St. Univ. (July 1985). Materials Science Research Vol 20 Plenum Press New York (1986) 549-560.

29. Minford, E.J. and Prewo, K.M.: Fatigue Behavior of SiC Fiber Reinforced LAS Glass-Ceramic, ibid.

30. Prewo, K.M., Brennan, J.J. and Layden, G.K.: Fiber Reinforced Glasses and Glass-Ceramics for High Performance Applications, Am. Cer. Soc. Bull. Vol. 65 No. 2 (Feb 1986).

31. Brennan, J.J.: Interfacial Chemistry and Bonding in Fiber Reinforced Glass and Glass-Ceramic Matrix Composites, Proc. of the Conf. on Ceramic Microstructures '86: Role of Interfaces Univ of Calif Berkeley (July 1986) Materials Science Res Vol. 21 Plenum Press NY (1987) 387-400.

32. Mah, T. Mendiratta, M.G., Katz, A.P., Ruh, R. and Mazdiyasni, K.S.: Room Temperature Mechanical Behavior of Fiber-Reinforced Ceramic-Matrix Composites, J. Am. Cer. Soc. 68 [1] (1985) C-27-30.

33. Cooper, R.F. and Chyung, K.: Structure and Chemistry of Fibre-Matrix Interfaces in SiC Fibre-Reinforced Glass-Ceramic Composites: An Electron Microscopy Study, J. Mat. Sci. 22 (1987) 3148-3160.

34. Fitzer, E. and Gadow, R.: Fiber Reinforced Composites Via the Sol/Gel Route, Materials Sci. Res. Vol. 20 Plenum Press NY (1986) 571-608.

35. Jamet, J., Spann, J.R., Rice, R.W., Lewis, D. and Cobleuz, W.S.: Ceramic-Fiber Composite Processing via Polymer Filled Matrices, Cer. Eng. Sci. Proc. 5 [7-8] (1984) 677-694.

36. Antolin, P.B., Schiroky, G.H., and Andersson, C.A.: Properties of Fiber-Reinforced Alumina Matrix Composites, Presented at 12th Annual Conf. on Composites and Advanced Ceramics Cocoa Beach FL (Jan 1988) (Paper 40-C-88F).

37. Bhatt, R.T.: Mechanical Properties of SiC Fiber-Reinforced Reaction Bonded Si_3N_4 Composites, Mat. Sci. Res. Vol. 20 Tailoring Multiphase and Composite Ceramics Plenum Press NY (1986) 675-686.

38. Warren, J.W.: Fiber and Grain-Reinforced Chemical Vapor Infiltration (CVI) Silicon Carbide Matrix Composites, Ceram. Eng. Sci. Proc. 5 [7-8] (1985) 684-93.

39. Caputo, A.J. and Lackey, W.J.: Fabrication of Fiber-Reinforced Ceramic Composites by Chemical Vapor Infiltration, Ceram. Eng. Sci. Proc. 5 [7-8] (1984) 654-67.

40. Caputo, A.J., Lackey, W.J. and Stinton, D.P.: Development of a New, Faster Process for the Fabrication of Ceramic Fiber-Reinforced Ceramic Composites by Chemical Vapor Infiltration, ibid. 6 [7-8] (1985) 694-706.

41. Naslain, R. and Langlais, F.: CVI-Processing of Ceramic-Ceramic Composite Materials, Conf on Tailoring Multiphase and Composite Ceramics Penn St. Univ (July 1985) Plenum Press NY 145-164.

42. Fitzer, E. and Gadow, R.: Fiber-Reinforced Silicon Carbide, Am. Cer. Soc. Bull. 65 [2] (1986) 326-35.

43. Lamicq, P.J., Bernhart, G.A., Dauchier, M.M. and Mace, J.G.: SiC/SiC Composite Ceramics ibid. 336-38.

44. Stinton, D.P., Caputo, A.J. and Lowden, R.A.: Synthesis of Fiber-Reinforced SiC Composites by Chemical Vapor Infiltration, ibid. 347-50.

45. Capouto, A.J., Stinton, D.P., Lowden, R.A. and Besmann, T.M.: Fiber-Reinforced SiC Composites with Improved Mechanical Properties, Am. Ceram. Soc. Bull. 66 [2] (1987) 368-72.

46. Moeller, H.H., Long, W.G., Caputo, A.J. and Lowden, R.A.: SiC Fiber Reinforced SiC Composites Using Chemical Vapor Infiltration, SAMPE Quart. (April 1986) 1-4.

47. Colmet, R., Lhermitte-Sebire, I. and Naslain, R.: Alumina Fiber/Alumina Matrix Composites Prepared by a CVI Technique, Adv. Cer. Mat. 1 [2] (1986) 185-191.

48. Stinton, D.P., Besmann, T.M. and Lowden, R.A.: Advanced Ceramics by Chemical Vapor Deposition Techniques, Am. Cer. Soc. Bull. 67 [2] (1988) 350-356.

49. Strife, J.R. and Sheehan, J.E.: Ceramic Coatings for Carbon-Carbon Composites, ibid., 369-374.

50. Lowden, R.A. and Stinton, D.P.: Interface Modification in Nicalon/SiC Composites, presented at the 12th Annual Conf. on Composites and Advanced Ceramics Cocoa Beach FL (Jan 1988) (Paper 34-C-88F).

51. Lowden, R.A. (private communication).

52. Brennan, J.J.: Interfacial Characteristics of Glass-Ceramic Matrix/SiC Fiber Composites, Proceedings of Interface Science and Engineering '87 Lake Placid NY (July 1987) (to be published).

53. Brennan, J.J.: The Evaluation of Dow Corning Fibers, Annual Rept R86-917103-12 on Contract F33615-83-C-5006 (Feb. 1986).

TABLE I

RT FLEXURAL STRENGTH (3-PT) OF 1/4 SEGMENTS OF
CVI SIC MATRIX COMPOSITES 7-8-18

Fiber	Condition	Flexural Strength-ksi(MPa)
Nicalon	As-Fabricated	30 (207)
"	1000°C, 120 hrs, O_2	16 (110)
Nextel	As-Fabricated	37 (255)
"	1000°C, 120 hrs, O_2	23 (159)

TABLE II

CVI SIC MATRIX COMPOSITES AND COATED FIBERS

Hydrogen/MDS=3.25/1, 1080°C, Evap. at 1028 mm, Cond. at 11°C
50 cc/min H_2

Run #	Form	SiC Prec.	Fiber	Time	Flush Gas	Comments
4-3-12	Comp	MDS	Nicalon	70hrs	CH_4+H_2	Deliberate PG interfacial layer, SAM found PG, O in coating next to PG, stoich. SiC surface
7-8-18	Comp	MDS	Nicalon	100hrs	Ar	Quite brittle fracture, very thick C interfacial layer found, stoich. SiC surface, some O
7-8-18	Comp	MDS	Nextel 440	100hrs	Ar	Semi-brittle fracture surface, thin C rich interfacial layer, stoich. SiC surface, some O
7-8-18	Comp	MDS	Nextel 440	10hrs	Ar	1000Å C coating on both fibers
7-9-14	Coated Fiber	MDS	Nextel 440	2hrs	Ar	Weakly bonded 2μ thick coating almost pure C under stoich SiC
7-9-15	Coated Fiber	MDS	Nicalon	2hrs	Ar	~ 1μ thick C rich coating
7-10-2	Fiber	None	Nextel 440	2hrs	Ar	Minor C on fiber surface
7-10-6	Fiber	None	Nicalon	2hrs	Ar	Minor C on fiber surface
7-10-22	Coated Fiber	MDS	Nextel 440	2hrs	H_2	Very strong interfacial bond, no C at interface, stoich SiC
7-10-23	Coated Fiber	MDS	Nicalon	2hrs	H_2	Very strong interfacialbond, no C at interface, stoich SiC
8-1-14*	Coated Fiber	MTS	Nextel 440	2hrs	H_2	Weakly bonded coating, thin C interface, silica layer, stoich SiC
8-11-18*	Coated Fiber	MTS	Nextel 440	13/4hrs	Ar	0.5μ coating of almost pure C, plus high C SiC overcoat, weak bond
8-1-15*	Coated Fiber	MTS	Nicalon	2hrs	H_2	Strongly bonded interface, slightly C rich (54%) SiC
8-11-25*	Coated Fiber	MTS	Nicalon	2hrs	Ar	2000Å C interface, high C (69%) SiC coating, weakly bonded

*Hydrogen/MTS = 4.8/1, Condenser at 22°

TABLE III

BULK COMPOSITION OF CVD SIC FROM MDS*

Run #	Flush Gas	Run Time	H_2[1] (cc/min)	H_2[2] (cc/min)	H_2/MDS	Bulk Composition-at% C	Si	O
9-1-28	Ar	4 hrs	10	990	328/1	49	49	2
9-1-26	Ar	4 hrs	50	450	32.8/1	53	45	2
9-1-25	Ar	4 hrs	50	-	3.28/1	53	43	4
9-3-2**	Ar	4 hrs	50	-	1/1	52	46	2

*Substrate temp - 1080°C, evaporator at 1028 mm Hg, condenser at 11°C
**Condenser at 28°C
[1] H_2 through evaporator
[2] H_2 added

TABLE IV

BULK COMPOSITION OF CVD SIC FROM MTS*

Run #	Flush Gas	Run Time	H_2[1] (cc/min)	H_2[2] (cc/min)	H_2/MTS	Bulk Composition-at% C	Bulk Composition-at% Si	Bulk Composition-at% O
9-4-14	Ar	2 hrs	100	-	4.8/1	25	66	9
9-4-14A	H_2	2 hrs	100	-	4.8/1	25	75	-
9-4-18A	Ar	2 hrs	100	900	48/1	48	45	7
9-5-9	H_2	2 hrs	100	900	48/1	47	47	6
9-5-18**	H_2	10 hrs	100	-	1/1	89-94	4-7	2-4

*Substrate temp - 1120°C, evaporator at 992 mm Hg, condenser at 22°C
**Condenser at 50°C

[1] H_2 flow through evaporator
[2] Added H_2

TABLE V

BULK COMPOSITION OF CVD SIC FROM DMDS*

Run #	Flush Gas	Run Time	H_2[1] (cc/min)	H_2[2] (cc/min)	H_2/DMDS	Bulk Composition-at% C	Si	O
12-5-31	Ar	30 min	100	400	38.5/1	28	58	14
12-6-14A	H_2	30 min	100	192	22.5/1	36	56	8
12-6-6B	Ar	30 min	100	-	7.69/1	39	51	10
12-6-7	H_2	30 min	100	-	7.69/1	49	49	2
12-6-16**	Ar	30 min	10	-	1/1	92	3	5

*Substrate temp - 900°C, evaporator at 992 mm Hg, condenser at 22°C
**Condenser at 50°C

[1] H_2 flow through evaporator
[2] Added H_2

TABLE VI

BULK COMPOSITION OF CVD SIC FROM MDS WITH METHANE ADDITIONS

Carrier Gas/MDS Ratio = 3.28/1, 1080°C, 100cc/min
flow rates, 30 min run time

Run Number	Conditions	Bulk Composition-% C	Si	O
12-6-27	H carrier, H flush	55	43	2
12-7-5	CH_4 carrier, H flush	54	42	4
12-7-7A	Ar carrier, H flush + CH_4	54	44	2
12-7-7	Ar carrier, Ar flush + CH_4	55	43	2
12-7-5B	H carrier, Ar flush + CH_4	54	45	1
12-7-5A	H carrier, H flush + CH_4	57	41	2
13-8-3	H carrier except 1120°C	54	46	0
13-8-3A	H carrier, H flush + CH_4 (200 cc/m)	58	39	3
13-8-15	H carrier, H flush + CH_4 (400 cc/m)	51-59	37-45	3
13-8-16	H carrier, H flush + CH_4 (600 cc/m)	56-60	40-44	0

R88-917779-2

FIG. 1

CVD SiC REACTOR

85—199—H

88—9—36—49

SCHEMATIC OF CVD SIC REACTION CHAMBER

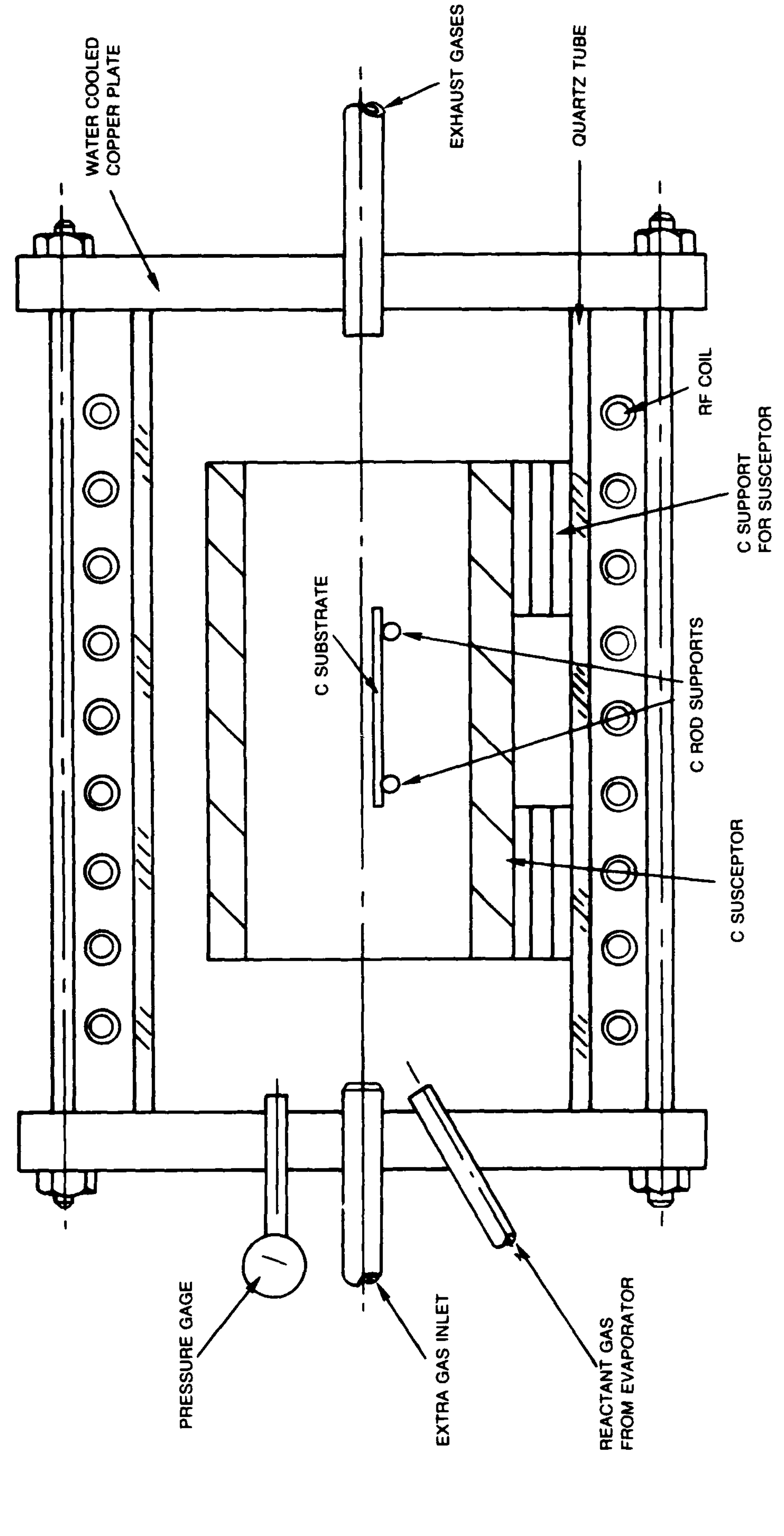

88—9—36—50

FRACTURE SURFACE OF CVI SiC MATRIX/PG/NICALON FIBER COMPOSITE #4-3-12

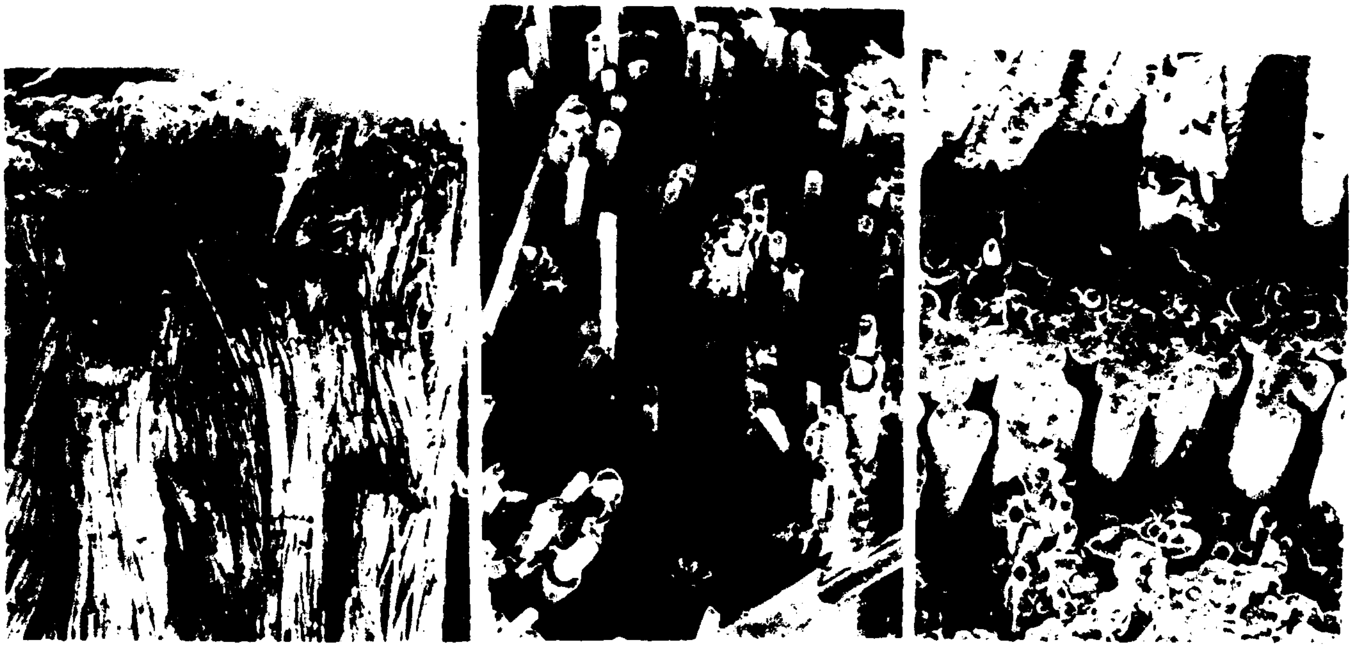

OVERALL FIBROUS REGION 70μm BRITTLE REGION 70μm

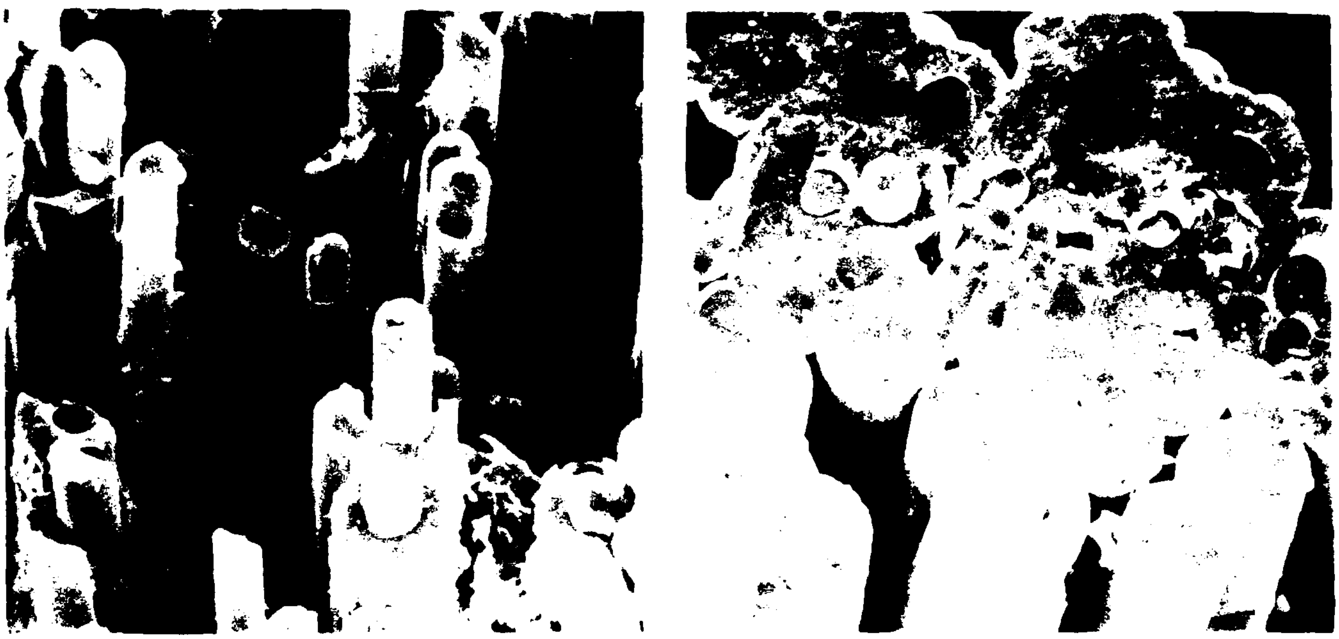

FIBROUS REGION 20μm BRITTLE REGION 20μm

SAM DEPTH PROFILE
INTERFACIAL CHEMISTRY OF CVI SiC MATRIX/PG/NICALON FIBER COMPOSITE #4-3-12
(MDS, Ar FLUSH)

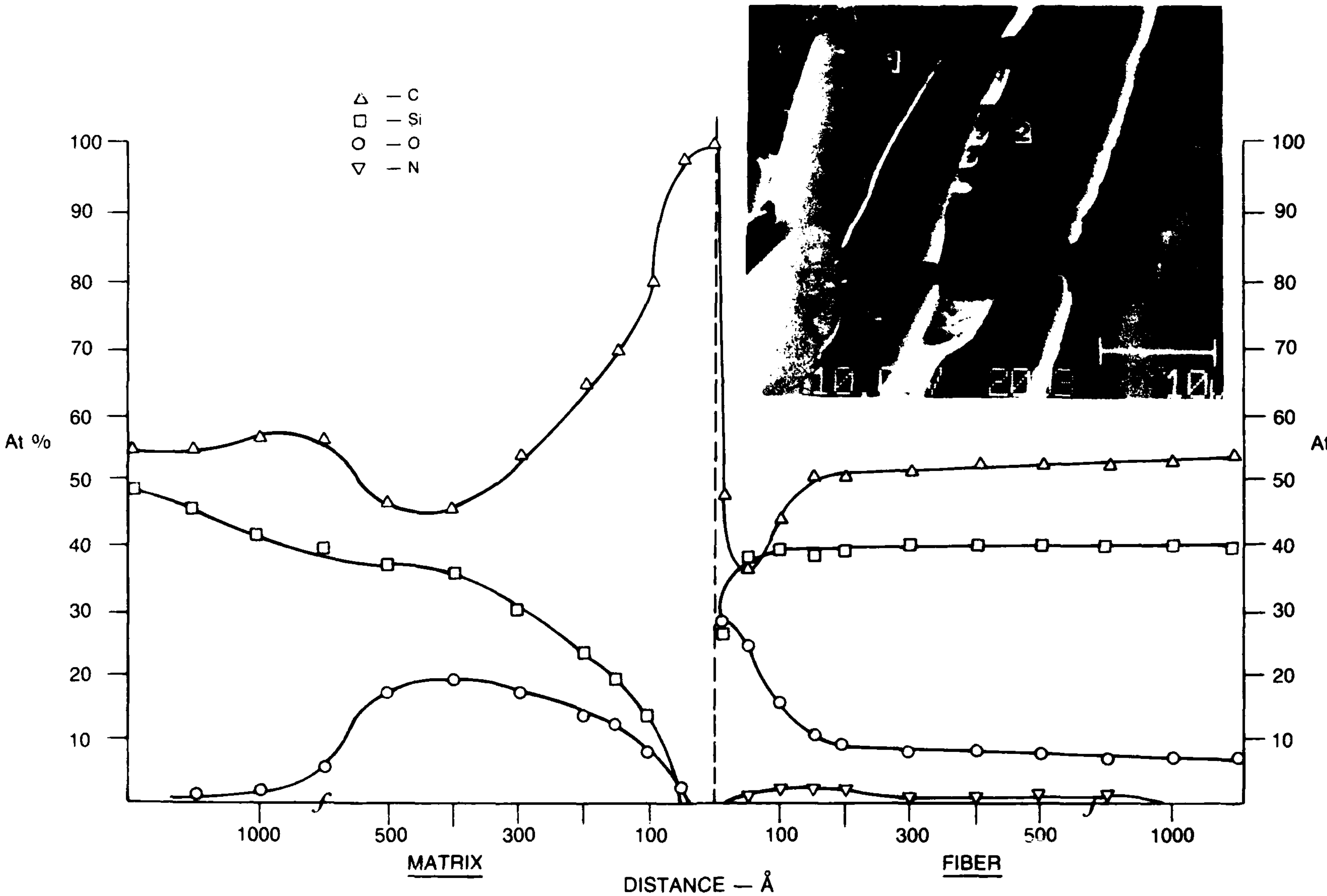

FIG. 4

TEM THIN FOIL CHARACTERIZATION OF CVI SiC MATRIX/PYROLYTIC GRAPHITE COATED NICALON FIBER COMPOSITE — (#4-3-12)

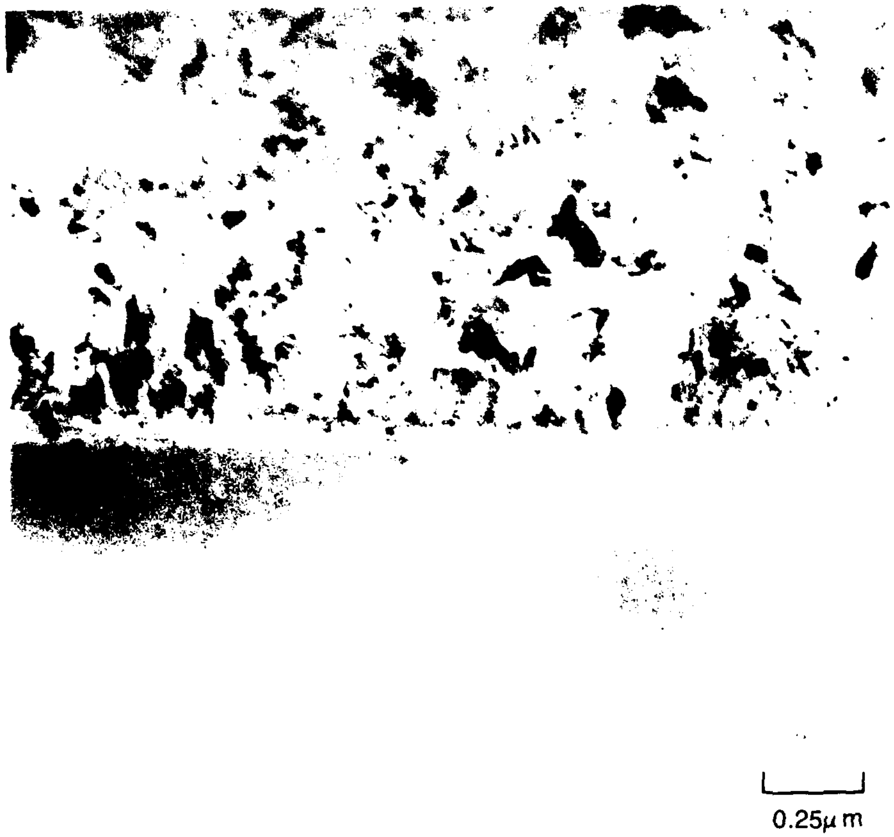

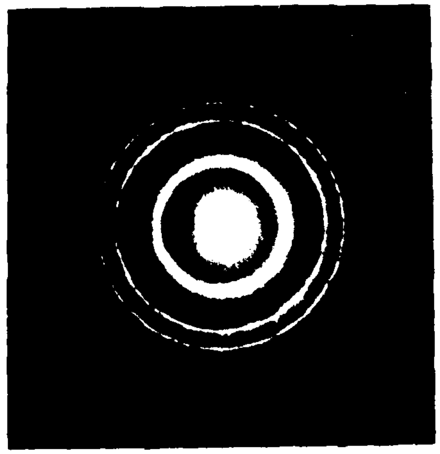

MATRIX

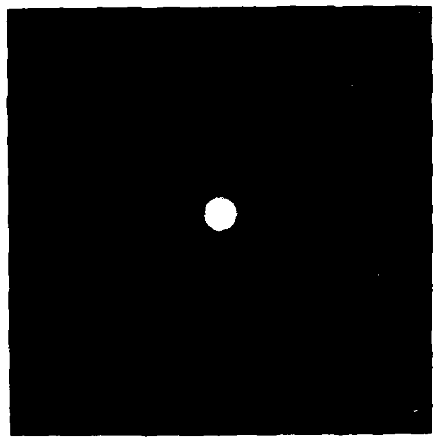

FIBER

FIG. 5

FIG. 6

TEM THIN FOIL CHARACTERIZATION OF CVI SiC MATRIX/PYROLYTIC GRAPHITE COATED NICALON FIBER COMPOSITE — (#4-3-12)

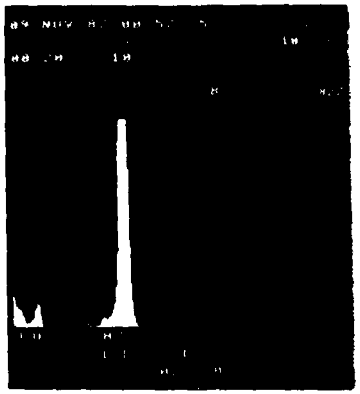

FIBER (a)

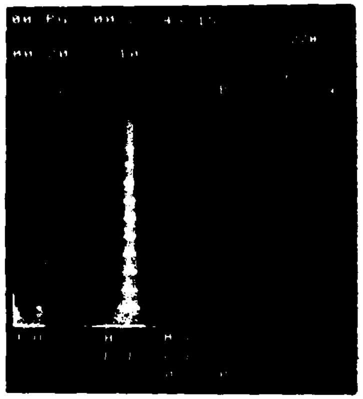

FIBER (b)

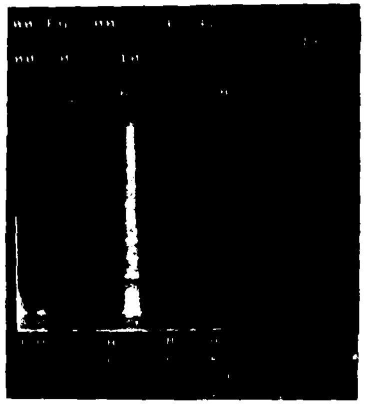

INTERFACE (c)

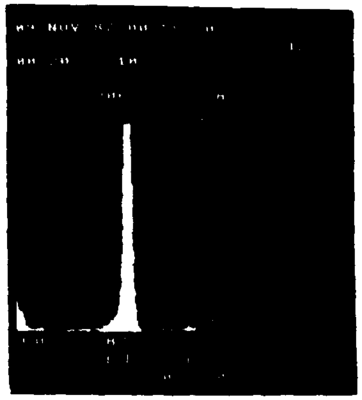

MATRIX (d)

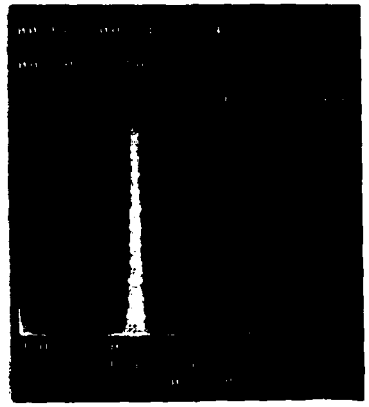

MATRIX (e)

a

88—9—36—4

TEM THIN FOIL CHARACTERIZATION OF CVI SiC MATRIX/PYROLYTIC GRAPHITE COATED NICALON FIBER COMPOSITE (#4-3-12) (POROUS MATRIX REGION)

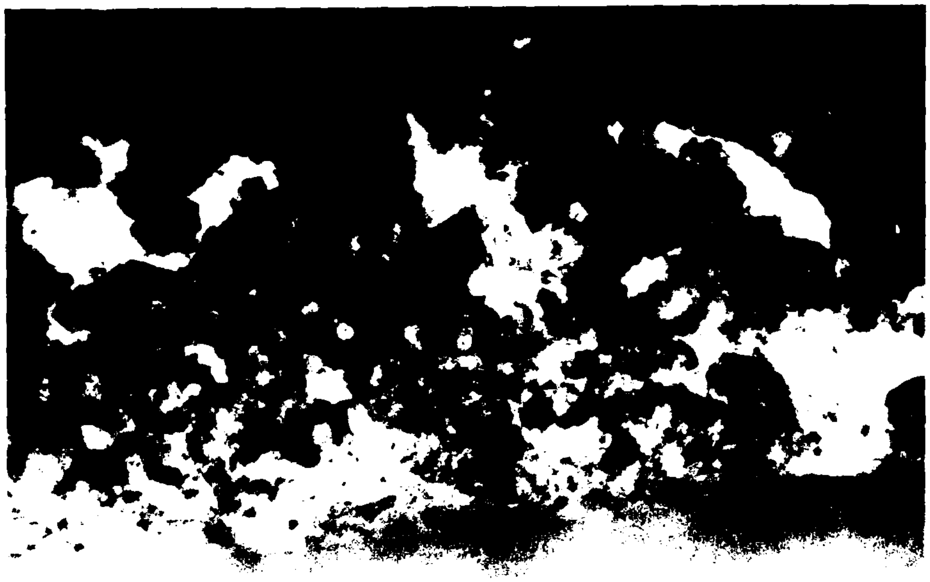

MATRIX

FIBER

0.25μm

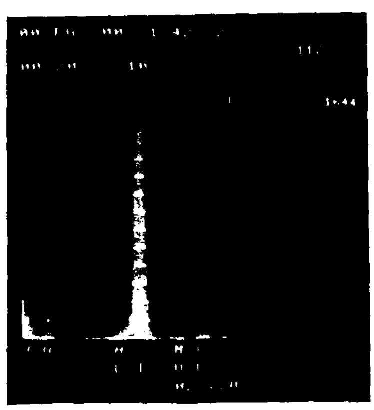

EDS OF POROUS MATRIX

FIG. 8

FRACTURE SURFACE OF ORNL CVI SiC MATRIX/NICALON FIBER COMPOSITE
(RTσ = 13 ksi (90 MPa)]

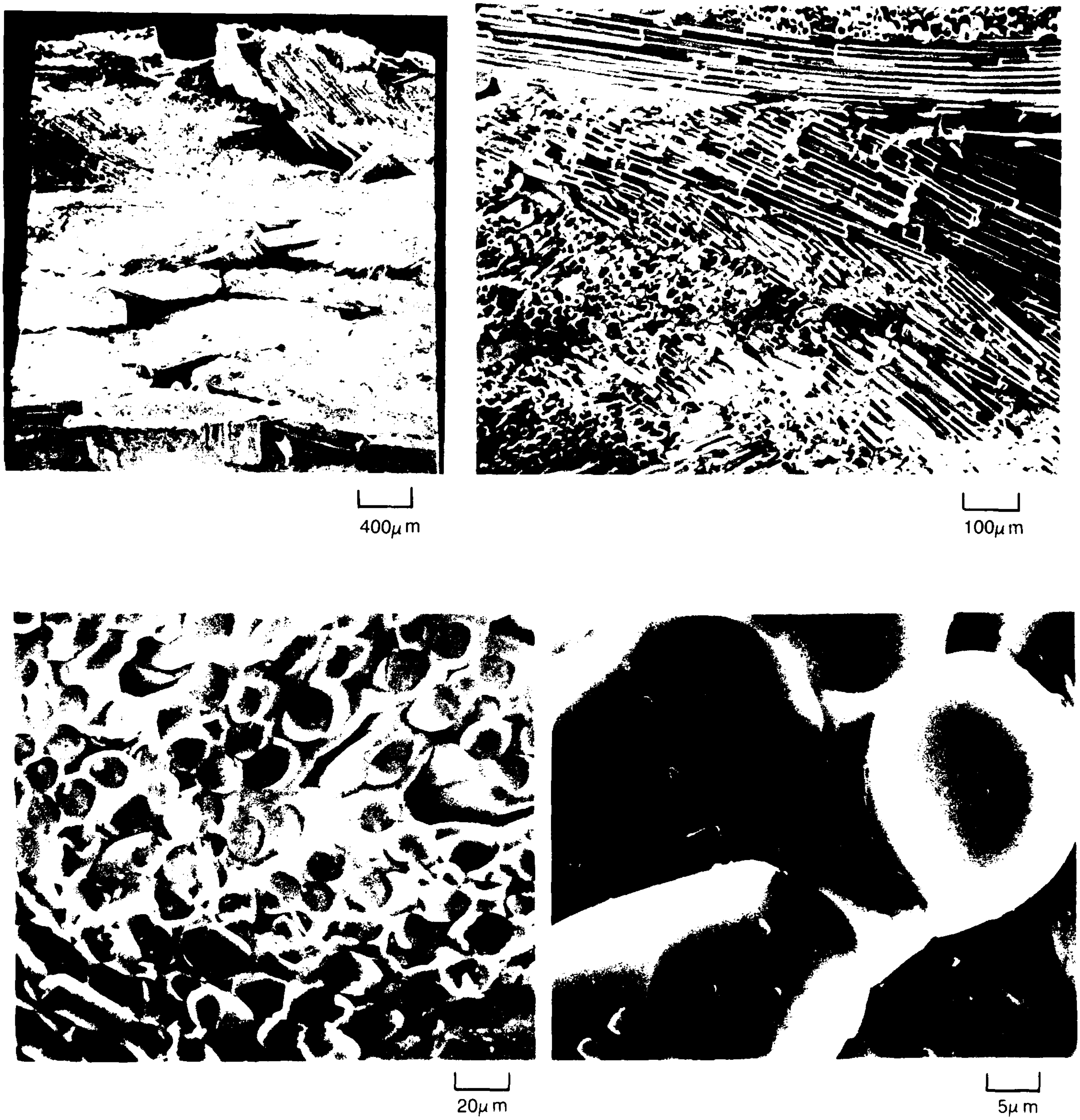

FRACTURE SURFACE OF ORNL CVI SiC MATRIX/CARBON COATED NICALON FIBER COMPOSITE [RT$\sigma\approx$55 ksi (380 MPa)]

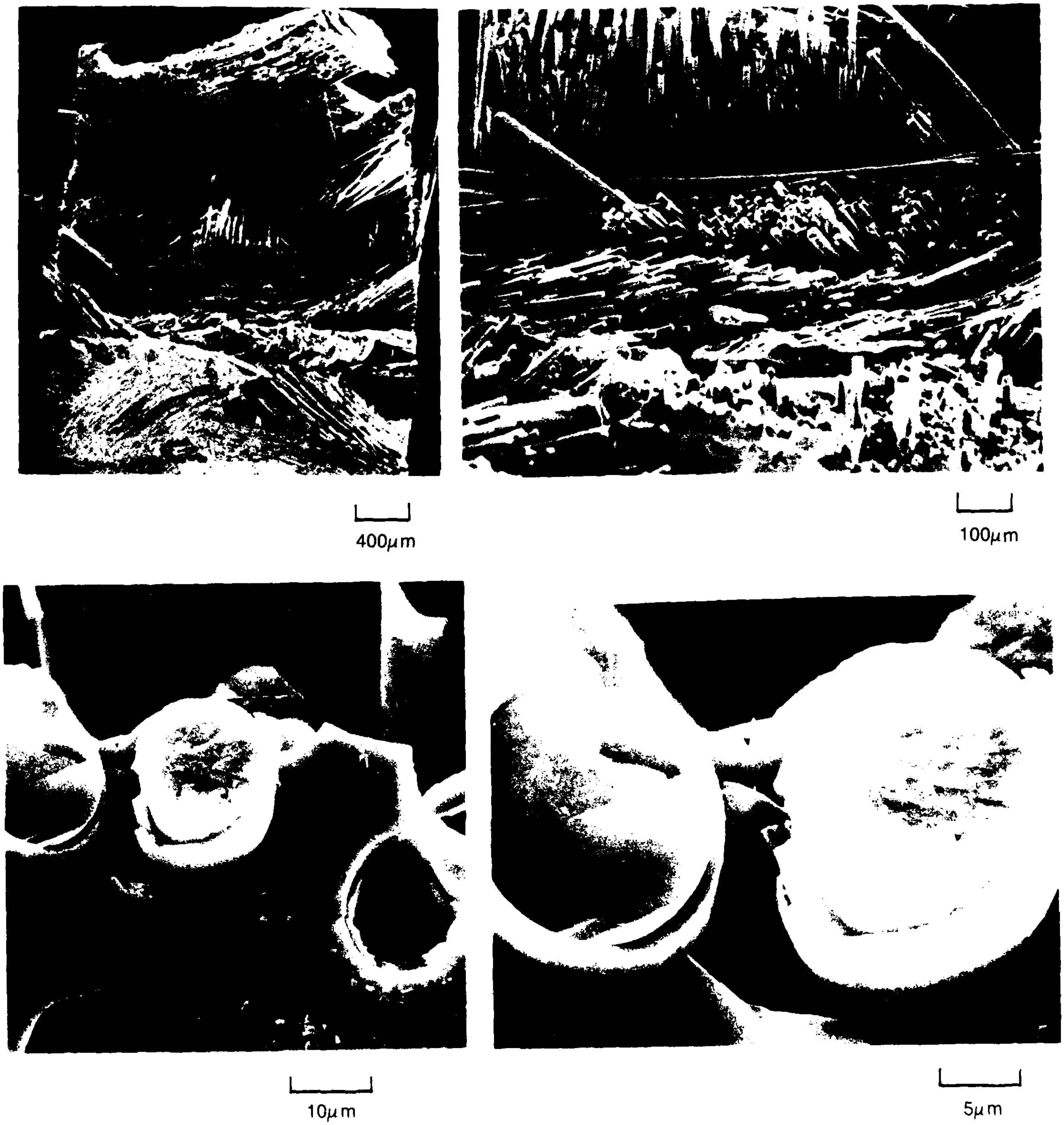

88—9—36—7

FIG. 10

FRACTURE SURFACE OF ORNL CVI SiC MATRIX/CARBON COATED NICALON FIBER COMPOSITE [OXIDIZED 1000°C, 70 hrs — RTσ = 11.2 ksi (77 MPa)]

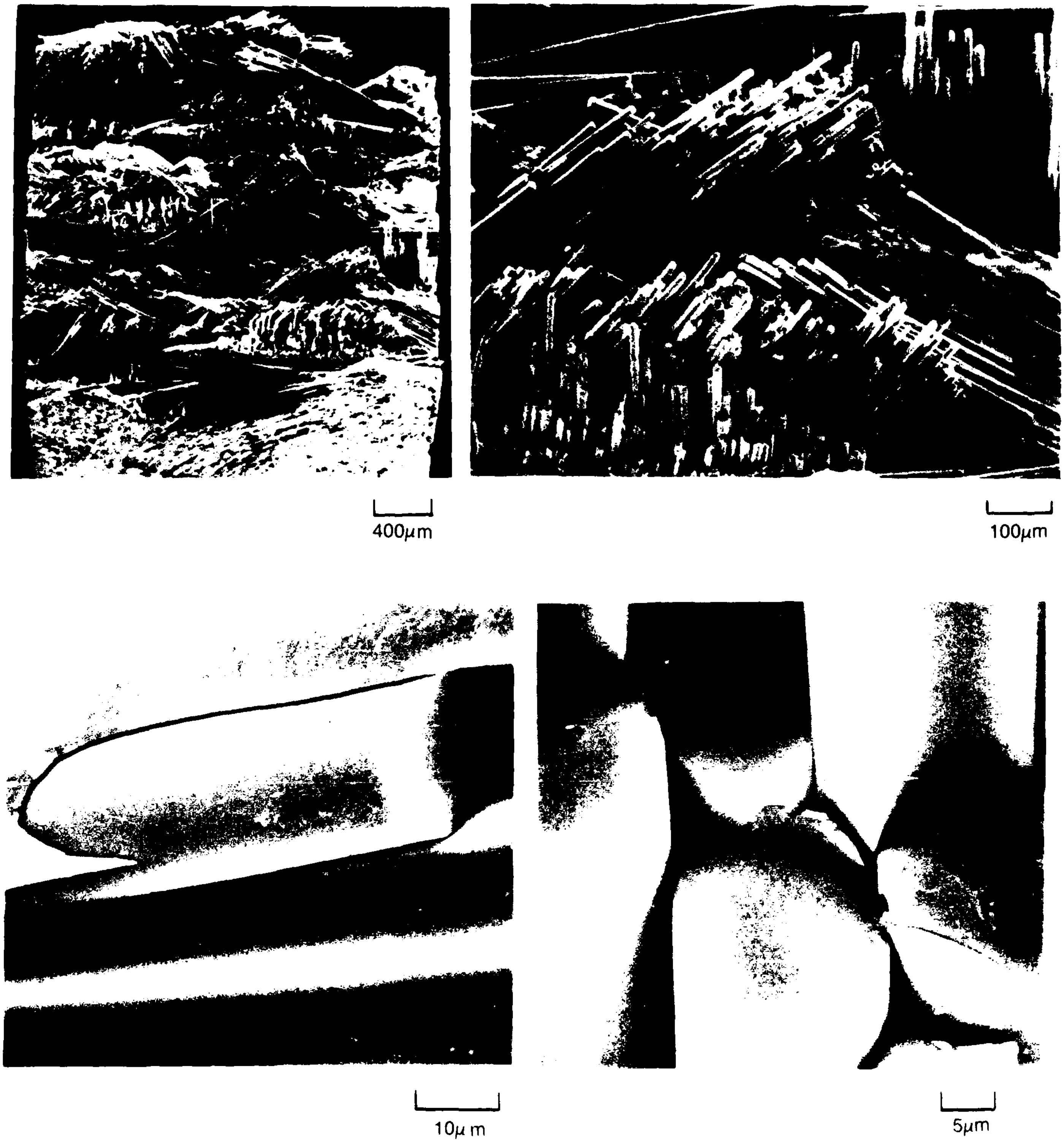

FRACTURE SURFACE OF CVI SiC MATRIX/NICALON FIBER COMPOSITE #7-8-18 (Ar FLUSH)

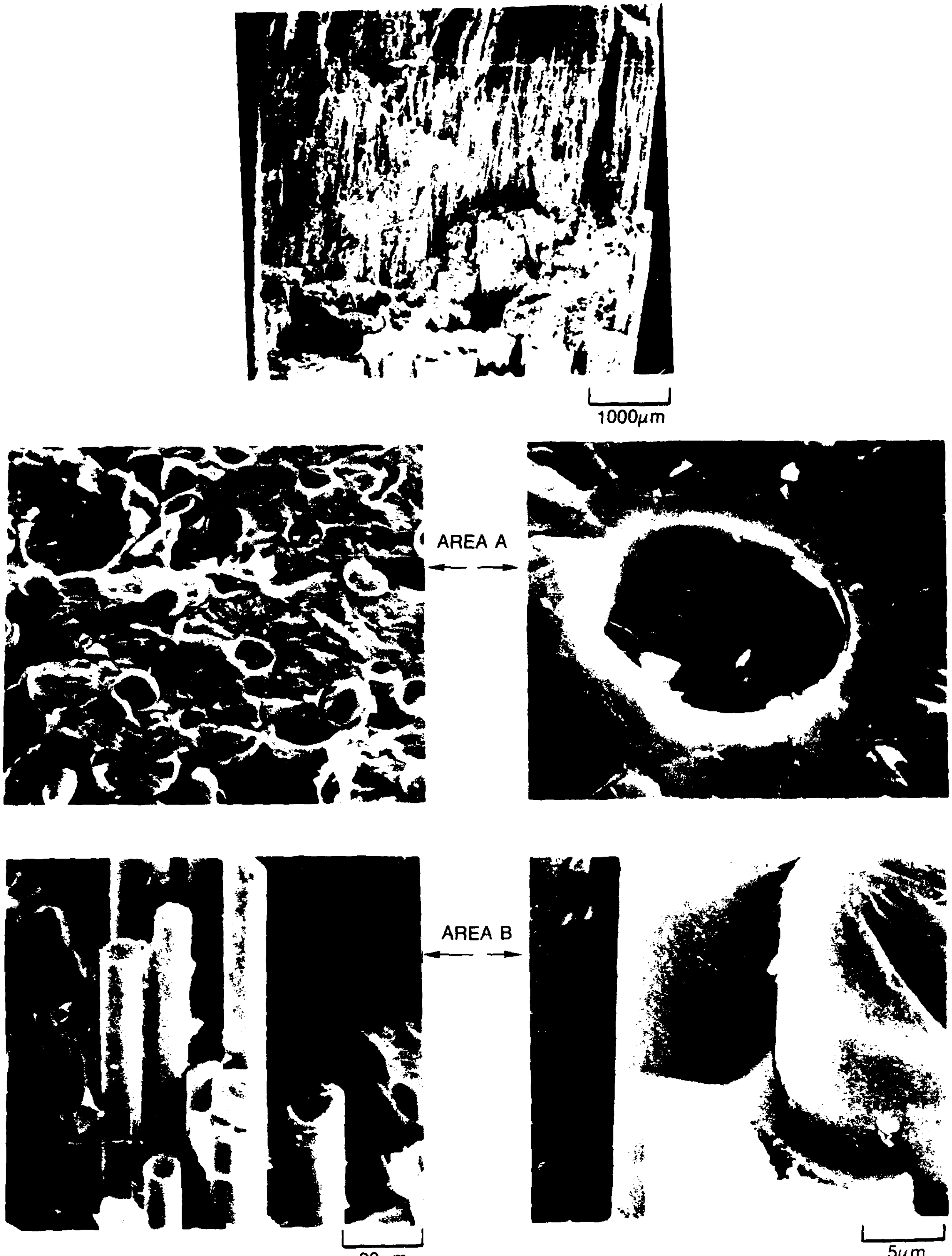

88—9—36—13

FIG. 12

CROSS-SECTION OF CVI SiC/NICALON FIBER COMPOSITE #7-8-18

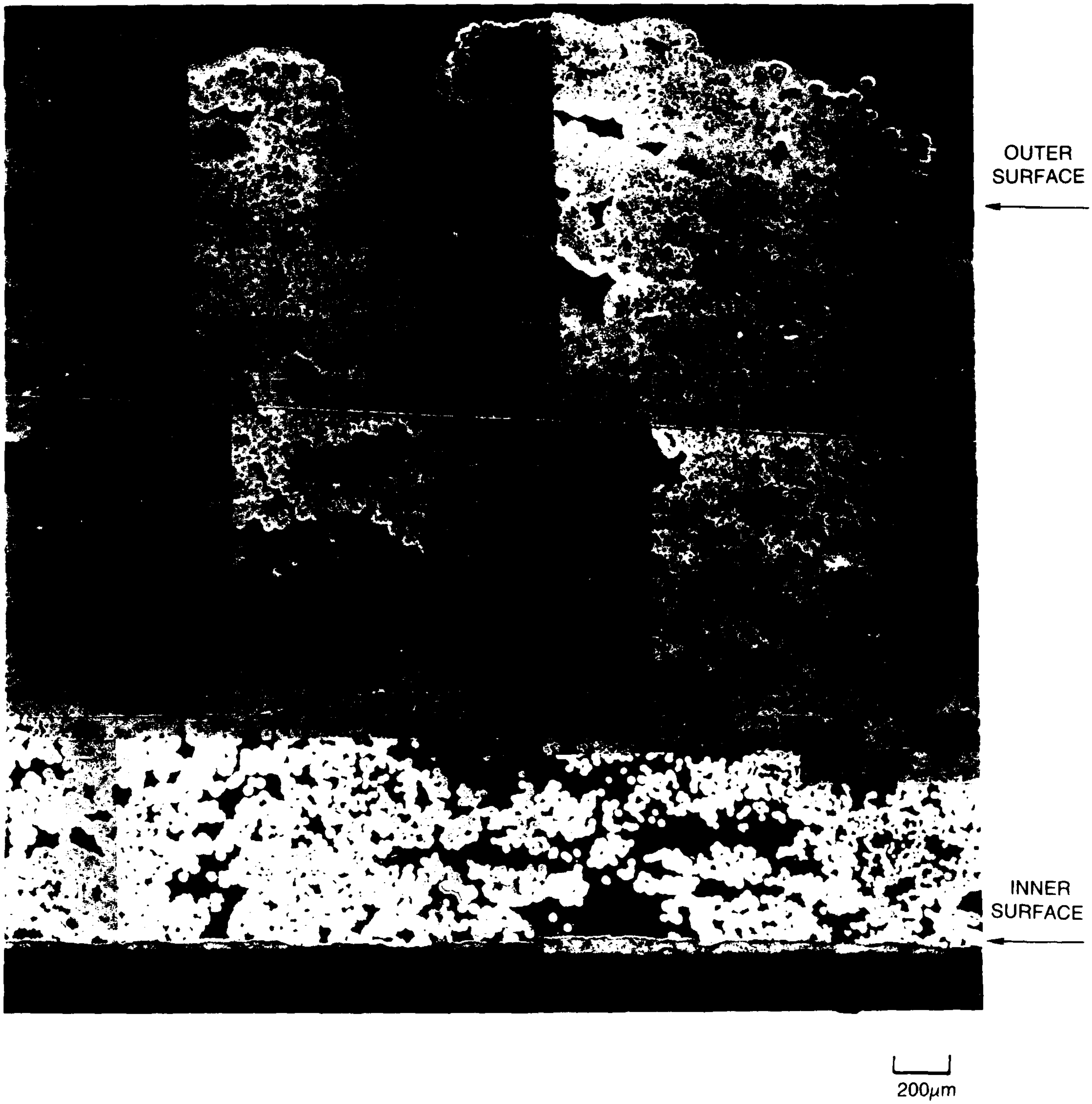

EDS ANALYSIS OF FIBER/MATRIX INTERFACIAL AREA NEAR OUTER SURFACE OF CVI SiC/NICALON FIBER COMPOSITE #7-8-18

20μm
(BSI)

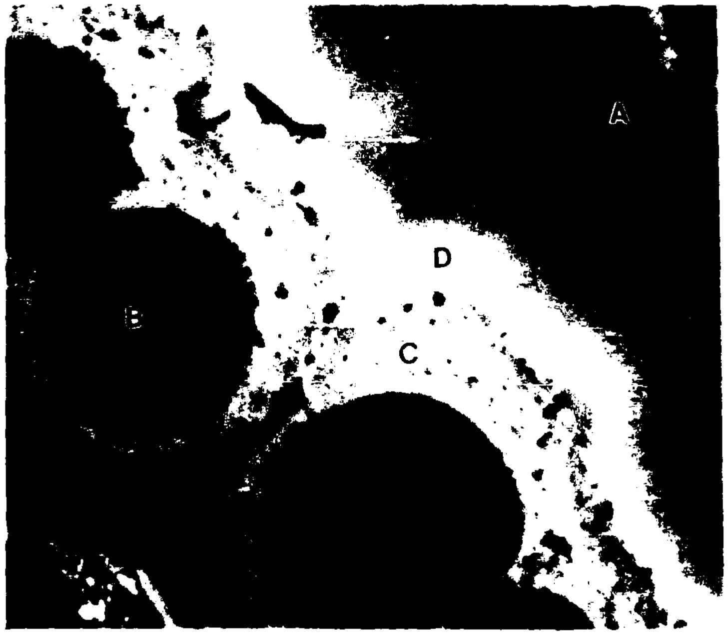

5μm
(BSI)

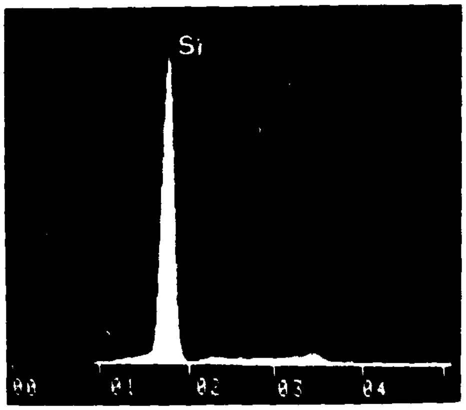

AREA A

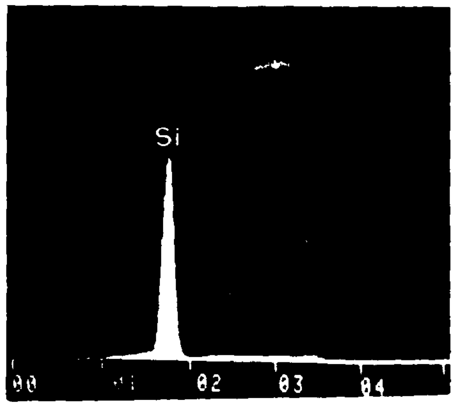

AREA B

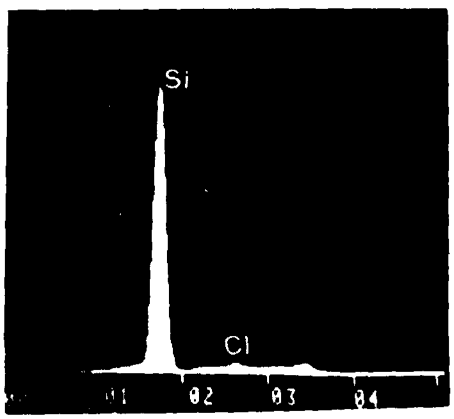

AREA C

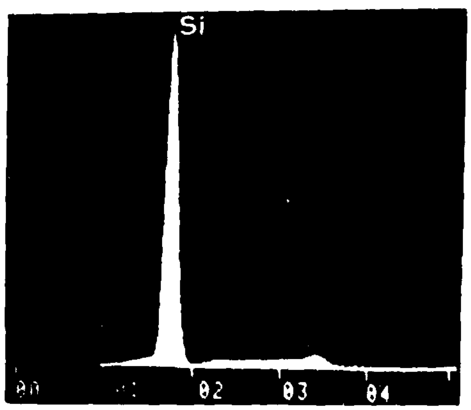

AREA D

88—9—36—11

SAM DEPTH PROFILE
INTERFACIAL CHEMISTRY OF CVI SiC/NICALON SiC FIBER COMPOSITE #7-8-18
(Ar FLUSH)

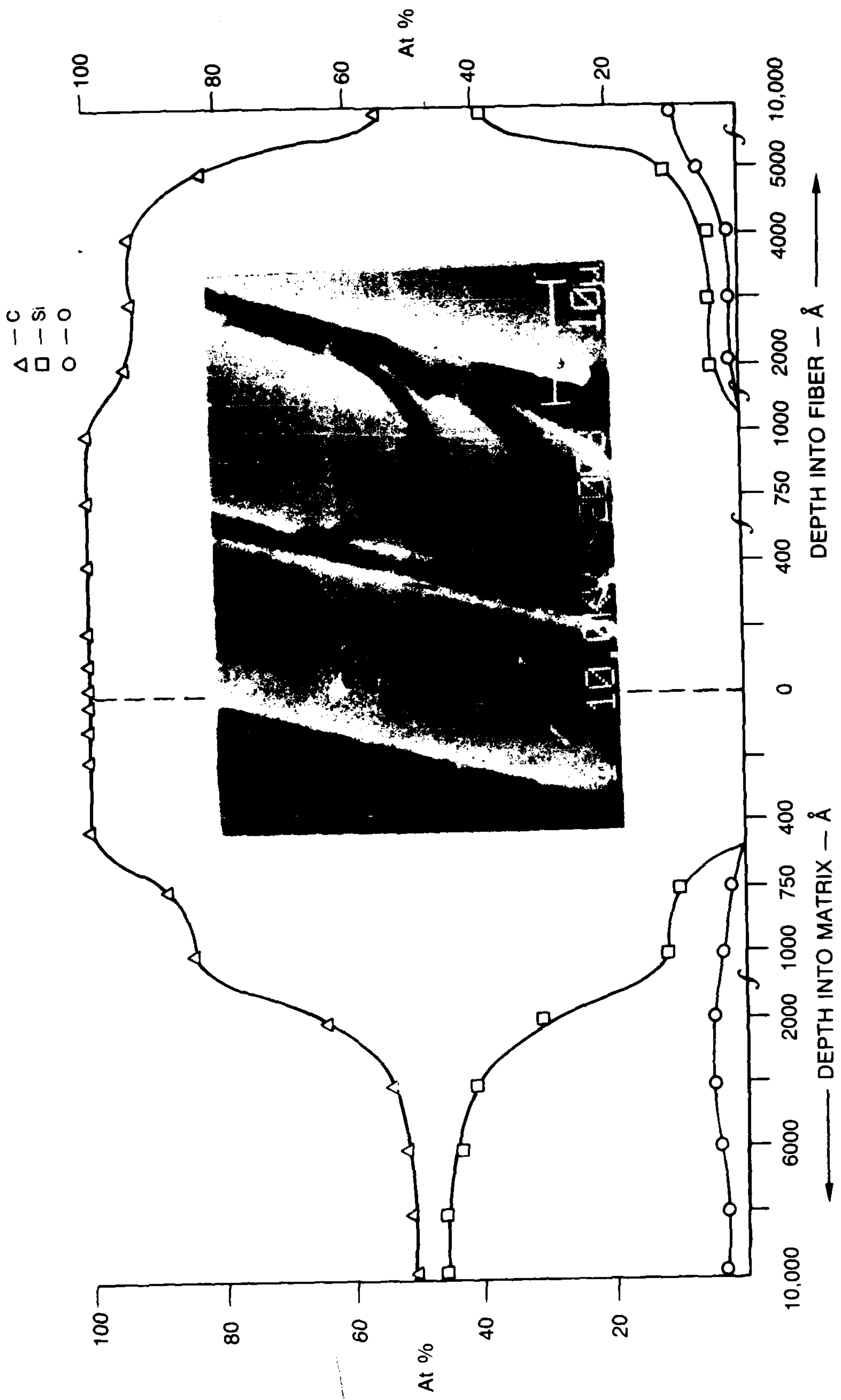

88—9—36—12

FRACTURE SURFACE OF CVI SiC MATRIX/NEXTEL 440 FIBER COMPOSITE #7-8-18 (Ar FLUSH)

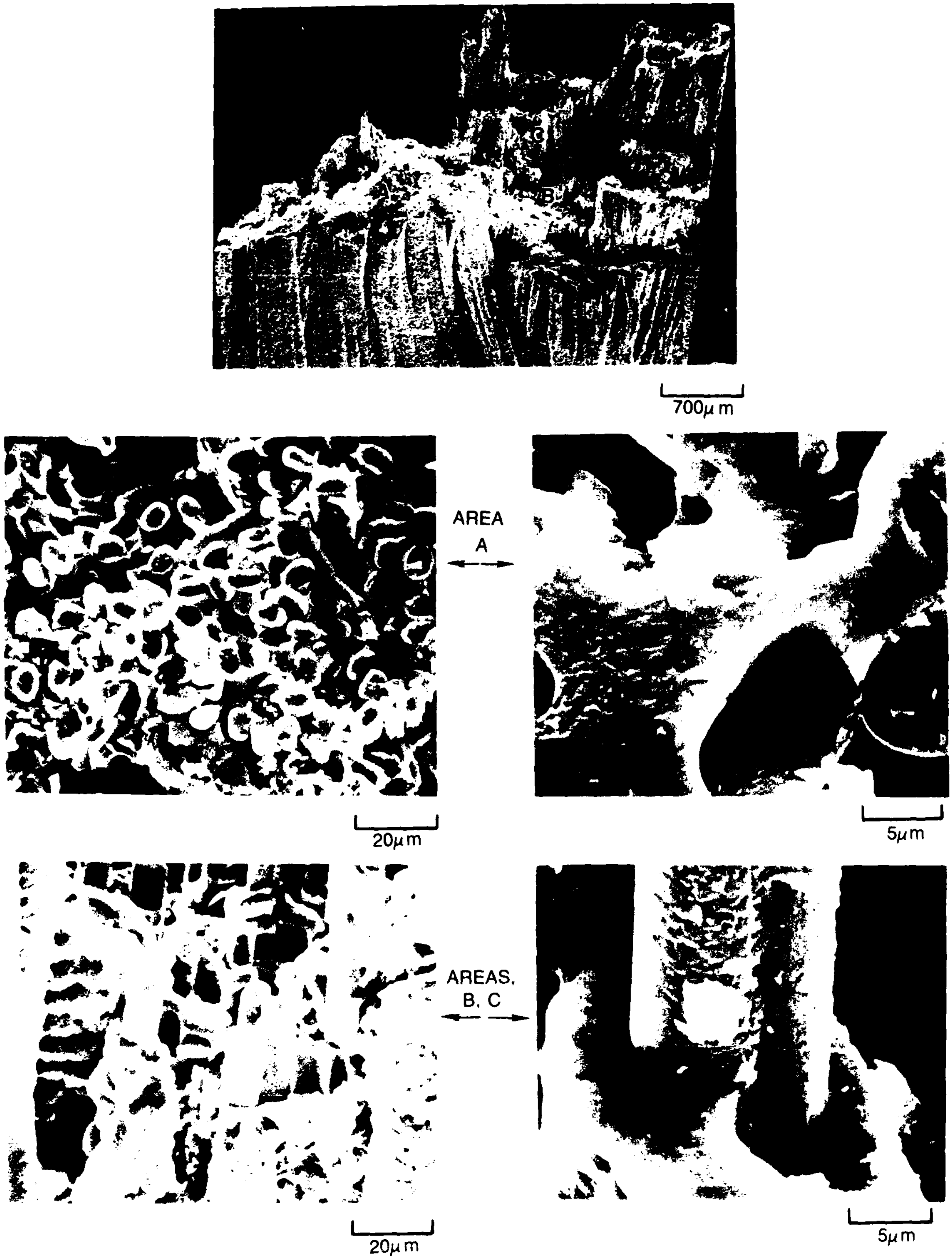

88—9—36—9

CROSS-SECTION OF CVI SiC/NEXTEL 440 FIBER COMPOSITE #7-8-18

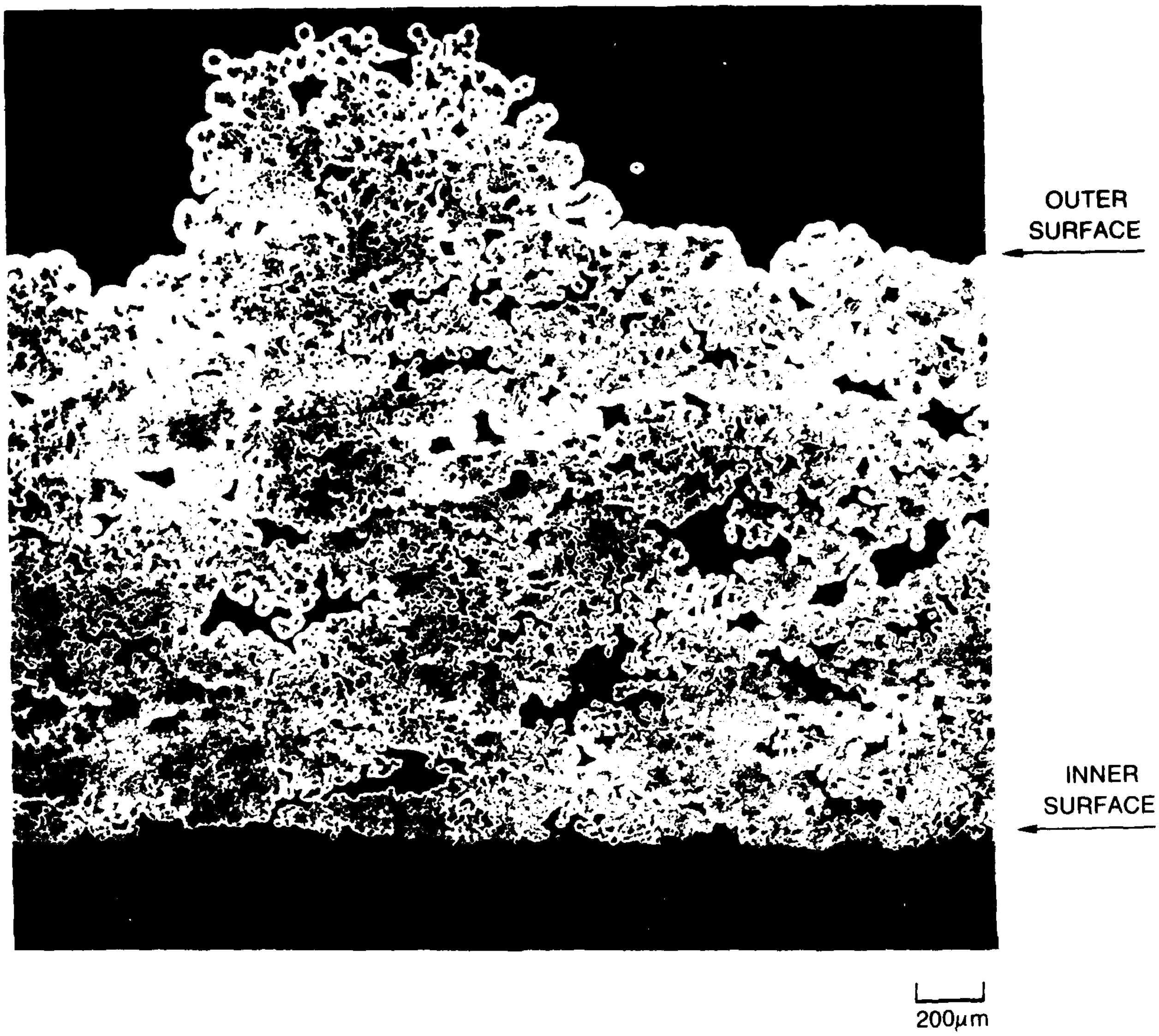

CROSS-SECTION OF CVI SiC/NEXTEL 440 FIBER COMPOSITE (#7-8-18) NEAR OUTER SURFACE

20μm

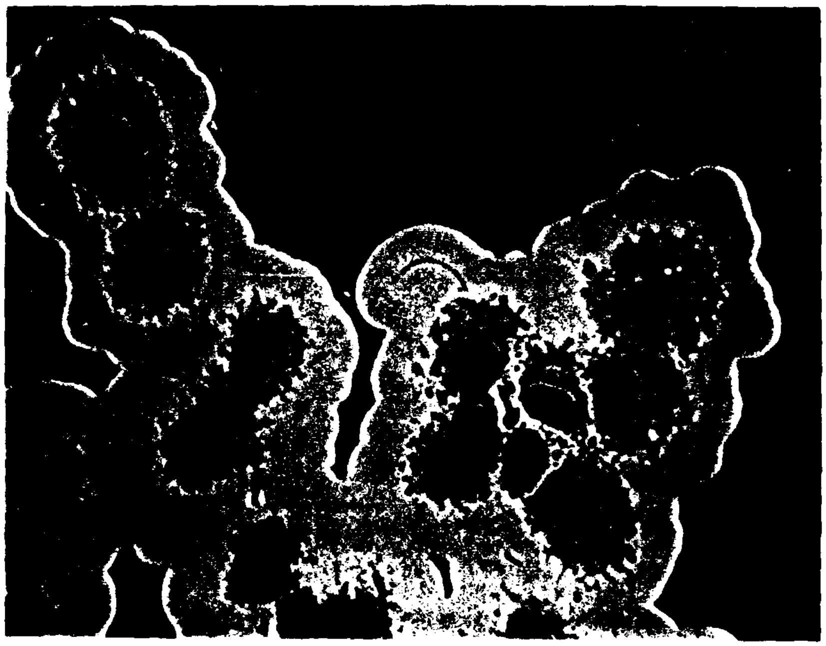

(BACKSCATTERED ELECTRON IMAGE)

88—9—36—15

EDS ANALYSIS OF FIBER/MATRIX INTERFACIAL AREA NEAR OUTER SURFACE OF CVI SiC/NEXTEL FIBER COMPOSITE #7-8-18

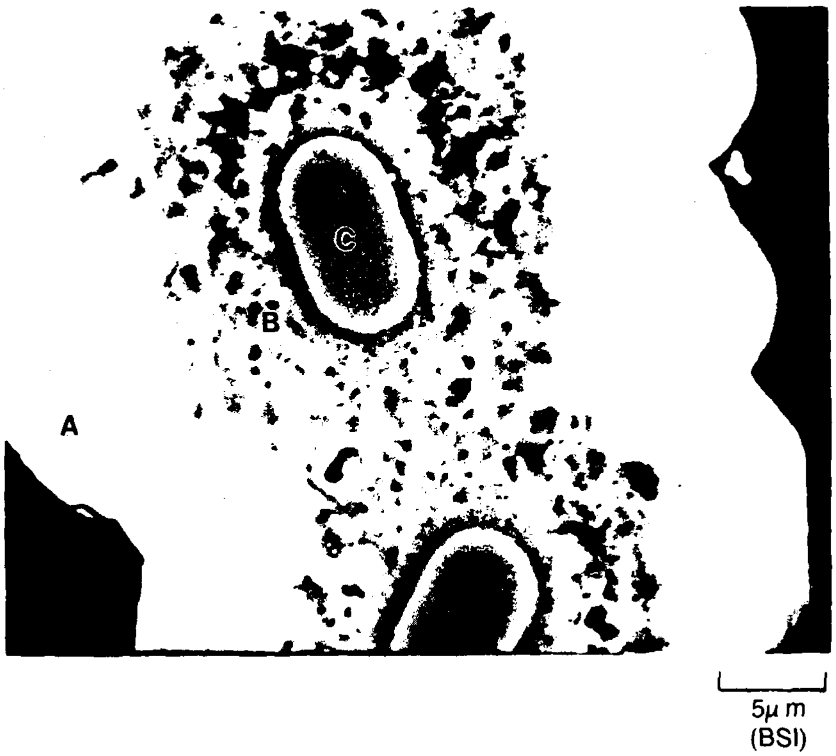

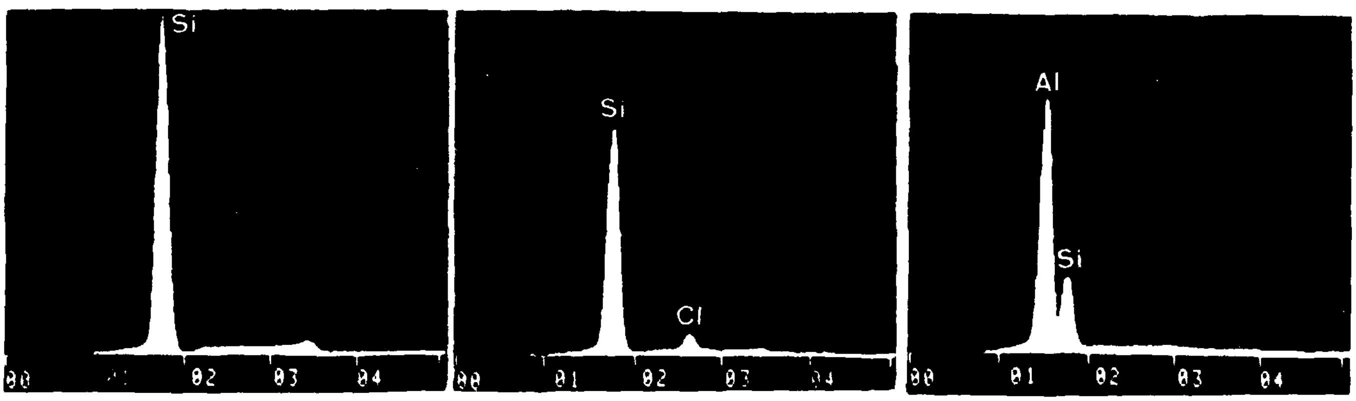

AREA A AREA B AREA C

SAM DEPTH PROFILE
INTERFACIAL CHEMISTRY OF CVI SiC/NEXTEL 440 FIBER COMPOSITE #7-8-18
(Ar FLUSH)

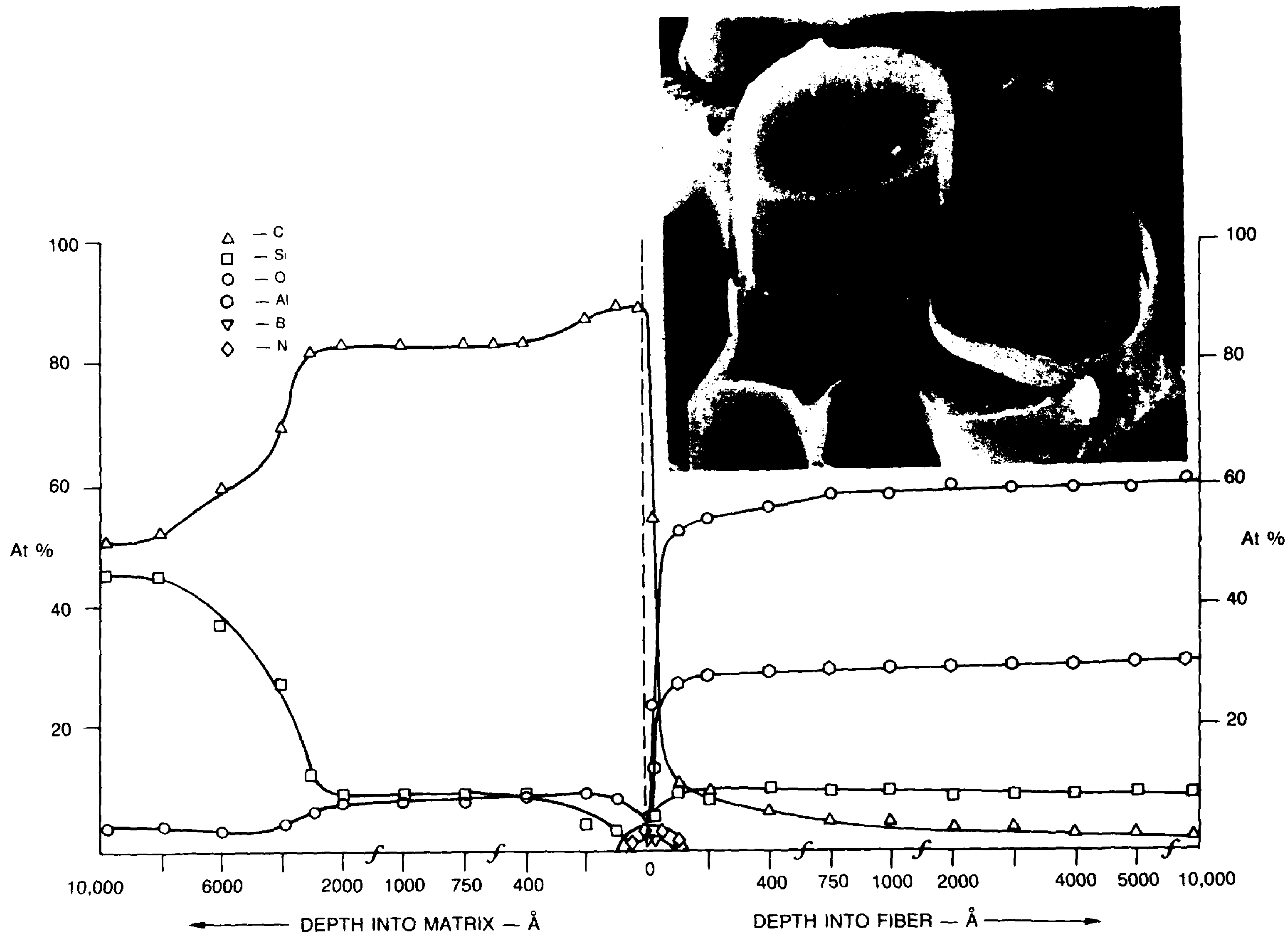

88-9-36-17

FIG. 19

SAM DEPTH PROFILE
CVD SiC ON NEXTEL 440 FIBER, (#7-8-18), (SMOOTH FIBER, Pt #1) MDS, 10 hrs, Ar FLUSH

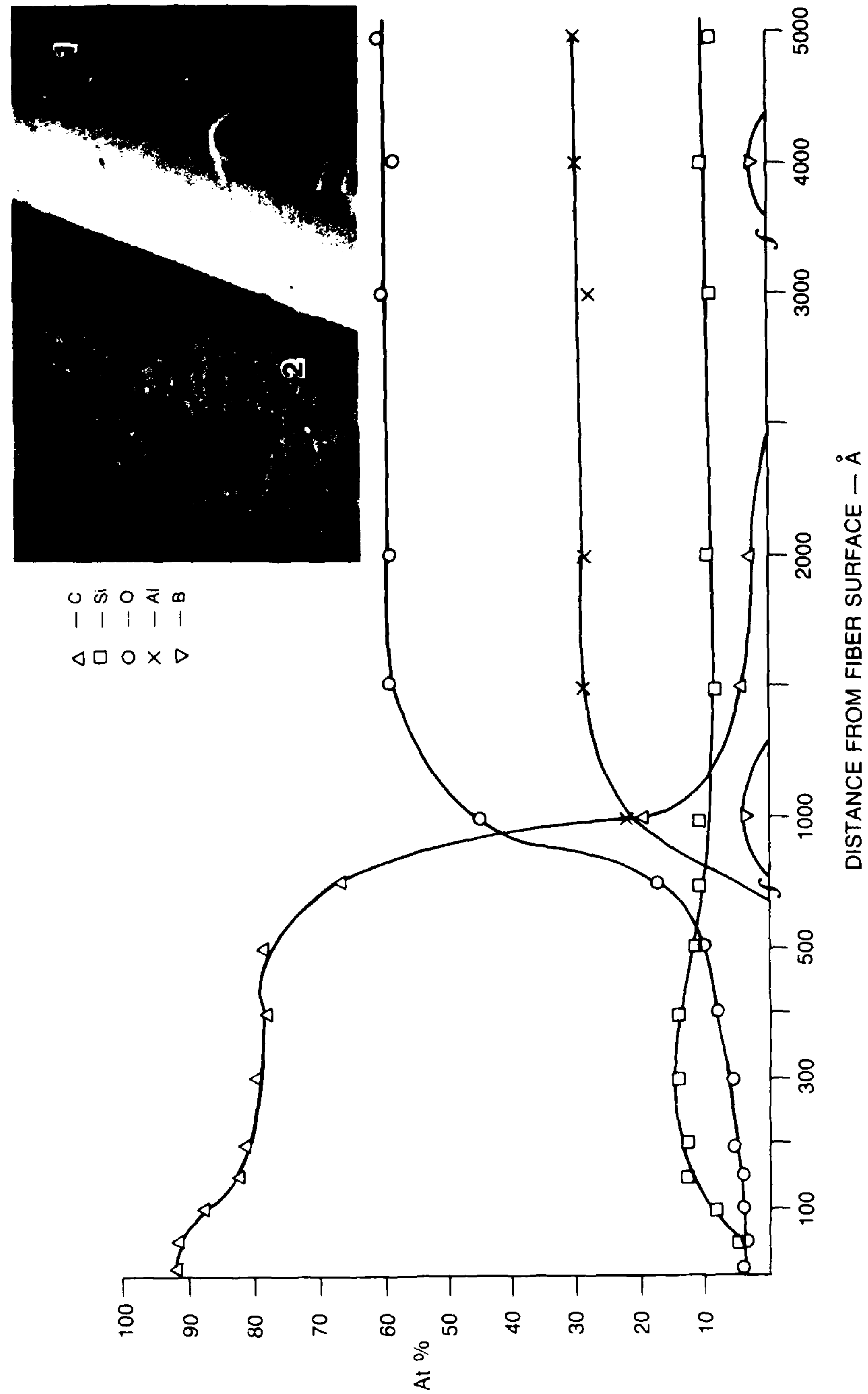

88—9—36—18

SAM DEPTH PROFILE
CVD SiC ON NEXTEL 440 FIBER, (#7-8-18), (ROUGH FIBER, Pt2) MDS, 10 hrs, Ar FLUSH

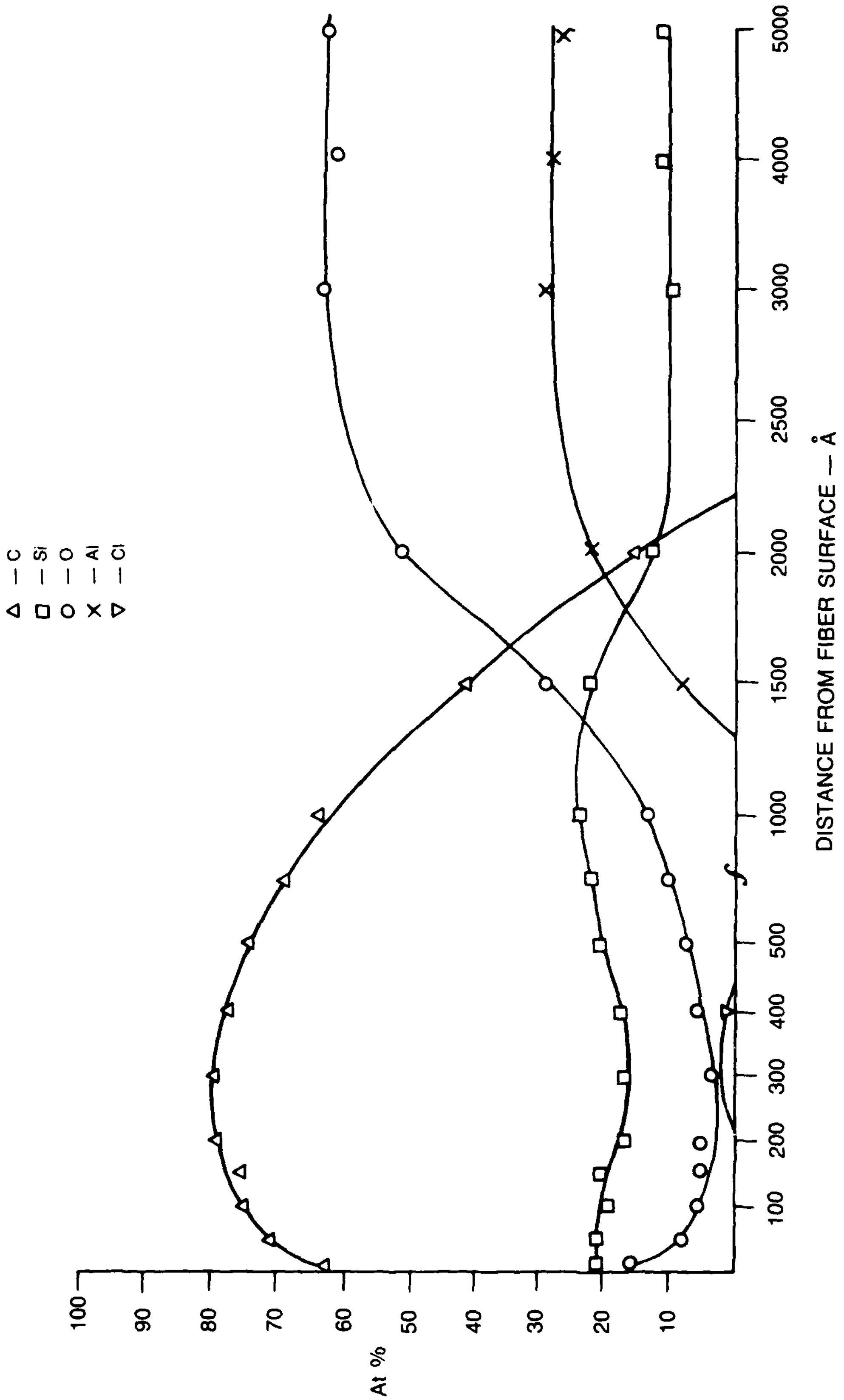

88—9—36—19

SEM OF CVD SiC ON NEXTEL 440 FIBERS (#7-9-14) (MDS, 2 hrs, Ar FLUSH)

10μm

1μm

88—9—36—

SAM DEPTH PROFILE
CVD SiC ON NEXTEL 440 FIBER — (#7-9-18) — FIBER SURFACE UNDER COATING (Pt #2)

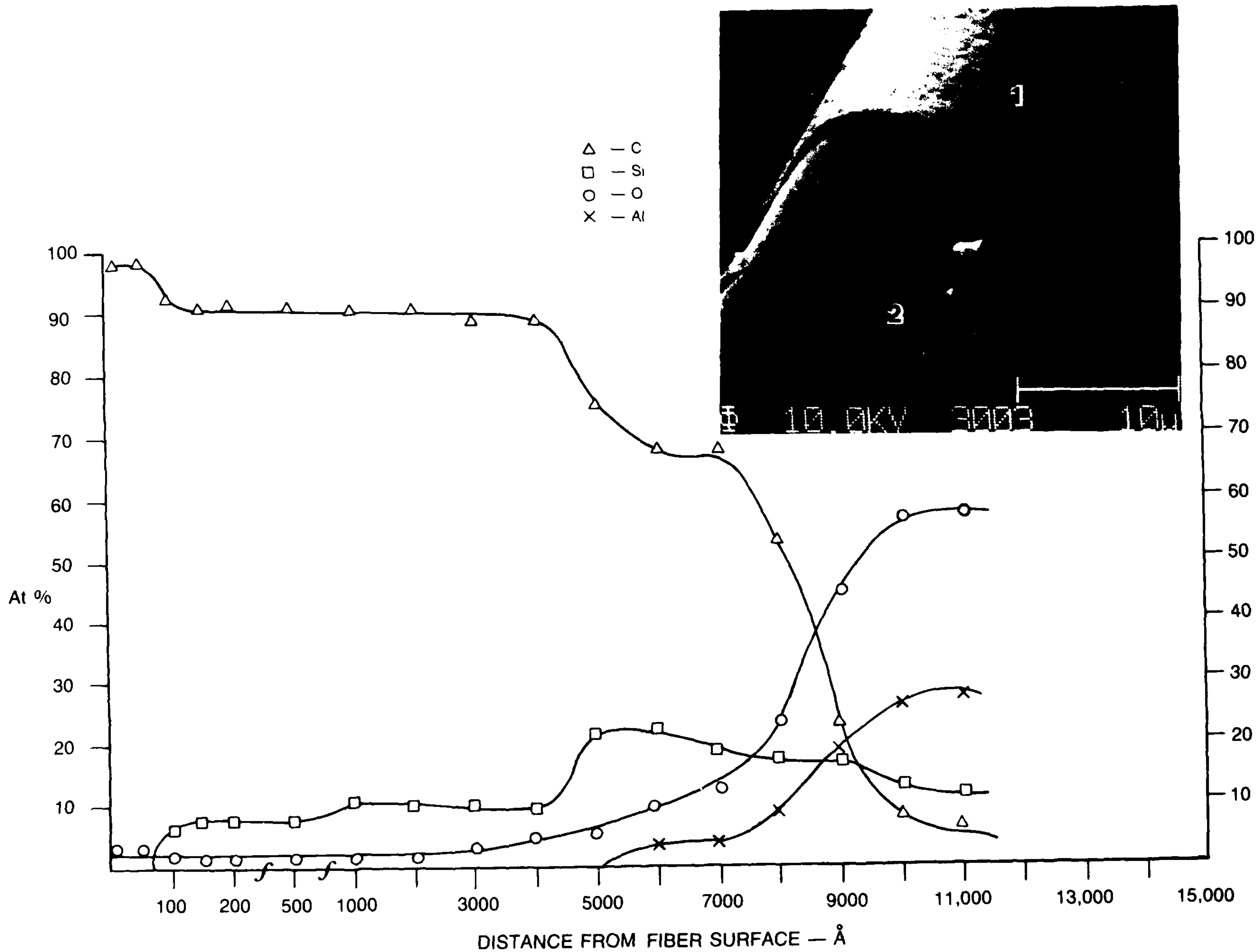

SAM DEPTH PROFILE
CVD SiC ON NEXTEL 440 FIBER (#7-9-14) — SiC SURFACE (Pt #1)

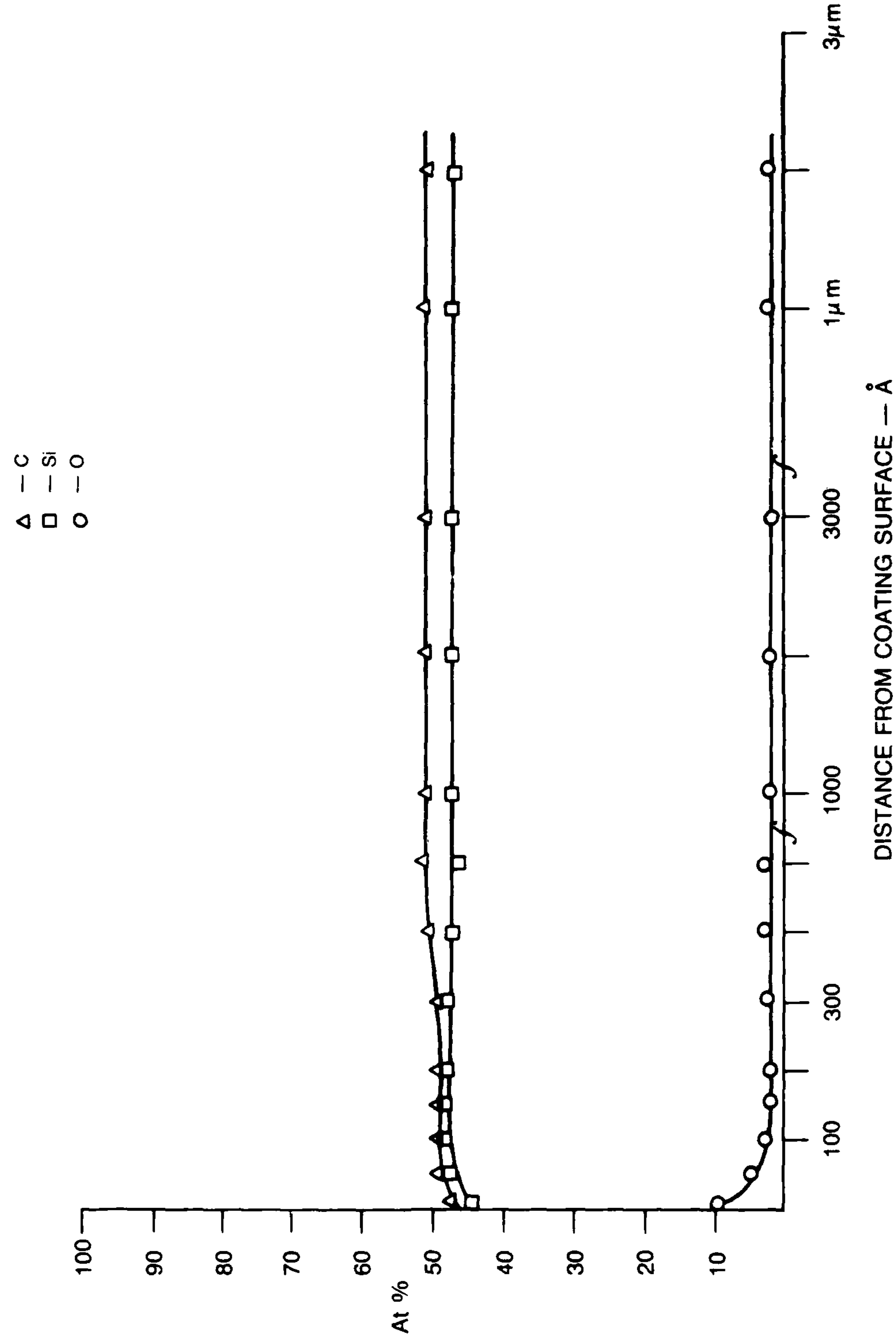

88—9—36—22

SEM OF CVD SiC ON NICALON FIBERS (#7-9-15) (MDS, 2 hrs, Ar FLUSH)

SAM DEPTH PROFILE
CVD SiC ON NICALON FIBERS — #7-9-15 (MDS, 2 hrs, Ar FLUSH)

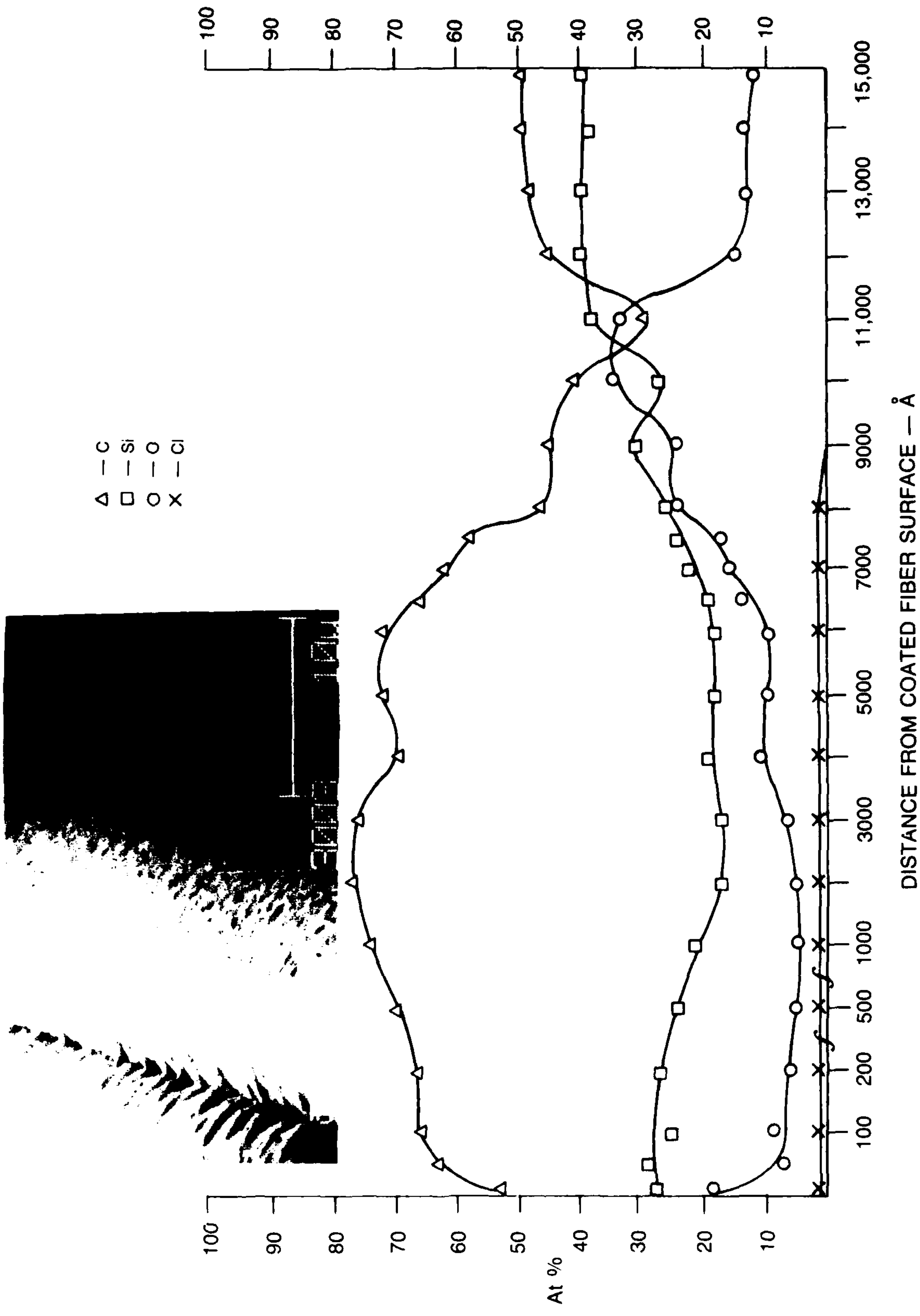

FIG. 27

TEM/SAED CHARACTERIZATION OF CVD SiC ON NICALON FIBERS — (#7-9-15)
(MDS, 2 hrs, Ar FLUSH)

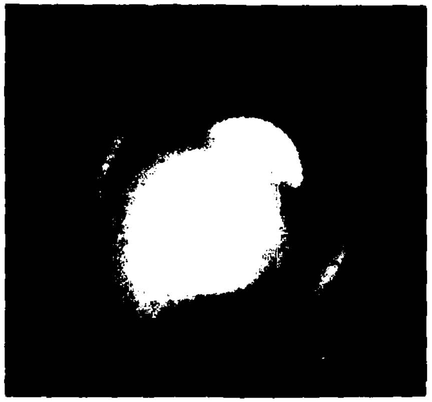

CARBON INTERFACE

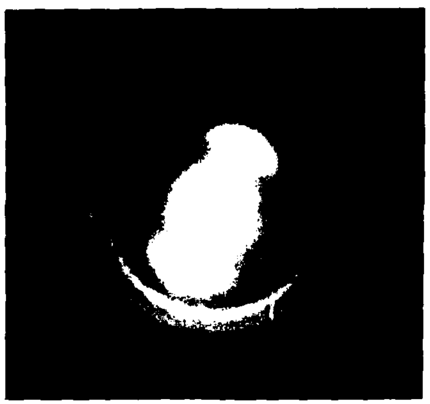

CARBON FILM +
SiC COATING

NICALON FIBER

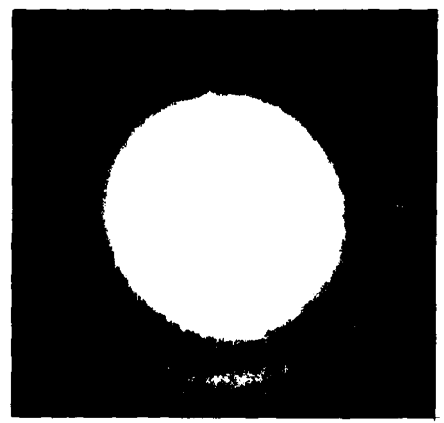

FIBER

88—9—36—25

SAM DEPTH PROFILE
NEXTEL 440 FIBER, NO COATING, 2 hrs, 1080°C, Ar, IN CVD CHAMBER (#7-10-2)

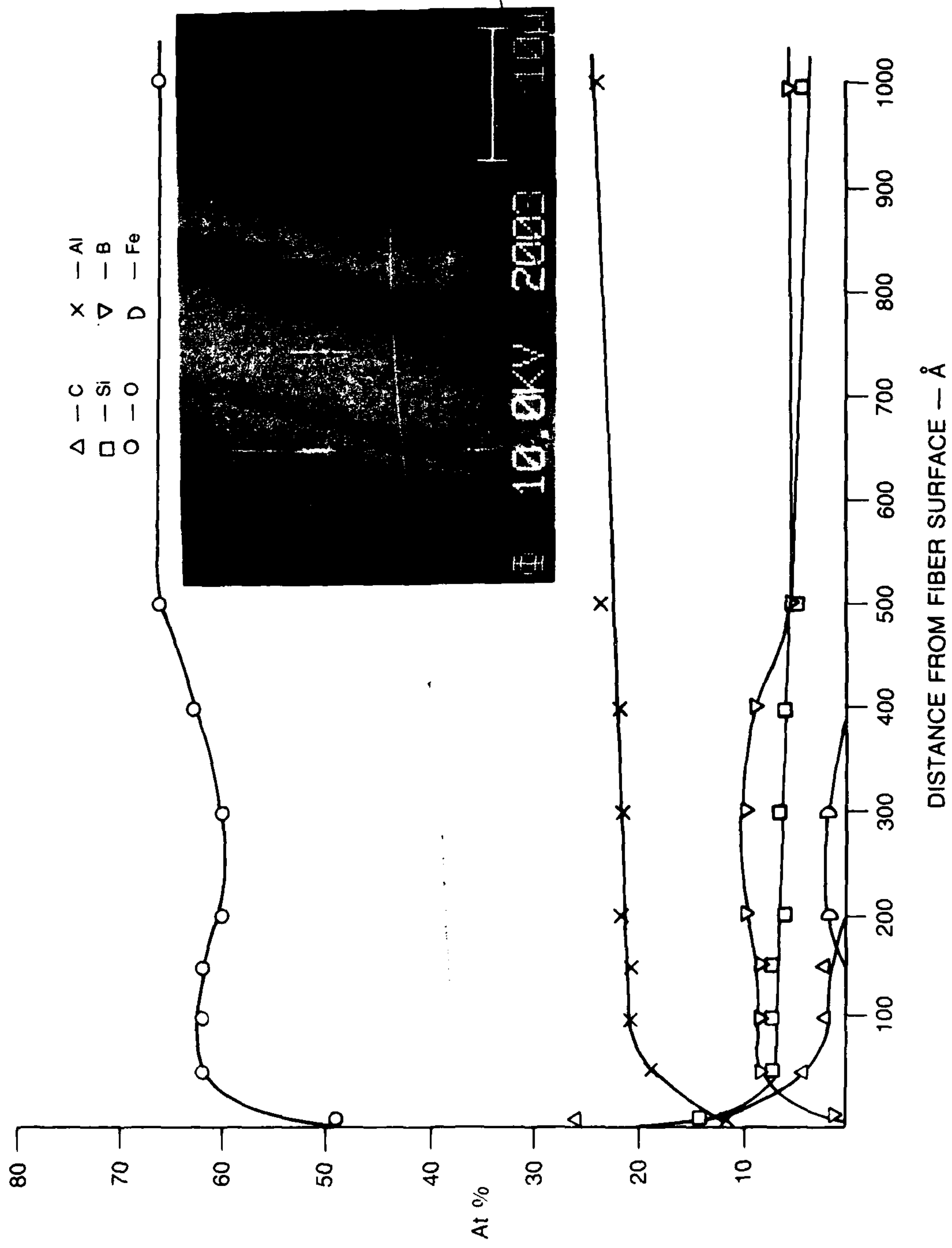

SEM OF CVD SiC ON NEXTEL 440 FIBERS (#7-10-22) (MDS, 2 hrs, H_2 FLUSH)

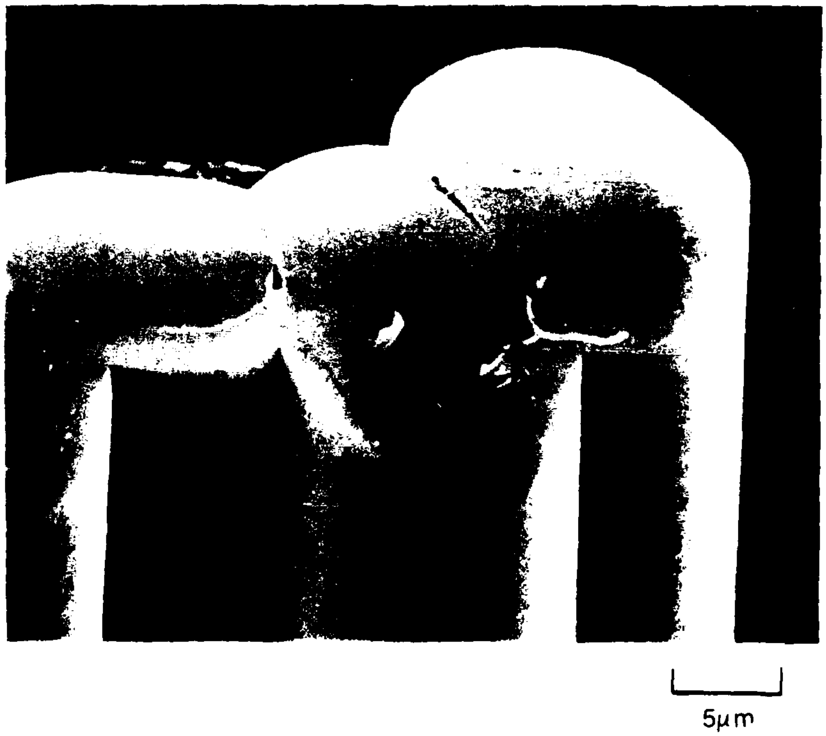

88—9—36—27

TEM/EDS CHARACTERIZATION OF CVD SiC ON NEXTEL 440 FIBER (#7-10-22) (MDS, 2 hrs, H_2 FLUSH)

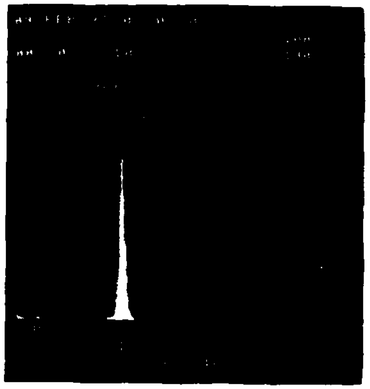

COATING 1×

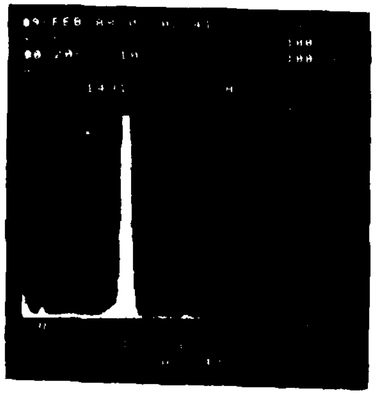

COATING 2×

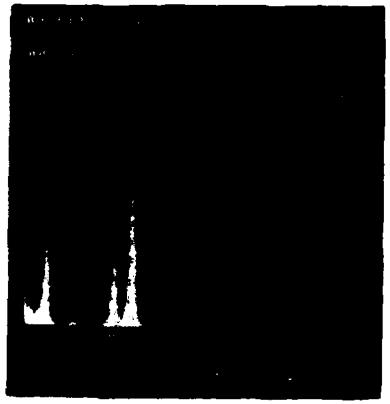

INTERFACE

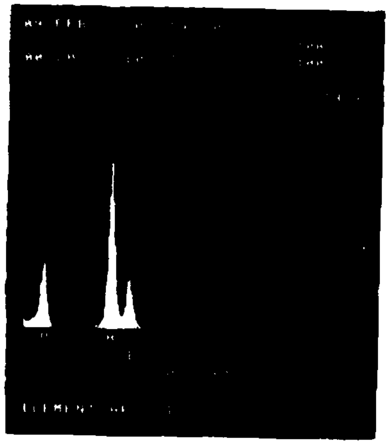

FIBER

FIG. 30

88—9—36—28

SEM OF CVD SiC ON NICALON FIBERS (#7-10-23) (MDS, 2 hrs, H_2 FLUSH)

10μm

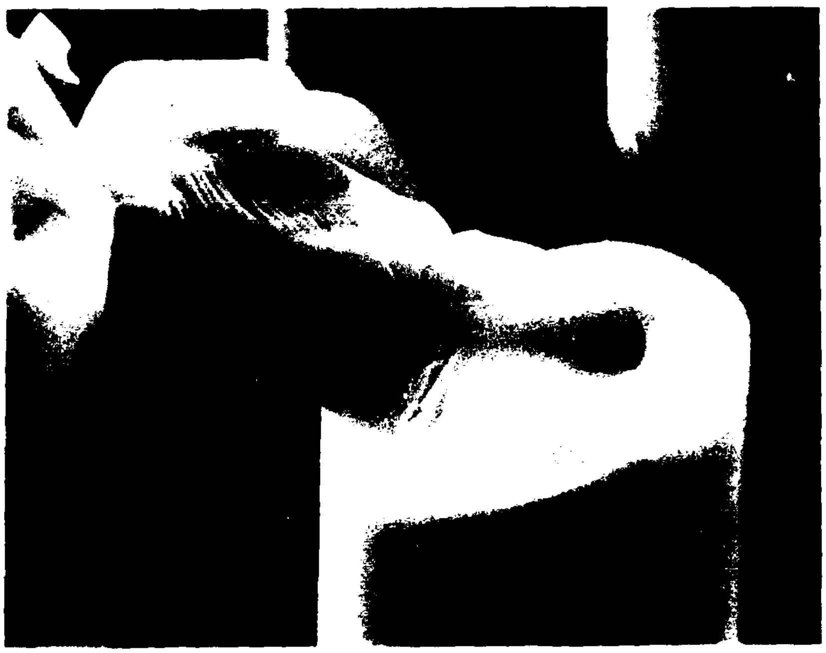

5μm

TEM/SAED CHARACTERIZATION OF CVD SiC ON NICALON FIBER — (#7-10-23)
(MDS, 2 hrs, H_2 FLUSH)

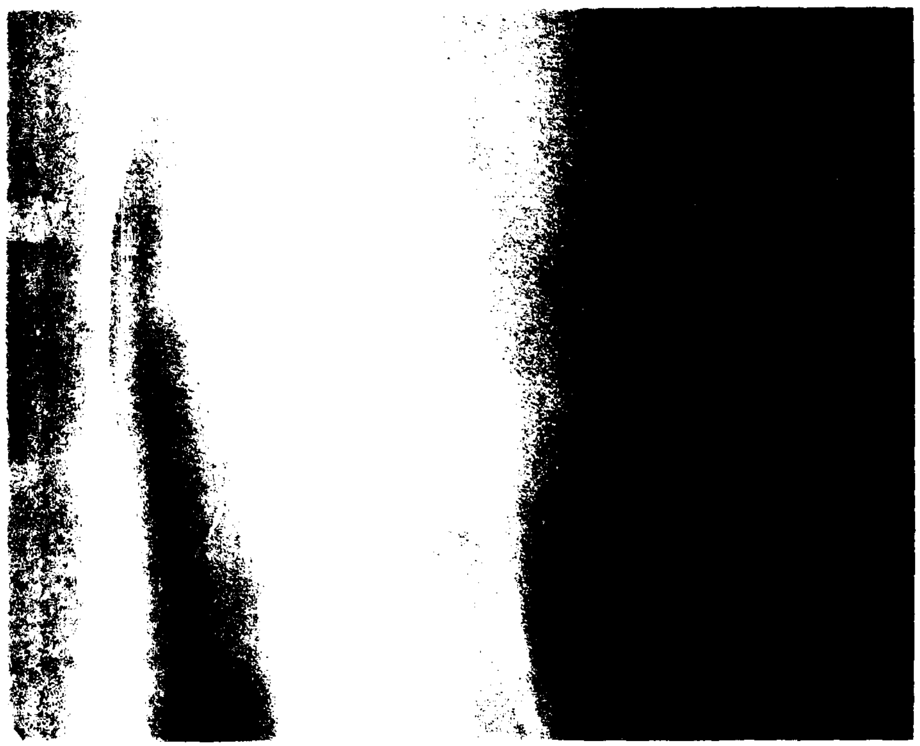

0.15μ m

CVD SiC COATING

NICALON FIBER

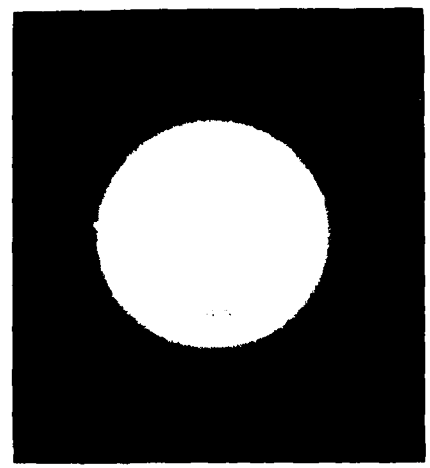

COATING

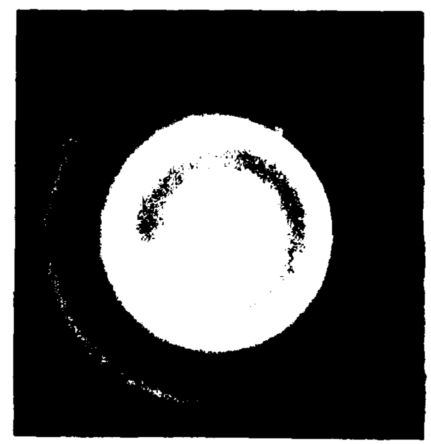

FIBER

88—9—36—30

SEM OF CVD SiC ON NEXTEL 440 FIBERS (#8-1-14) (MTS, 1 3/4 hrs, H_2 FLUSH)

SAM DEPTH PROFILE
CVD SiC ON NEXTEL 440 FIBERS — (#8-1-14) MTS, 1 3/4 hrs, H_2 FLUSH

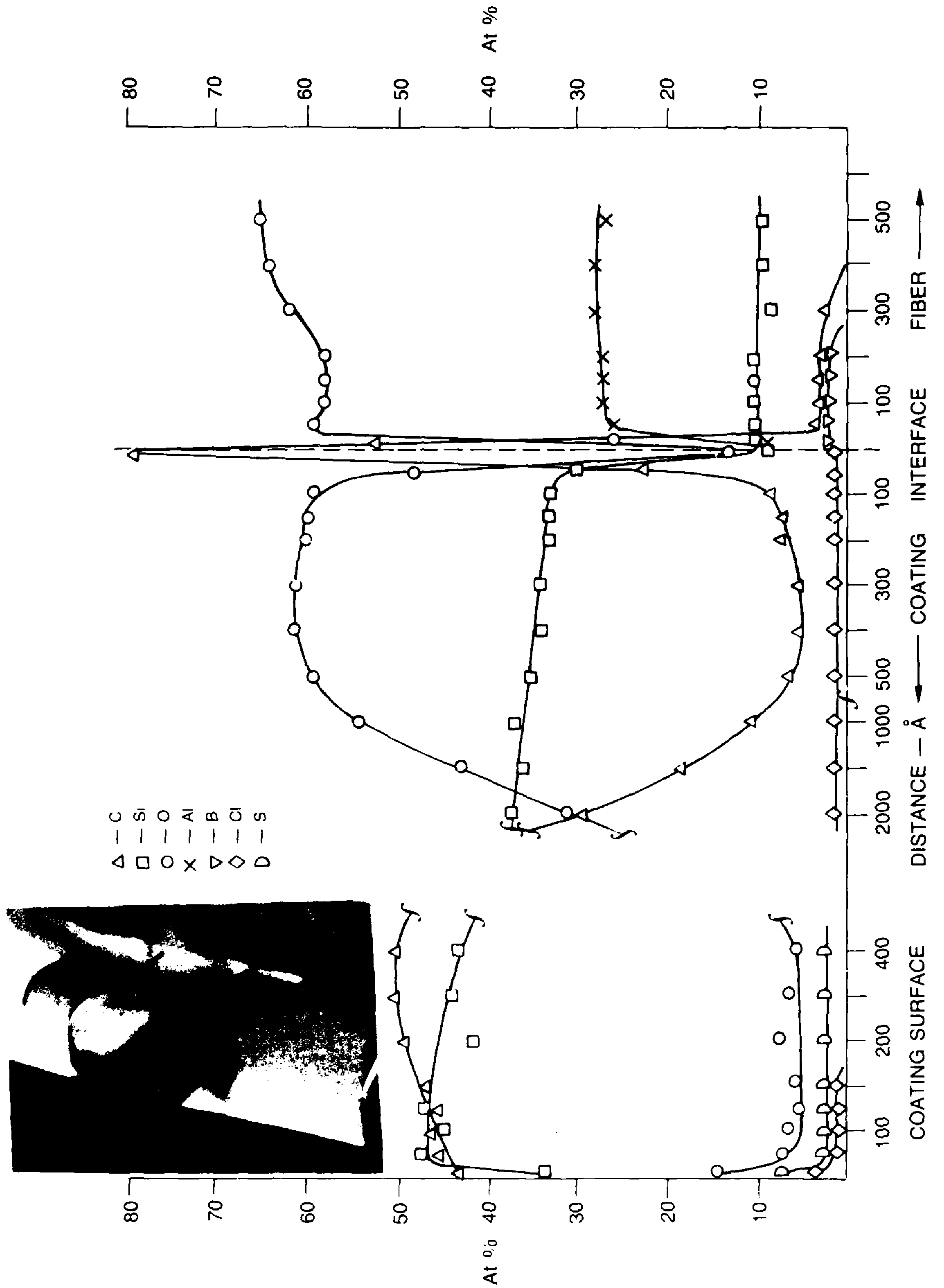

SEM OF CVD SiC ON NICALON FIBERS (#8-1-15) (MTS, 2 hrs, H_2 FLUSH)

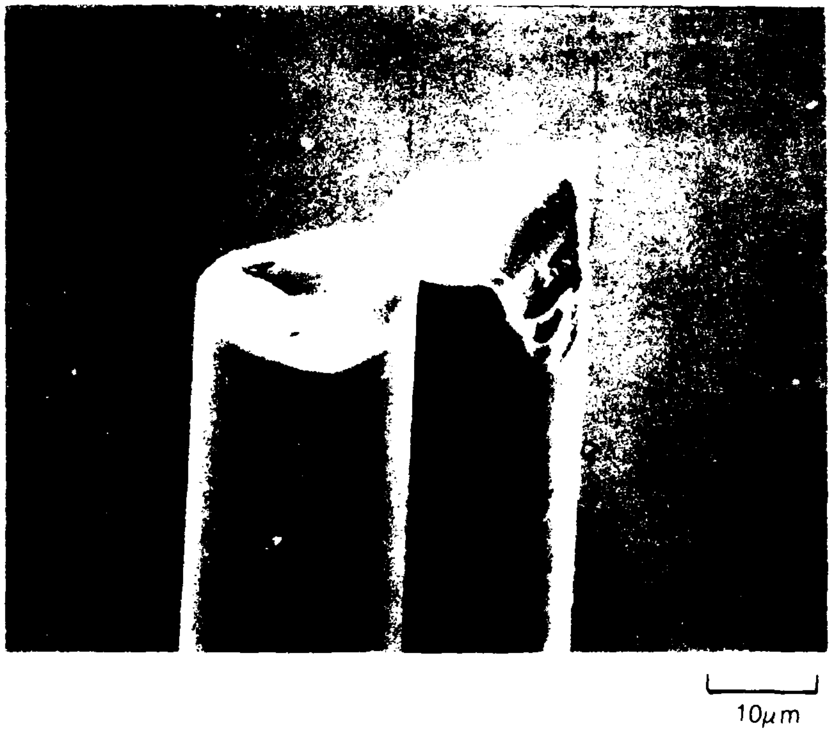

SAM DEPTH PROFILE
CVD SiC ON NICALON FIBERS (#8-1-15) MTS, 2 hrs, H_2 FLUSH

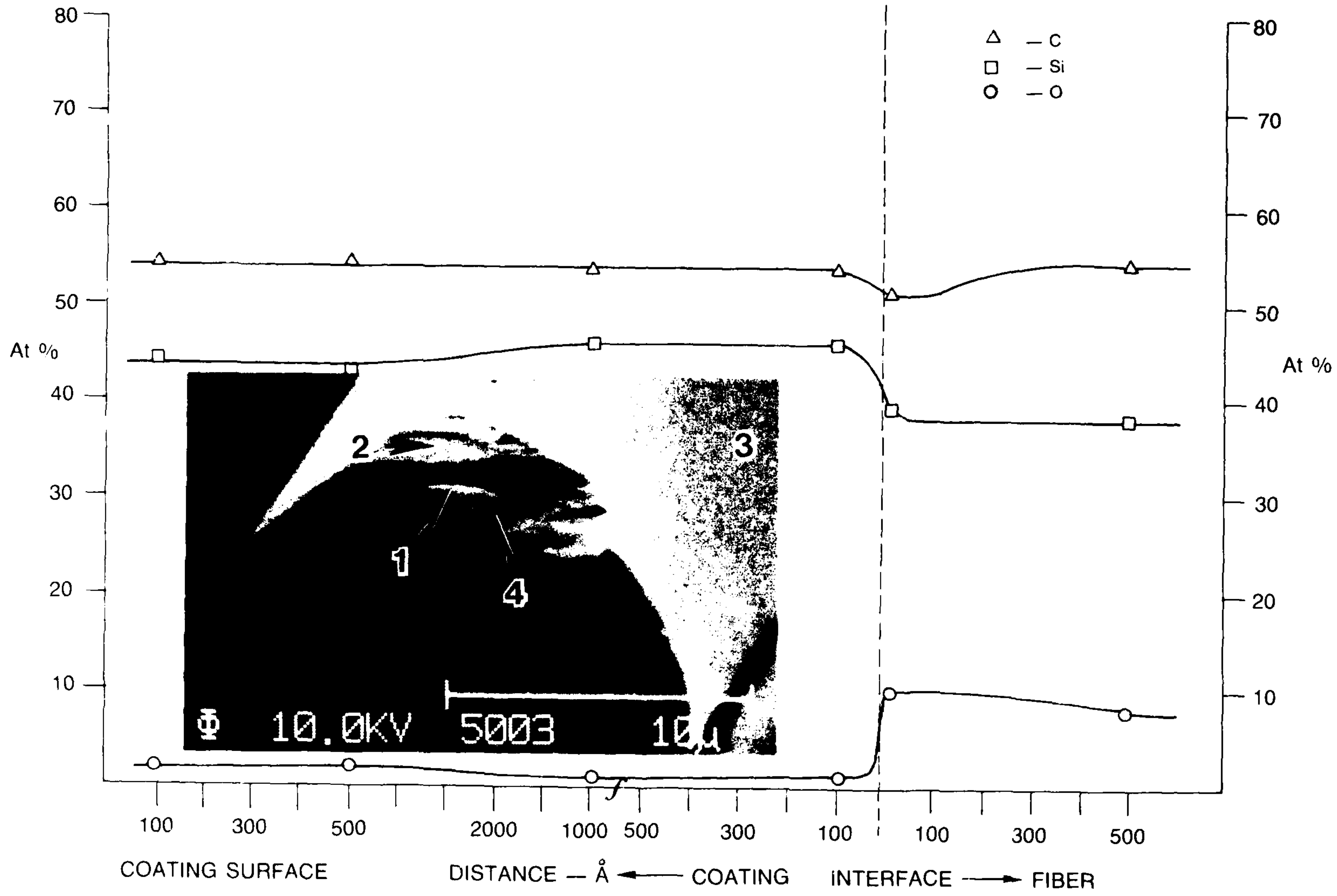

FIG. 36

88-9-36-38

SEM OF CVD SiC ON NEXTEL 440 FIBERS (#8-11-18) (MTS, 1 3/4 hrs, Ar FLUSH)

SEM OF CVD SiC ON NICALON FIBERS (#8-11-25) (MTS, 2 hrs, Ar FLUSH)

10μm

5μm

88–9–36–35

FIG. 39

SAM DEPTH PROFILE
CVD SIC ON NICALON FIBERS (#8-11-25) MTS, 2 hrs, Ar FLUSH

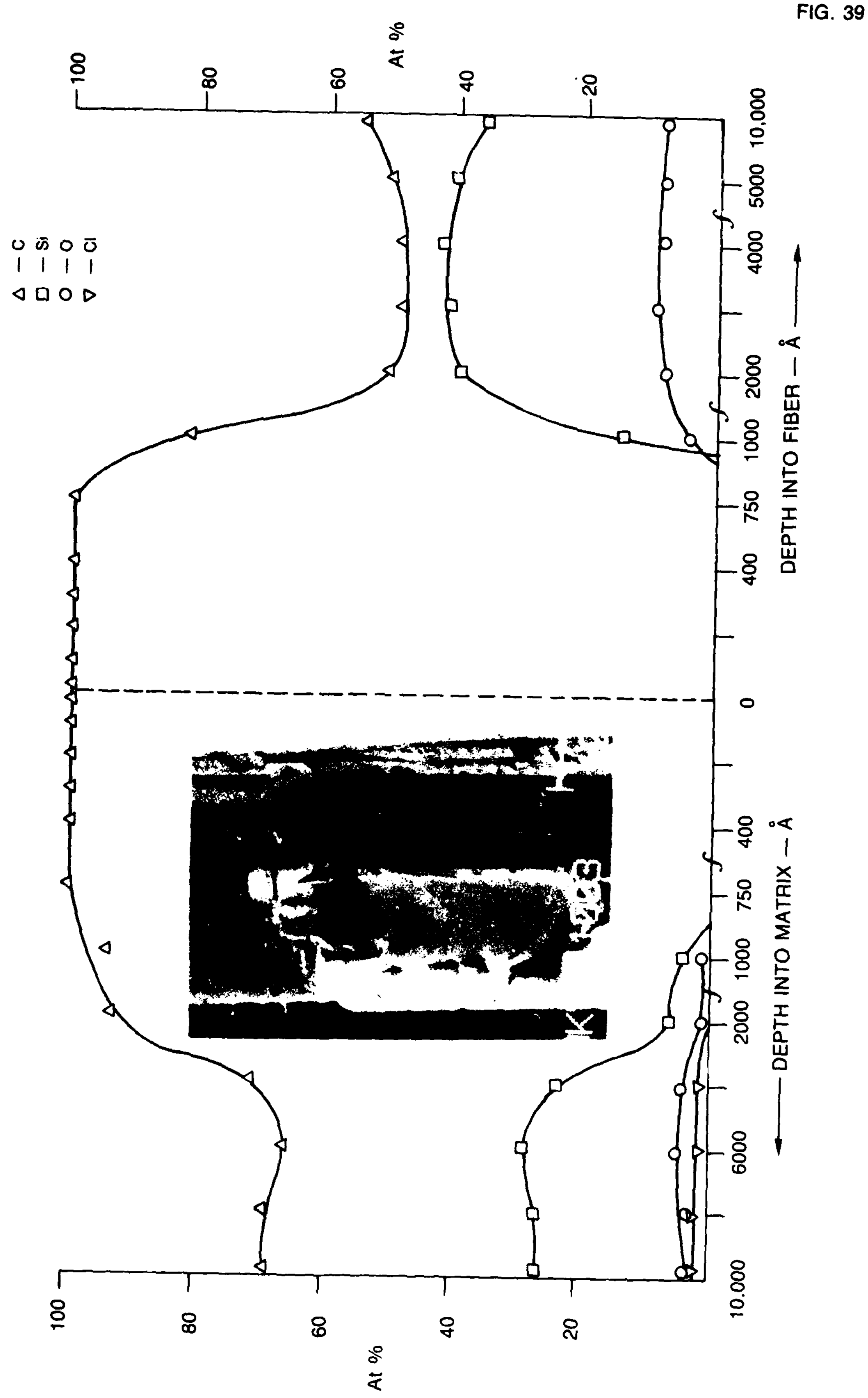

FIG. 40

SAM DEPTH PROFILE
CVD SiC ON CARBON PLATE (#9-1-28) — 328/1 — MDS, Ar FLUSH

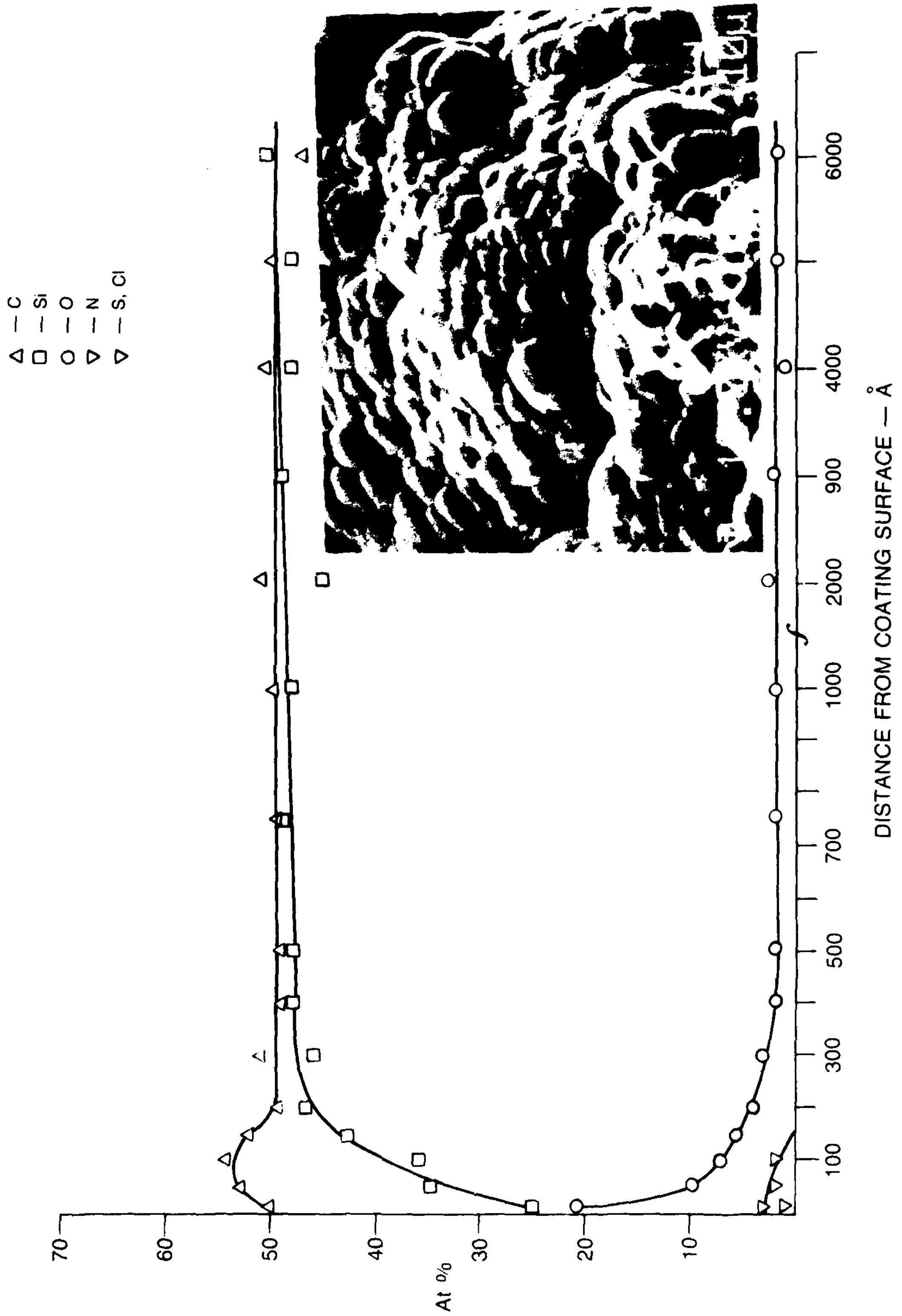

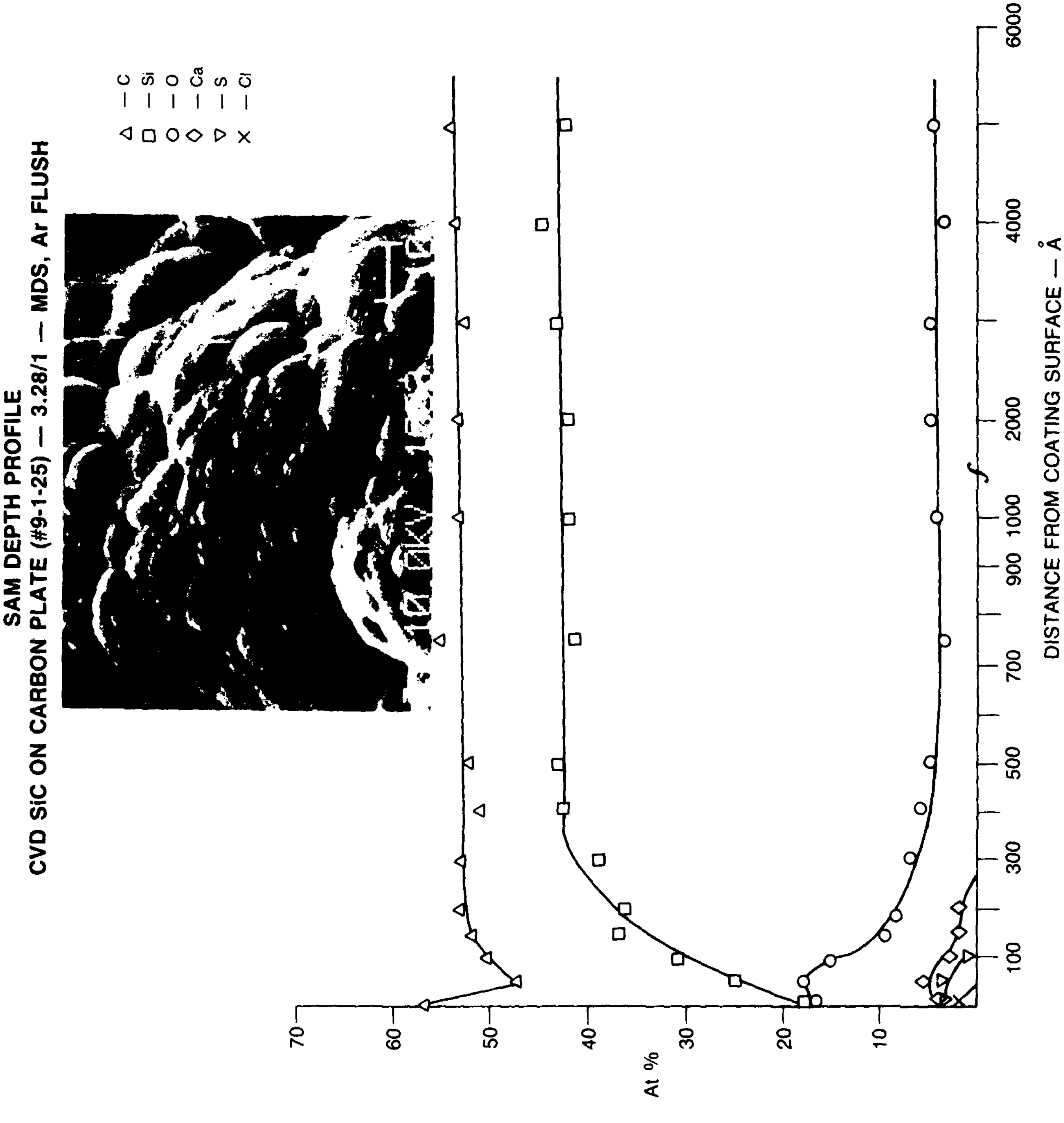
SAM DEPTH PROFILE
CVD SiC ON CARBON PLATE (#9-1-25) — 3.28/1 — MDS, Ar FLUSH
△ — C
□ — Si
○ — O
◇ — Ca
▷ — S
X — Cl
At %
70
60
50
40
30
20
10
100
300
500
700
900
1000
2000
4000
6000
DISTANCE FROM COATING SURFACE — Å

SAM DEPTH PROFILE
CVD SiC ON CARBON PLATE (#9-4-14) MTS 4.8/1, Ar FLUSH

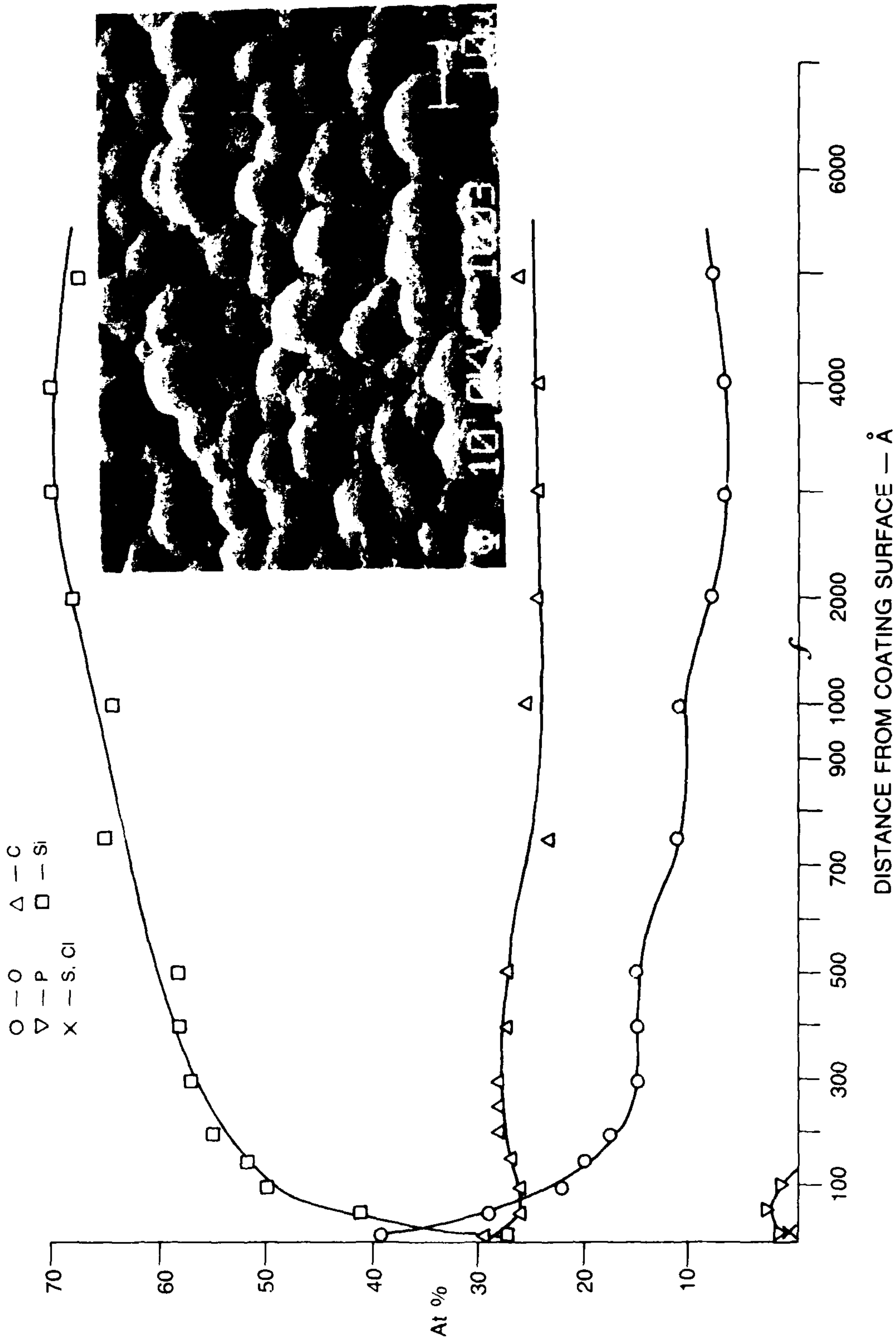

SAM DEPTH PROFILE
CVD SiC ON CARBON PLATE (#9-4-14A) MTS 4.8/1, H_2 FLUSH

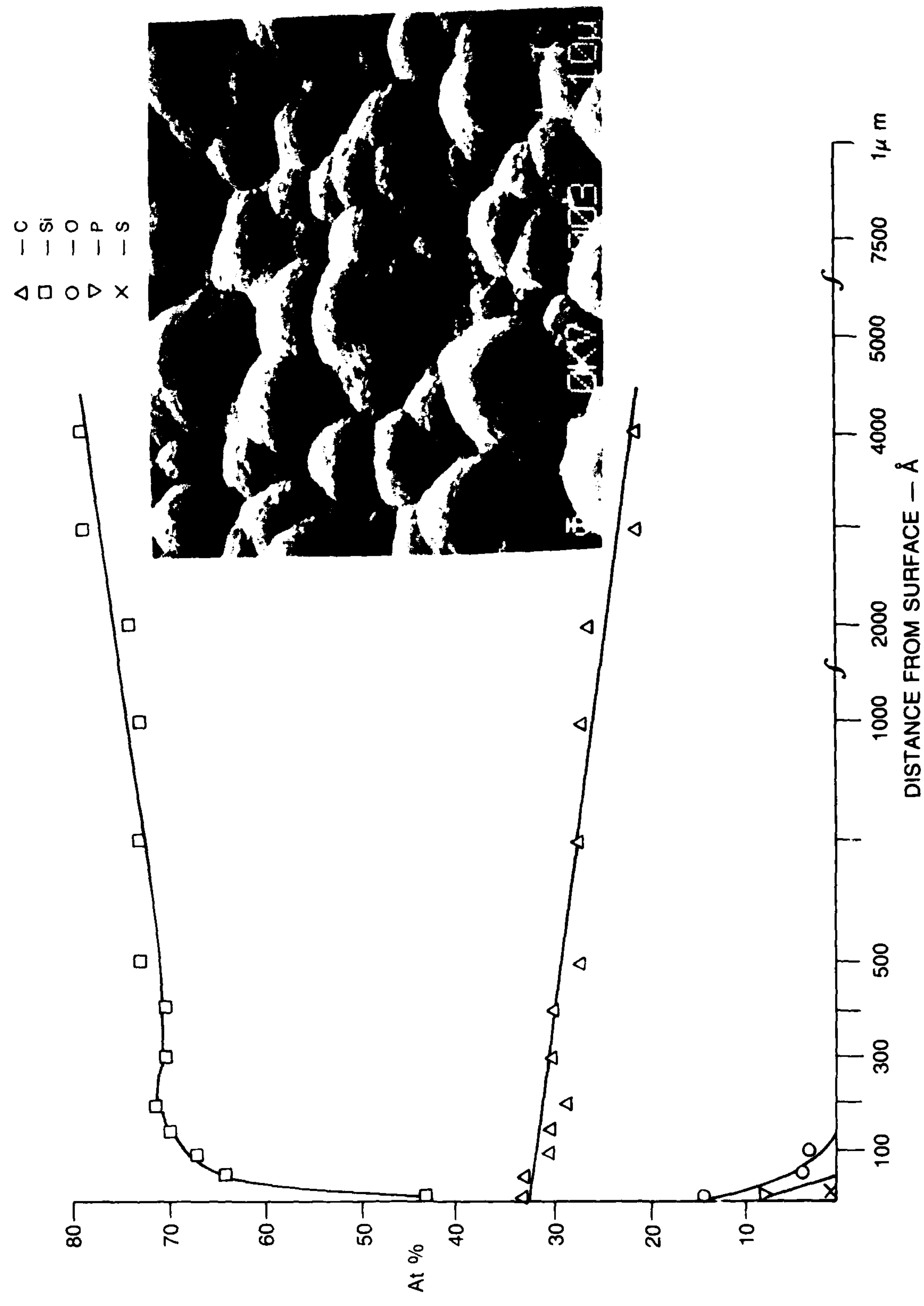

SAM DEPTH PROFILE
CVD SiC ON CARBON PLATE (#9-4-18A) MTS, 4.8/1, Ar FLUSH

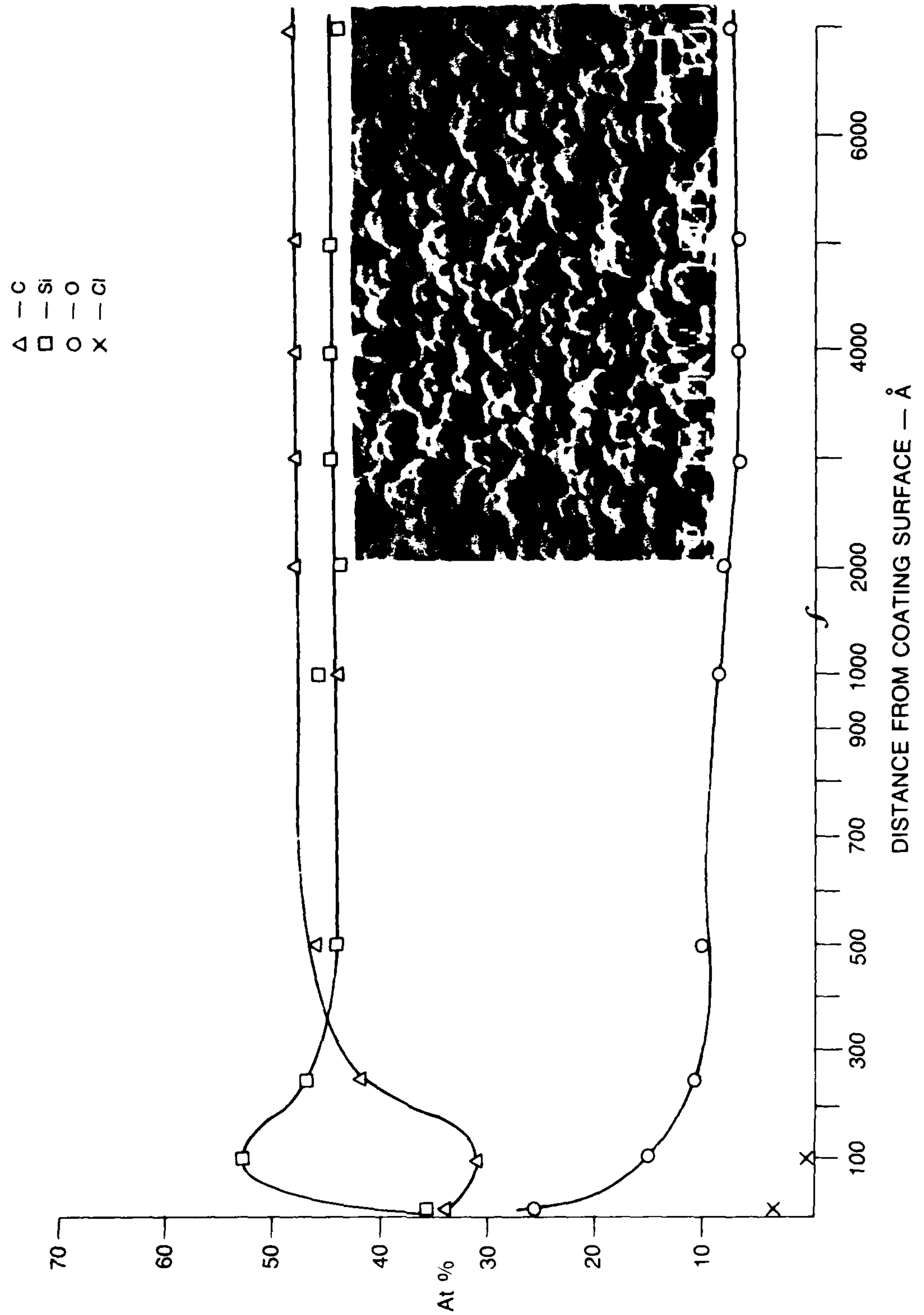

SAM DEPTH PROFILE
CVD SiC ON CARBON PLATE (#9-5-9) MTS, 4.8/1 H_2 FLUSH

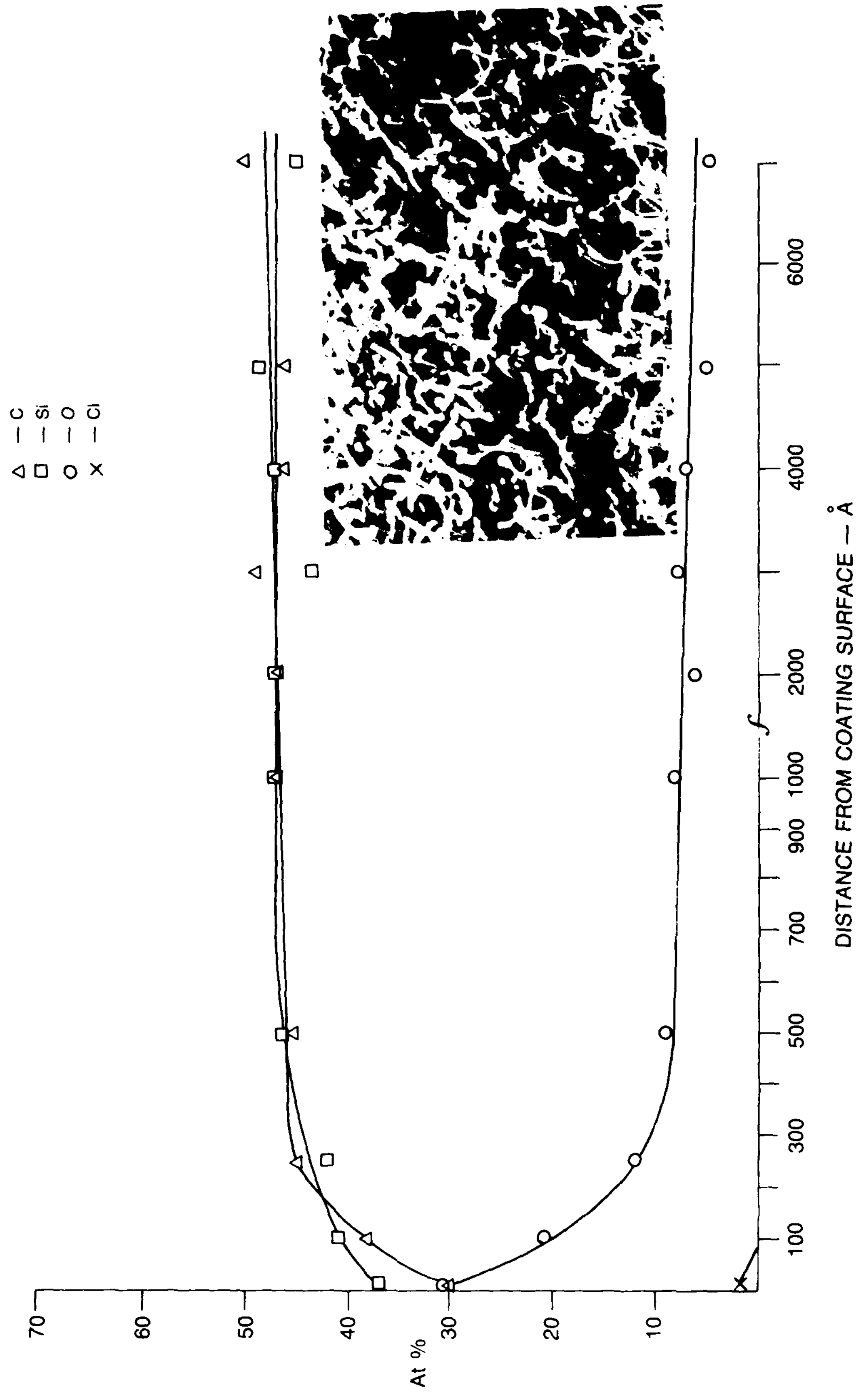

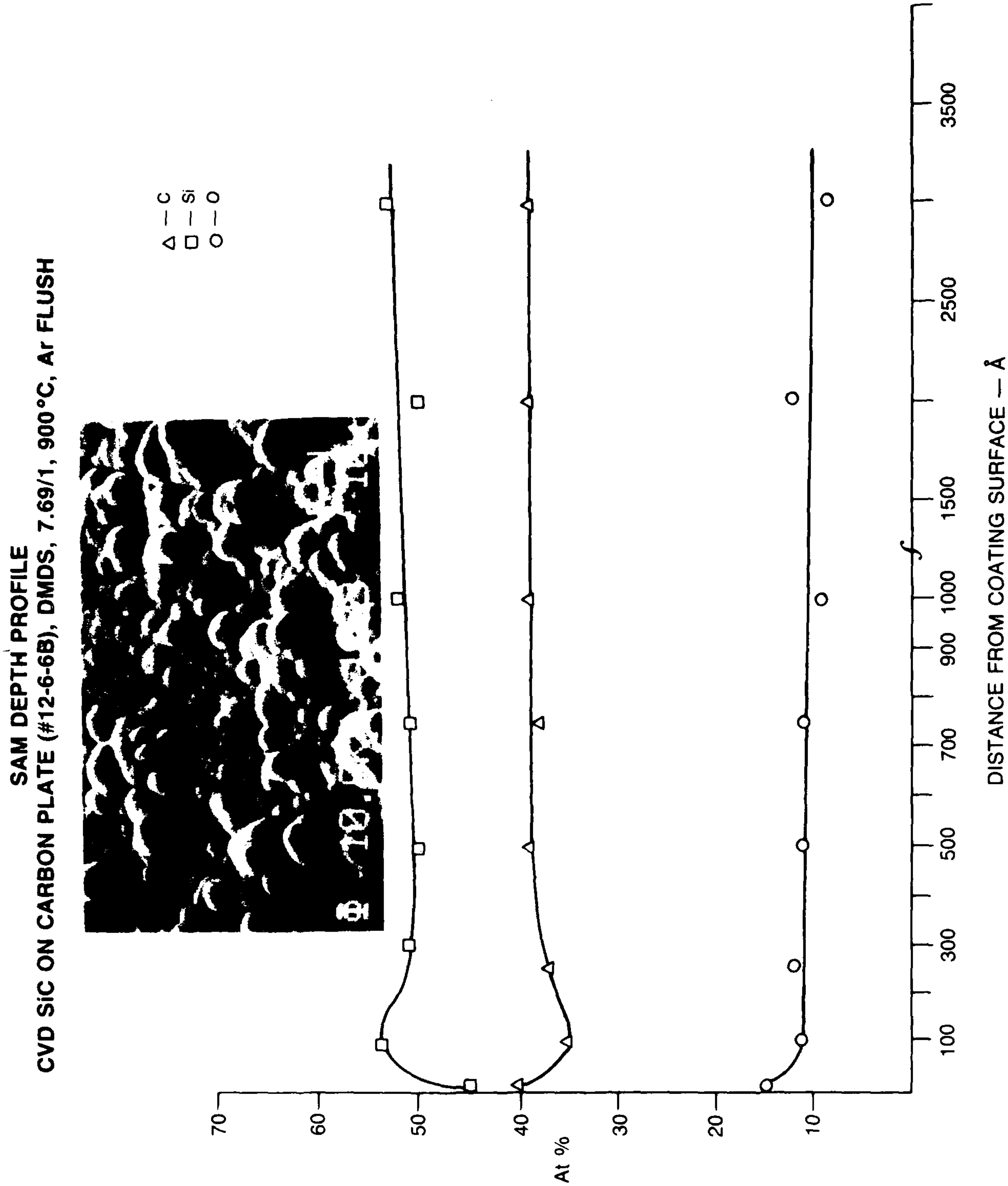
SAM DEPTH PROFILE
CVD SiC ON CARBON PLATE (#12-6-6B), DMDS, 7.69/1, 900°C, Ar FLUSH
△ — C
□ — Si
○ — O
At %
70
60
50
40
30
20
10
100
300
500
700
900
1000
1500
2500
3500
DISTANCE FROM COATING SURFACE — Å

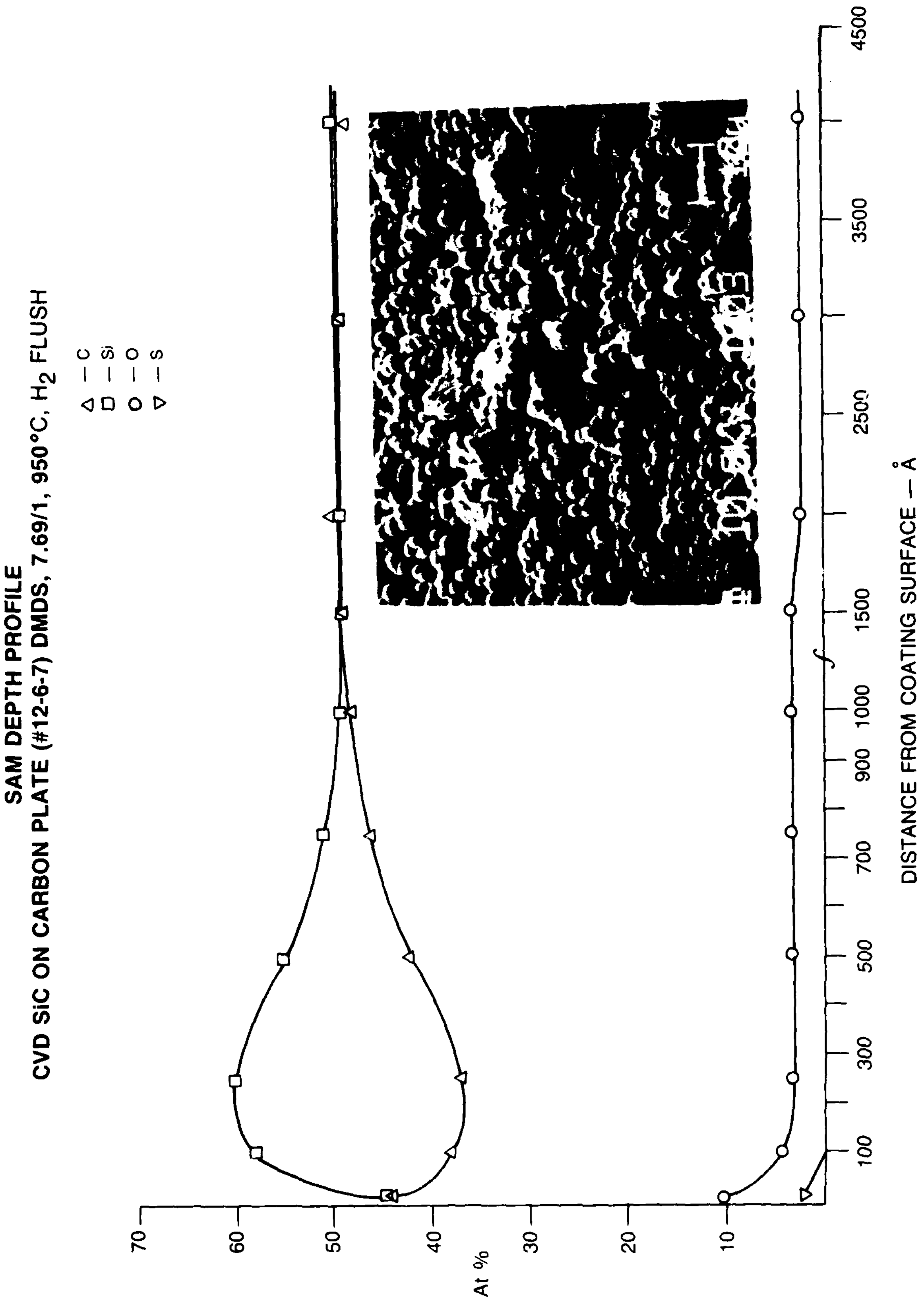
SAM DEPTH PROFILE
CVD SiC ON CARBON PLATE (#12-6-7) DMDS, 7.69/1, 950°C, H2 FLUSH
△ — C
□ — Si
○ — O
▽ — S
At %
70
60
50
40
30
20
10
100
300
500
700
900
1000
1500
2500
3500
4500
DISTANCE FROM COATING SURFACE — Å

FIG. 48

SAM DEPTH PROFILE

CVD SiC ON CARBON PLATE (#13-8-3A), H_2 CARRIER, H_2 FLUSH, CH_4 ADDED (200 cc/min)

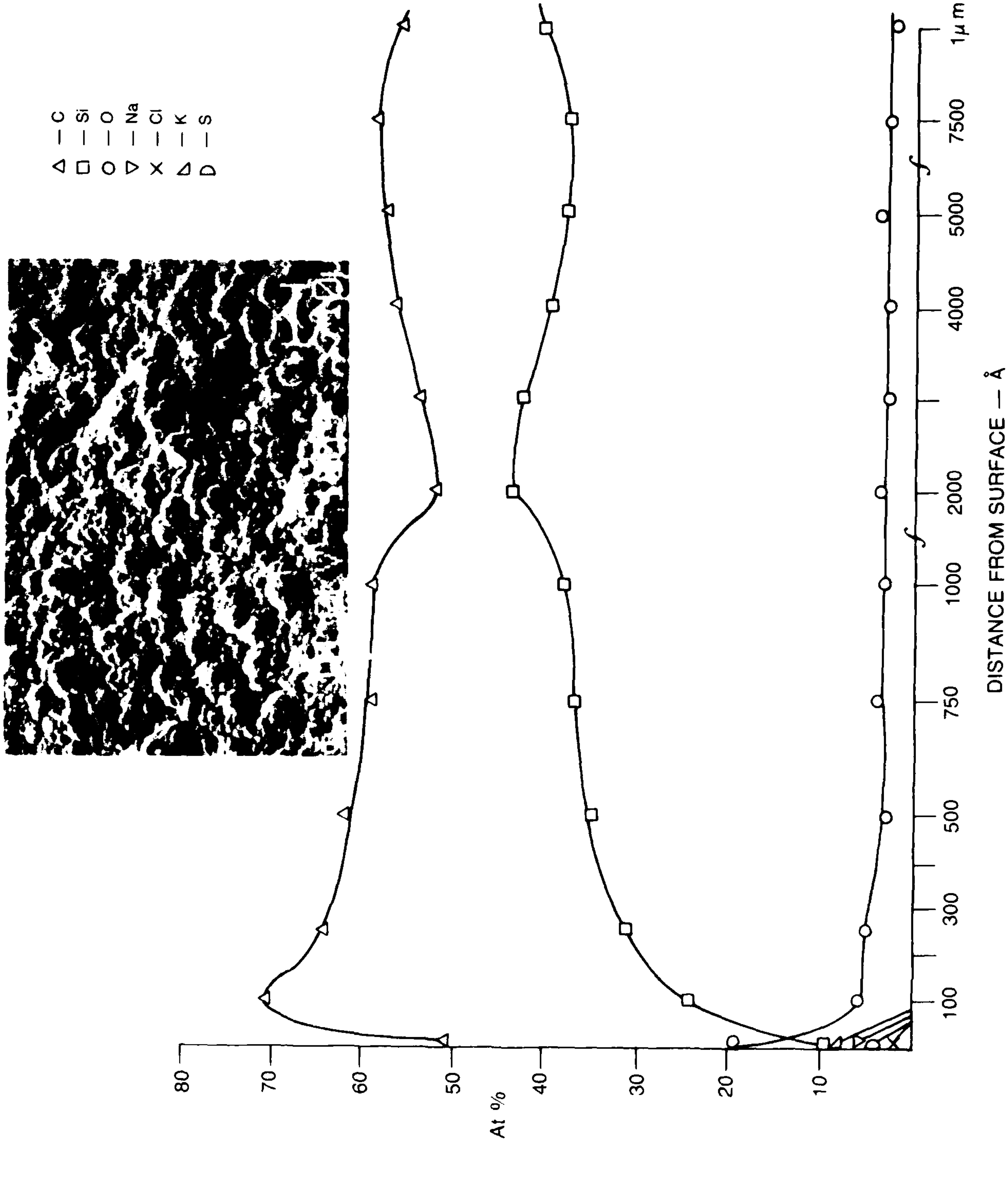

SAM DEPTH PROFILE

CVD SiC ON CARBON PLATE (#13-8-16) H_2 CARRIER, H_2 FLUSH, CH_4 ADDED (600 cc/min)

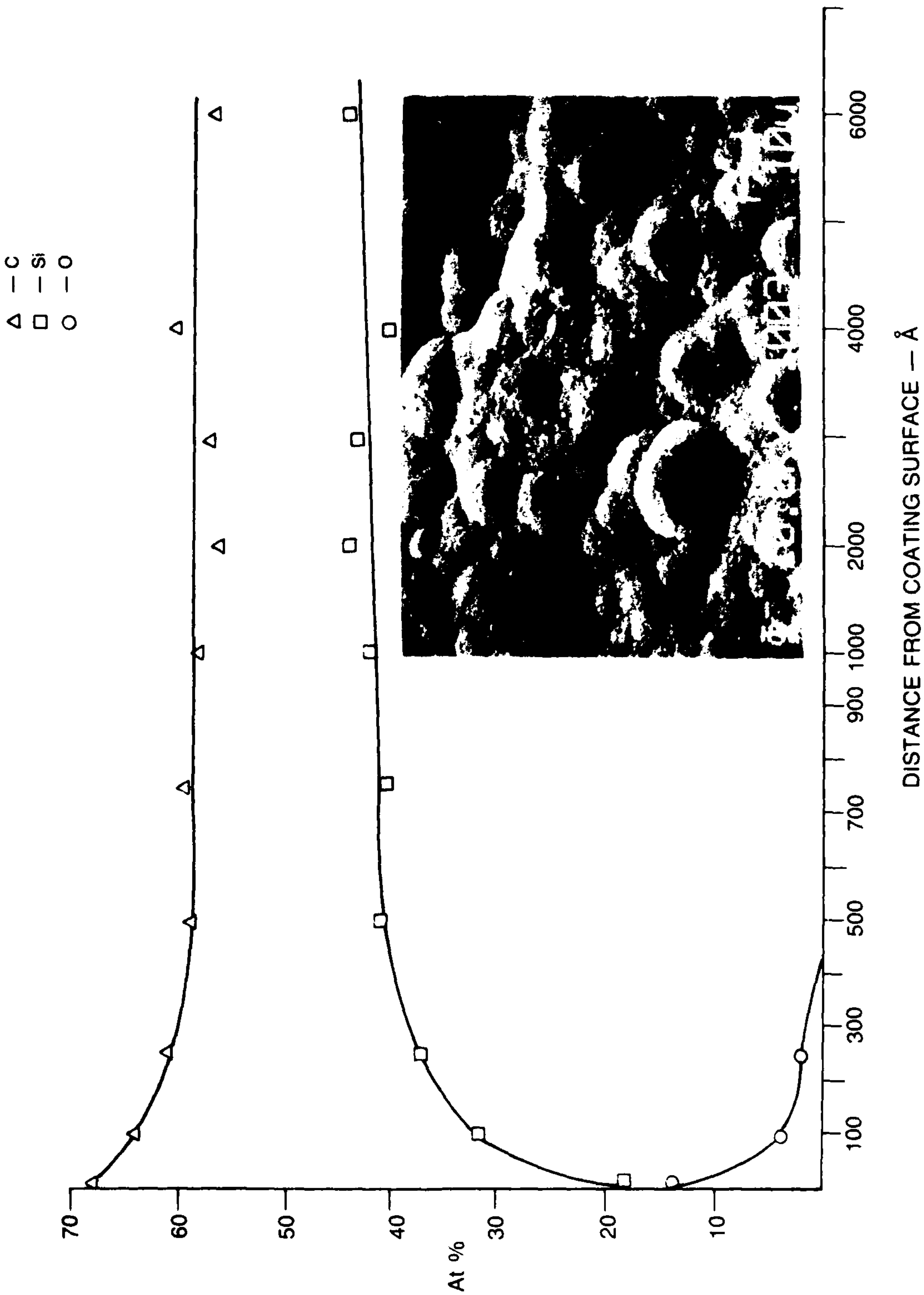

88—9—36—48